2019

The causes and consequences of mimicry in Limenitis butterflies in western North America

BOSTON UNIVERSITY

GRADUATE SCHOOL OF ARTS AND SCIENCES

Dissertation

THE CAUSES AND CONSEQUENCES OF MIMICRY IN *LIMENITIS* BUTTERFLIES IN WESTERN NORTH AMERICA

by

EVAN B. KRISTIANSEN

B.S., University of the Pacific, 2012
M.S., University of the Pacific, 2014

Submitted in partial fulfillment of the

requirements for the degree of

Doctor of Philosophy

2019

Approved by

First Reader

Sean Mullen, Ph.D.
Associate Professor of Biology

Second Reader

Michael Sorenson, Ph.D.
Professor of Biology

Third Reader

Erik B. Dopman, Ph.D.
Associate Professor of Biology
Tufts University, Department of Biology

ACKNOWLEDGMENTS

Completing a PhD and producing a dissertation is not a solitary endeavor, and I am indebted to a large number of people for their generosity in the last five years. I simply do not have the space to thank everyone individually, but if you are reading this, know that you have been an influential part of getting me this far. I want to especially thank my family: Mom, Dad, Kari Anne, Maria, for your love and support. Thank you especially for long phone calls, for patience with breaks and holidays, and for encouragement throughout my entire graduate school career.

My advisor, Sean Mullen, for steadfast support, writing help, encouragement, and banter. Without your help, my thesis would still be an uneven stack of unrelated paragraphs. Thank you for your advice, your instruction, and your friendship. I am also grateful for the advice and patience of my thesis committee: Mike Sorenson, Pete Buston, Chris Schneider, and Erik Dopman. In addition, I am thankful to those who have acted as advisors to me in other academic capacities, particularly Liz Co, Jenny Talbot, Sarah Davies, and Randi Rotjan.

I would also like to thank my friends, for keeping me sane, calling me to be better than I am, and providing support. Most especially Manuel Buen-Abad Najar, PJ Herrera, and Ben Castro. Everyone at the BU Catholic Center, but especially Fr. David Barnes for invaluable spiritual advice, and to Fran Boucher for what I'm sure amounts to a hundred pounds of pasta. Also, Karina Scavo, William Caffry, Katey Lesneski, and all of the other BU graduate students for being solid friends and excellent company in the department.

A large portion of my thesis research has involved fieldwork, and I have many to

thank for the help they offered me. Most especially I would like to thank Jeremy and Alex Gallus for providing me a place to stay for a whole month, this work would have been much more expensive and much less fun without you. Also, to Lily Tieu, field assistant extraordinaire. To Susan Finkbeiner, for company in both Idaho and Costa Rica, and for invaluable field advice. I would also like to thank the United States Forest Service, and the Office of Tropical Studies in Costa Rica for their help in procuring permits for some of this work.

Other parts of this research relied on extensive methodological support from collaborators, including Layla Freeborn, Katie Stryjewski, William Caffry, Ryan Hill, Louis Prusa, Cassidi Rush, Susan Finkbeiner, Michael Sorenson, and many others. I am especially thankful to the Office of Information Services Technology at BU, especially Katia Oleinik for invaluable support with large datasets in R and with high-throughput computing.

Thank you all most sincerely, and God bless you.

THE CAUSES AND CONSEQUENCES OF MIMICRY IN *LIMENITIS* BUTTERFLIES IN WESTERN NORTH AMERICA

EVAN B. KRISTIANSEN

Boston University Graduate School of Arts and Sciences, 2019

Major Professor: Sean P. Mullen, Associate Professor of Biology

ABSTRACT

Batesian mimicry is a classic example of adaptation wherein the benefit of bearing the mimetic trait is directly and positively correlated with fitness. This tangible fitness benefit makes mimicry an excellent model system for addressing one of the largest remaining questions in evolutionary biology, that of the origin and maintenance of adaptive phenotypic diversity. Here I set out to answer a small part of this larger question - namely, what maintains color pattern polymorphism between two hybridizing species of admiral butterflies (genus *Limenitis*) in western North America. I address this question by examining both predator-mediated selection on the phenotype, and by investigating phenotype-genotype association across the genome. In chapter one, I demonstrate the adaptive significance of the mimetic orange apical forewing patch (AFP) phenotype in *Limenitis lorquini* through the use of a large-scale predation experiment. In the chapter two, I localize the genomic region responsible for this color pattern variation using a mapping cross and quantitative trait locus (QTL) analysis. Finally, in chapter three I identify putative causal variants that are associated with the phenotype using linear modeling in a genome wide association study (GWAS). Collectively, my results suggest that the presence or absence of the orange AFP phenotype is associated two separate

regions of the genome. The first region includes an undescribed gene, while the second contains variation near the known color patterning gene *optix*. Studies of the functional relationship between these gene regions and phenotype will be necessary to confirm this hypothesis and examine how selection acting on these regions of the genome impact patterns of introgression and gene flow across the species boundary between these two hybridizing admiral lineages.

PREFACE

Diversity of form is one of the most striking features of the natural world. Endeavoring to categorize and understand how such diversity comes about has been a key focus of biologists since antiquity. From Aristotle's "the parts of animals" (Aristotle 350BC) -- where he describes the life cycle of a butterfly (likely *Pieris brassicae*) in great detail and contrasts it with that of other insects -- to more modern scientists like Henry Walter Bates, the diversity of life has been a constant source of fascination. In Bates' case, he became fascinated with the diversity of butterfly color patterns that he encountered during his famous voyage to South America in 1848 with fellow scientist Alfred Russel Wallace. During this journey he was struck both by the diversity of butterfly color pattern and the degree to which many unrelated species closely resemble each other when occurring in the same environment. He remarked:

> In tropical South America a numerous series of gaily-colored butterflies and moths, of very different families, which occur in abundance in almost every locality a naturalist may visit, are found to change their hues and markings together, as if by the touch of an Enchanter's wand, at every few hundred miles". (Bates 1879; Harrison 1993)

The interesting thing was not that there was so much diversity, according to Bates, but rather that there was so much similarity between seemingly unrelated species. For these, and other reasons, butterflies have become a model system for understanding the origin and maintenance of diversity at multiple levels of biological organization. Butterflies have featured heavily, for example in studies of adaptation and speciation, evolutionary

genetics, evolutionary developmental biology, and the genetic and genomic basis of mimetic color pattern variation. Great strides, particularly with respect to mimicry, have allowed researches to begin to understand the genetic and developmental basis of color pattern variation and the evolutionary processes that shape adaptive phenotypic diversity in natural populations.

In this preface I provide a brief overview of **1)** convergent evolution and Batesian mimicry theory, **2)** what is known about the genetics of color pattern variation in Lepidoptera, and **3)** the genus *Limenitis*. I conclude with a summary of the main questions motivating each of my dissertation chapters.

Convergent evolution: Convergent evolution is an evolutionary phenomenon wherein two organisms independently evolve similar phenotypes. These new convergent phenotypes may introduce barriers to gene flow within a population, thereby driving the formation of independent convergent and non-convergent populations. It is these barriers to gene flow, which lead to differential fixation of alleles between populations, that set the stage for lineage divergence, may lead to speciation. Convergent evolution between species can occur in three different ways. First, independent mutations can affect different genes or developmental pathways that nonetheless produce similar phenotypic outcomes; this is classically exemplified by cave tetra, in which independent mutations in *Oca2* or *Mc1r* are both known to induce blindness (Gross, Borowsky, and Tabin 2009). Second, independent mutations can affect the same gene or the same developmental pathway, resulting in a similar phenotypic outcome; this appears to be a common

occurrence and can stretch across wide gulfs of phylogenetic time (e.g., Hoekstra et al. 2006). Finally, convergent evolution between interfertile species can occur via introgression of a mutated gene region; identifying this mode of convergent evolution, sometimes called "collateral evolution" (Stern 2013), is complicated by the difficulty associated with differentiating introgression events from incomplete lineage sorting, but examples of convergence due to introgression have slowly begun to emerge (e.g., Mullen et al. 2019 (in press)). In each case, the result is that two phenotypically distinct species begin to resemble one another, which has the net effect of increasing intraspecific color pattern variation. Importantly, if this intraspecific color pattern variation associated with fitness differences, then it could introduce a barrier to gene flow in the form of reduced fitness, infertility, or hybrid inviability (Coyne and Orr 2004) and possibly speciation (Jiggins et al. 2008).

Genetics of color pattern variation: Experiments aimed at understanding the genetics of butterfly color pattern began roughly 100 years ago with crossing experiments performed by Leigh and Poulton (1909). This early work, along with similar work in *Heliconius* (Beebe 1955, Turner and Crane 1962), was able to infer that a relatively small number of loci of major effect exerted binary (present/absent) control over the variation in color pattern in red and yellow color pattern elements. Additionally, control of color is very similar to the modular control of pattern in that a relatively small number of co-opted genes are responsible (Nijhout 2001; Carroll et al. 1994). Later work using modern techniques and DNA sequencing has also revealed a remarkable amount of homology

between species in both how they regulate color and pattern (Nadeau et al. 2014; Carroll et al. 1994; Papa, Martin, and Reed 2008). However, because pattern and color are independently controlled (Brunetti et al. 2001) and often unlinked, the result is additional modularity and potential diversity produced by different combinations of patterning loci and color loci. When paired with gene regulation in time and space, this modularity is a possible explanation for the evolution of widespread diversity in butterfly wing color patterns despite the relatively small number of genes.

Many of the loci underlying color have been identified in recent years. Pioneering work by Sheppard et al. (1985b), Mallet (1989), and Jiggins and McMillan (1997) and further characterized by Riccardo Papa et al. (2013) identified a small handful of important genetic loci that control color patterning in *Heliconius* (reviewed by Kronforst and Papa (2015)). Red and yellow patterning in *Heliconius* is controlled by the BD gene region, which contains the transcription factor *optix. Optix* is expressed during the development of red wing regions prior to ommochrome pigmentation (Reed et al. 2011), which demonstrates a functional link between this gene region and red color. The yellow locus (called Cr by Jiggins and McMillan (1997) , now called Yb/N (Kronforst and Papa 2015)) has been shown to control the size, shape, and pattern of the yellow hindwing bar, and recently was found to be homologous with the supergene P in *H. numata* (Joron et al. 2006). A candidate gene within this locus is *cortex* which is differentially expressed in black and yellow regions of the wing during development (Nadeau et al. 2016). Finally, a third locus has been implicated in the control of forewing band shape and melanization (Kronforst, Kapan, and Gilbert 2006). QTL analyses in two different species (Gallant et

al. 2014; Kronforst and Papa 2015) reveal that this locus contains the gene WntA, and functional demonstrations have revealed consistency between WntA expression and melanic patterning. This example is particularly interesting because it demonstrates convergence in the genetic basis of color patterning between two species (*Limenitis arthemis* and *Heliconius erato*) that are highly diverged (~65mya). This remarkable convergence in the genetic basis of color patterning points to the possibility that color pattern evolution is due primarily to changes at a few genomic "hotspots" (Martin and Orgogozo 2013; Papa, Martin, and Reed 2008), and further demonstrates the clear need for broadening the scope of study to include additional species.

Mimicry: In his famous work, cited above, H.W. Bates pointed out the similarity between the patterns of co-occurring butterfly species that he encountered in the tropics. This, he postulated, was due to the fact that some of the butterflies were toxic, and that the non-toxic butterflies were "mimicking" them; a phenomenon that has since been termed "Batesian" mimicry in recognition of his observations. Batesian mimicry is a classic example of adaptation where, as Bates predicted, palatable individuals gain protection from predation by resembling an unpalatable model species (Bates 1862). Batesian mimicry theory makes three concrete predictions: First, the model organism is unpalatable, leading to reduced predation because of learned avoidance (Bates 1862; Ruxton, Sherratt, and Speed 2004). Second, because the unpalatability of the model is be correlated with its phenotype, predators should also reduce their predation of organisms that resemble the model. Finally, this protection should disappear in areas where

predators have not learned to avoid the phenotype of the model. Despite these clear and highly testable predictions, very few field experiments of Batesian mimicry have been published. It is very common to infer a mimetic relationship between species that are similar in appearance and share a habitat, but this hypothesis goes untested surprisingly often. Among those studies that do have experimentally demonstrated mimicry, experiments are often conducted in laboratory settings, or are restricted to a handful of organisms including snakes (Wster et al. 2004; Pfennig, Harcombe, and Pfennig 2001), hoverflies (Rashed and Sherratt 2007), beetles (Hetz and Slobodchikoff 1988), and poison-dart frogs (Darst and Cummings 2006). More recently, studies have begun to emerge that utilize new techniques to assess the consequences of mimetic resemblance (Kristiansen et al. 2018; Palmer et al. 2018), but this new field is still developing. In the era of big data and spurious correlation it is increasingly important to establish firm biological basis for hypotheses of adaptation.

Batesian mimicry provides important insights into the evolution of diversity because it posits a clear mechanism to explain the initial evolution of mimetic novelty following a two-step hypothesis. In this hypothesis an initial shift towards highly fit mimics dominating a landscape of relatively unfit non-mimetic individuals (Nicholson 1927) may result in the non-mimic being supplanted by the mimic -- even in the presence of ongoing gene flow -- due to the selective advantage of bearing the mimetic phenotype (Ruxton, Sherratt, and Speed 2004). However, in areas where the Batesian model organism does not occur the selective landscape may be more variable due to associated costs of bearing the mimetic (often conspicuous) phenotype, which results in a

heterogeneous distribution (Ruxton, Sherratt, and Speed 2004). It is important to note that mimics routinely extend outside of the range of their models (Pfennig and Mullen 2010). Such cases, however, do not undermine the theoretical framework underlying a process of speciation via divergent selection resulting from mimicry, but merely demonstrates that traits that have positive fitness effects in some niches need not simultaneously have strongly negative fitness effects in other, unoccupied, niches. The outcome of the evolution of mimicry is often two distinct populations (mimetic and non-mimetic) and therefore a net increase in diversity. These populations may be genetically separated by only one or a small handful of loci that are responsible for the mimetic trait, while the remainder of the genome remains relatively similar until the subsequent evolution of additional divergent characteristics.

It remains unclear how quickly porous species boundaries harden, and to what extent the genomic architecture of traits experiencing divergence (i.e., "Speciation phenotypes") influence the speciation process (Mullen and Shaw 2014; Shaw and Mullen 2011). Furthermore, while divergent regions in the genome are often thought to play a critical role in the evolution of reproductive isolation, few studies have successfully linked genomic divergence at the molecular level to patterns of reproductive isolation in natural populations, though some evidence is emerging (Cruickshank and Hahn 2014; Marques et al. 2016). To study the possibility that Batesian Mimicry may lead to speciation, a group that exhibits the hallmarks of early stage divergent selection for a mimetic phenotype is needed.

***Limenitis*:** Limenitidine butterflies (*Limenitis* and *Adelpha*) are emerging as excellent model systems for studying mimicry because of their extreme diversity and widespread convergent evolution (Ebel et al. 2015; Porter 1990; Ritland and Brower 1991; Savage and Mullen 2009; Willmott 2003). The *Limenitis* genus is unusual among other temperate butterfly species in that mimicry has evolved multiple times, and hybridization is common among the species and forms (J. V. Z. Brower 1958a; Mullen 2006; Porter 1989; 1990). Admiral butterflies (genus *Limenitis*) are a diverse radiation of butterflies found throughout North America. They are notable for the repeated evolution of mimicry within the genus, with mimicry having evolved at least three separate times within the radiation. The most famous mimetic relationship in *Limenitis* is between the Viceroy (*Limenitis archippus*) and the Monarch (*Danaus plexippus*), but significant attention has also been paid to mimicry between the eastern Red Spotted Purple (*Limenitis arthemis astyanax*) and the Pipevine Swallowtail (*Battus philenor*). In each case, a palatable *Limenitis* mimic resembles an unpalatable model, and gains protection from predation as a result. However, upon closer investigation, Ritland and Brower (Ritland and Brower 1991) demonstrated that the relationship between the Monarch and Viceroy is variable throughout their shared range, with the Viceroy sometimes exhibiting lower palatability than the monarch. This led to the coining of the term "quasi-Batesian" mimicry, and also points to the importance of testing mimetic hypotheses.

Less attention has been paid to the mimetic relationship between Lorquin's Admiral (*Limenitis lorquini*) and the California Sister (*Adelpha californica*). *L. lorquini* is an Admiral butterfly which is found primarily in California and the Pacific Northwest.

These two butterflies are similar in appearance to most North American limenitidine butterflies, with dark brown ground color and a single longitudinal white column or band that is colored white/cream in the central symmetry system. Unlike other related butterflies with similar color patterns however, *L. lorquini* bears on its forewing an orange apical forewing patch (AFP) which appears to mimic the wing pattern of *Adelpha californica* in the geographic areas where the two species occur. Previous studies have demonstrated both the unpalatability of *A. californica* and the relative palatability of *L. lorquini*, which suggests that *L. lorquini* is a Batesian mimic of *A. californica* (Prudic, Shapiro, and Clayton 2002). Further tentative supporting evidence, such as a delayed brood emergence time for *L. lorquini* relative *A. californica* (Shapiro 2016), which may indicate an adaptive strategy that allows predators to be educated by the model before emergence; phenotypically stable populations of *L. lorquini* and it's close Great-Basin relative, *L. weidemeyerii*, despite ongoing hybridization; and changes in the geographic width of these hybrid zones based on the presence or absence of *A. californica* further support the theory of a Batesian relationship between the two western butterfly species (Boyd et al. 1999). Simultaneously, extensive hybridization between these two groups suggests a lack of strong prezygotic barriers to gene flow and indicated relatively recent divergence. When taken together, these two qualities -- 1) Batesian mimicry, and 2) distinct yet hybridizing populations -- make *L. lorquini* an attractive study system for the effects of selection on gene flow, the species boundary continuum, and the origins and maintenance of color pattern diversity. Despite this, field tests of mimicry between these two species have never been conducted and the genomic basis of their phenotypic

divergence remains unexplored.

Therefore, the aim of the research I present here is twofold: To explore the adaptive significance of convergent evolution between *L. lorquini* and *A. californica* to test the hypothesis of Batesian mimicry between these two species.

1. To test the adaptive significance of the orange AFP by investigating the hypothesis of mimicry.
2. To identify the gene(s) or genomic region(s) that is(are) responsible for the orange AFP in *L. lorquini*.

To accomplish this, I first present the results of a field study which tests the efficacy of Batesian mimicry inside and outside the geographic range *of A. californica* using actual predators in their natural habitat. Then I test for an association between the presence or absence of the mimetic phenotype and a genomic region using restriction site associated DNA (RAD) sequencing data to create a linkage map and to perform a QTL experiment. Finally, I utilize whole-genome sequencing and high-throughput genomics to assess the relationship between genomic variation at the previously identified QTL and the orange AFP phenotype in a natural population of hybridizing *Limenitis.*

TABLE OF CONTENTS

ACKNOWLEDGMENTS iv

ABSTRACT vi

PREFACE viii

TABLE OF CONTENTS xviii

LIST OF TABLES xx

LIST OF FIGURES xxi

LIST OF ABBREVIATIONS xxii

CHAPTER ONE: 1

Introduction 1

Methods 5

Results 14

Discussion 17

CHAPTER TWO: 29

Introduction 29

Methods 34

Results 39

Discussion 43

CHAPTER THREE 62

Introduction 62
Methods 66
Results 71
Discussion 77
CONCLUSION 95
APPENDIX 96
BIBLIOGRAPHY 109
CURRICULUM VITAE 126

LIST OF TABLES

Table 1.1 Probability of Attack Relative to *J. coenia*. 28

Table 1.2 Goodness of Fit Tests for Predation Data. 28

Table 2.1 Results of the Mapping Brood Crosses. 56

Table 2.2 Number of linked SNPS used to create Linkage Groups. 57

Table 2.3 Number of Scaffolds Used to Create Linkage Groups. 57

Table 2.4 BLAST Alignment of QTL Regions 58

Table 2.5 Linkage Group Expectations Based on Synteny. 59

Table 2.6 Linkage Group/Chromosome Associtions Based on BLAST. 60

Table 2.7 Proteins Proximate to BLAST Alignments in *Heliconius*. 61

Table 3.1 GWAS Sample Collection Statistics 90

Table 3.2 Whole Genome Sequencing Results 90

Table 3.3 Filtering Parameters Used in GWAS Pipeline. 91

Table 3.4 GWAS Results in Unfiltered Dataset 92

Table 3.5 GWAS Result in Filtered Dataset. 93

Table 3.6 QTL Results Brief 94

Table 3.7 Comparison of GWAS and QTL Results. 94

LIST OF FIGURES

Figure 1.1 Geographic Range Map and Predation Study Sites. 23

Figure 1.2 Attacks on Butterfly Facsimiles 24

Figure 1.3 Variation in Mean Time in Residence of *L. lorquini* Males. 25

Figure 1.4 Variation in AFP Size Between Sites. 26

Figure 1.5 Wing Variation and Distribution in Hybrid Zones. 27

Figure 2.1 Mapping Brood Graphical Methods. 50

Figure 2.2 Variance in Mapping Brood Phenotypic Results. 51

Figure 2.3 Linkage Map of the 30 Largest Linkage Groups 52

Figure 2.4 Results of the QTL analysis on the top 15 Linkage Groups. 53

Figure 2.5 LOD Score Distribution on LG8 and LG12 54

Figure 2.6 Schematic of QTL loci BLAST alignments. 55

Figure 3.1 Geographic Range Map and Approximate GWAS Sample Localities. 86

Figure 3.2 Principal Components Analysis of Unfiltered Data. 87

Figure 3.3 Results of GWAS using Unfiltered Dataset. 88

Figure 3.4 Results of GWAS using Filtered Dataset 88

Figure 3.5 Schematic of GWAS loci BLAST alignments. 89

LIST OF ABBREVIATIONS

AFP ..... Apical Forewing Patch

bp ..... Nucleotide Base-Pair

BU ..... Boston University

BWA ..... Burrows-Wheeler Aligner

GEMMA ..... Genome-Wide Efficient Mixed-Model Association

GWAS ..... Genome-Wide Association Study

MAF ..... Minor Allele Frequency

NGS ..... Next Generation Sequencing

PCA ..... Principal Components Analysis

QTL ..... Quantitative Trait Locus

SNP ..... Single Nucleotide Polymorphism

VCF ..... Variant Call Format

CHAPTER ONE:

Testing the adaptive hypothesis of Batesian mimicry among hybridizing North American admiral butterflies

Introduction

Predator avoidance is a key adaptive requirement for most animal species. A common survival strategy is to adopt phenotypes which can serve one of three functions: 1) to reduce the number of predator-prey interactions 2) to reduce predation via warning signaling or deflection markings or 3) to dupe predators into mistaking the organism for an unpalatable species. The latter case, known as Batesian mimicry, is a classic example of adaptation in which a palatable mimic is protected from predation by resembling an unpalatable model (Bates 1862). Although lab-based experiments have provided compelling evidence that predators learn to recognize unpalatable prey based on their warning coloration (J. V. Z. Brower 1958a; Exnerová et al. 2015; Huheey 1980; Ruxton, Sherratt, and Speed 2004), and therefore avoid palatable mimics, field-based tests of Batesian mimicry theory are far less common (Finkbeiner, Briscoe, and Mullen 2017; Hetz and Slobodchikoff 1988; Howarth, Edmunds, and Gilbert 2004; Jeffords, Sternburg, and Waldbauer 1979; Rashed and Sherratt 2007; Winand et al. 1993)

Perhaps the best experimental evidence for Batesian mimicry in nature comes from studies of predation on coral snake mimics (Harper and Pfennig 2007; Kikuchi and Pfennig 2010; Pfennig, Harcombe, and Pfennig 2001; Pfennig et al. 2007). By taking advantage of geographic variation in abundance of a venomous Batesian model, Pfennig (Pfennig, Harcombe, and Pfennig 2001) demonstrated that a) predators avoid coral snake mimics where the model is common, and b) that protection from predation breaks down

outside the range of the model, and this trend is consistent across gradients from sympatry to allopatry. This frequency-dependent dynamic strongly implies that Batesian mimics should only be found in geographic sympatry with their model (Ruxton, Sherratt, and Speed 2004). Surprisingly, however, many Batesian mimics also occur in allopatry with their models (Carpenter and Ford 1933; Pfennig and Mullen 2010; Poulton 1909; Waldbauer 1988), and evidence suggests that sympatric and allopatric mimics may experience strongly divergent selection over narrow spatial scales (Harper and Pfennig 2007; Ries and Mullen 2008). Indeed, more recent findings (Pfennig, Akcali, and Kikuchi 2015) found that predator-imposed selection disfavors immigrants and non-mimetic hybrid phenotypes, leading to reproductive isolation between sympatric and allopatric populations.

Taken together with evidence from Müllerian systems that selection for mimicry leads to reproductive isolation via similarly predator-driven mechanisms (Jiggins et al. 2001; Mallet et al. 1990; Mallet and Barton 1989; Twomey, Vestergaard, and Summers 2014), these findings suggest that mimetic traits may represent "speciation phenotypes" (i.e., - traits whose divergence predictably leads to a reduction in gene flow and/or speciation) (Mullen and Shaw 2014; Shaw and Mullen 2011; 2014). However, any attempt to draw this conclusion is premature given the lack of a robust set of experimental field tests of Batesian mimicry in other systems. As noted above, Batesian mimicry theory makes three predictions that can be tested directly. First, the model must be unpalatable to a predator of both the model and the mimic (Bates 1862; Ruxton, Sherratt, and Speed 2004). Second, the unpalatability of the model should lead to reduced

predation on organisms that closely resemble it in areas where predators are educated to the model's appearance (Pfennig, Harcombe, and Pfennig 2001; Pfennig et al. 2007). Third, barring a confounding complex dynamic like sensory bias or migration of educated predators, both model recognition and mimic protection should erode outside of the usual geographic range of the model.

North American admiral butterflies (genus *Limenitis*) provide an ideal opportunity to investigate these predictions because mimicry has evolved in this lineage multiple times, and hybridization is very common among species and forms (J. V. Z. Brower 1958b; Gunder 1932; Platt and Brower 1968; Platt, Coppinger, and Brower 1971; Porter 1989; 1990; Poulton 1909). While significant attention has focused on the polytypic *Limenitis arthemis-astyanax* mimicry complex in the eastern United States (Gallant et al. 2014; Platt and Brower 1968; Platt, Coppinger, and Brower 1971; Ries and Mullen 2008; Savage and Mullen 2009), convergent evolution is also observed between *Limenitis lorquini* and *Adelpha californica* in the western U.S. (Figure 1.1). This lack of attention is surprising because of the seemingly complex relationship between *L. lorquini* and its parapatric relative *L. weidemeyerii.* The two species hybridize extensively wherever their ranges overlap but remain phenotypically distinct (Austin and Murphy 1987; Boyd et al. 1999; Porter 1990; Remington 1968). Despite this evidence for ongoing gene flow, the two species do vary in the presence or absence of a conspicuous orange patch (Apical Forewing Patch or AFP; Figure 1.1), suggesting that divergent selection for mimicry may play an important role in maintaining the species boundary between these butterfly species.

Previous studies in this system with caged jays (Corvidae) found evidence for both the unpalatability of *A. californica* and the relative palatability of *L. lorquini* (Prudic et al. 2002). The mechanism of unpalatability of *A. californica* is not well known, but is thought to be linked to sequestration of distasteful tannins from Oaks (*Quercus*), the hostplant of *A. californica* (L. P. Brower 1984; Prudic, Shapiro, and Clayton 2002). However, despite the known palatability differences between these two butterflies, rigorous field experiments have never been conducted to test the adaptive significance of convergence between *Limenitis* and *Adelpha* in a natural setting or to explore how the dynamics of interactions between predators and these two species vary as a function of the frequency of the model.

To address these issues, and to evaluate the potential role that natural selection may play in limiting gene flow between *L. lorquini* and *L. weidemeyerii*, we conducted a large-scale predation experiment using facsimile butterflies, at field sites where the putative mimic (*L. lorquini*) is sympatric (California) vs. allopatric (Idaho) with the unpalatable model (*A. californica*). Based on Batesian mimicry theory, we predicted that facsimiles resembling the putative mimic (*L. lorquini*) would receive less predation in sympatry with the model. We also estimated the longevity of the putative mimic, using mark-recapture, at two sympatric field sites varying in their relative abundance of *A. californica* to test whether protection from predation was correlated with the frequency of the putative model. Finally, we analyzed the morphology of the orange AFP in sympatric, allopatric, and hybrid zone populations to quantitatively test the hypothesis that selection for Batesian mimicry maintains convergence between *L. lorquini* and *A. californica*.

Specifically, we predicted that the range of phenotypic variance in this hypothesized mimetic trait would be higher in populations of *L. lorquini* where the model is absent and/or in areas where *L. lorquini* has historically been known to hybridize with its congener, *L. weidemeyerii*. We discuss our results in light of the ongoing hybridization between these two species, and the potential role that selection for mimicry may play in the maintenance of species boundaries in this system.

Methods

Site Selection: To study the relationship between predation rates on *Limenitis lorquini* in the presence and absence of its putative Batesian model *Adelpha californica,* we selected two geographically separate study areas in which the model and mimic are sympatric (California study area) or allopatric (Idaho study area), approximate locations of the study areas can be seen labeled in Figure 1.1. Geographic range data for each species was compiled from a combination of sources including: historical records (Boyd et al. 1999; Lepidopterist's Society 2016; Scott 1992), citizen science databases (Lotts and Naberhaus 2017), long-term monitoring data (Shapiro 2016), field guides (Brock and Kaufman 2003), and direct field observations (Kristiansen pers. obs.). *L. weidemeyerii* was used as an allopatric control for novelty in all of our experiments because it does not occur in any of the study areas we selected. Study sites were intentionally selected to reduce ecological variability by selecting sites with similar ecological and climatic variables, primarily upper-sonoran mountain canyons featuring willow trees, habitat types where both *A. californica* and *L. lorquini* are known to occur (Scott 1992).

The sympatric study area was in Northern California's Yuba Pass and in

surrounding recreational use areas (Figure 1.1, see Table S1.1 for exact GPS coordinates of sites). The Yuba pass study area was originally selected based on the extensive long-term records of A. Shapiro's group which preforms weekly transects through a nearby site at Bowman Lake Road and has established the presence of both *A. californica* and *L. lorquini* at this site. Subsequent sites in the surrounding area were selected based on the presence of suitable riparian habitat, and on the observed presence of the putative model and mimic.

The allopatric study area was in the Boise National Forest (Figure 1.1, GPS localities in Table S1.2) near Placerville and Idaho City. Site selection in Idaho was primarily based on field observations and reported geographic ranges for these butterflies (Brock and Kaufman 2003; Scott 1992). Data was also incorporated from the Butterflies and Moths of North America website (Lotts and Naberhaus 2017), which reported the presence of the relevant species in or near each of the study sites. These reports were subsequently supported by field observations before and during our field experiments (Kristiansen pers. obs.).

***Artificial Butterfly Facsimile Construction*:** Individually fabricated paper butterfly models (hereafter called "facsimiles") were used to test the hypothesis of Batesian mimicry in field predation studies. Specifically, facsimiles were constructed for four species: *A. californica* (the putative model), *L. lorquini* (the putative Batesian mimic), *Junonia coenia* (known local, palatable control), and *L. weidemeyerii* (non-local, palatable control). Facsimile construction followed Finkbeiner et al. (Finkbeiner, Briscoe,

and Mullen 2017; Finkbeiner, Briscoe, and Reed 2012) with some modification. Butterfly facsimile design was based on high resolution dorsal-view images of wild-caught butterflies in an open-winged posture, imported into Adobe® Photoshop, and adjusted for color accuracy. Images were printed onto Grade 1 Whatman filter paper sheets (#1001-931), which produces spectral reflectance similar to the brightness of actual wings (Finkbeiner, Briscoe, and Mullen 2017; Finkbeiner, Briscoe, and Reed 2012). Facsimiles were double-printed using an Epson Stylus Pro 4900 printer and UltraChrome® High Dynamic Range ink. This process involves printing the same image twice on the same sheet of paper to achieve appropriate color saturation. These double-printed sheets were then individually colored with either Crayola® brand crayons, or with Up and Up® brand colored pencils to match the spectral reflectance of specific color pattern elements, as measured by an Ocean Optics® USB2000 fiber optic spectrometer with a bifurcating cable (R400-7-UV-vis Ocean Optics, Winter Park, FL) and a deuterium-halogen tungsten light source (Model MINIDT1000-027; Analytical Instrument Systems, Flemington, NJ), with the facsimile placed on a cardboard backing material during measurements to simulate the influence on reflectance from the backing that would later be adhered to the facsimile. The spectrometer was calibrated using a spectralon white standard (WS-1-SL; Labsphere, North Sutton, NH) approximately every 5 measurements. The detection probe was held at a constant 45^{o} angle to the plane of the butterfly (or facsimile) wing in a machined probe holder (Ocean Optics RPH-1). Measurements were taken in triplicate from three facsimiles and three wild caught butterflies, resulting in nine measurements per color pattern element per species for both the facsimile and the wild caught

butterflies. These data were analyzed with R statistical software (R Core Team 2016), to assess the accuracy of the facsimiles (Figure S1.1) by calculating just noticeable differences (JND).

The JND values were determined by estimating quantum catches using the "*pavo*" package (Maia et al. 2013) in R. Quantum catches for color stimuli were estimated by using a tetrachromatic bird-vision model, following previous work (Vorobyev and Osorio 1998). Comparisons were made using the blue tit (*Cyanistes caeruleus*) cone sensitivities, which represents the UV-type avian visual system. Following the established norms (Hart et al. 2000), we used a relative cone abundance of (UV=0.37, S=0.7, M=0.99, L=1), a blue sky illuminant, and a von Kries transformation for green backgrounds. Comparisons were made at each of three possible colors on each species wing: Brown (or black), orange, and white. Note that not all the butterflies used in this study have all three colors on all four wings. JND calculations used a receptor noise model to calculate color distances from quantum catch data (Vorobyev and Osorio 1998).

Facsimiles that were determined to be accurately colored were then adhered to a Bazzil® cardstock paper backing (Color: Mocha Divine) using Krylon® High-strength Spray adhesive and allowed to dry overnight. The cardstock provides support and lends a suitably shade-darkened appearance to the ventral side of the final facsimile. Models were then individually cut out using a Brother Scan 'n Cut™ CM250 craft cutting machine and remaining excess was trimmed by hand. Individual facsimiles were sealed along the edges and across the body with clear candle wax to prevent layer separation and to increase water resistance and durability. Careful attention was paid to avoid obscuring

important color pattern elements with the wax, and facsimiles were discarded if wax penetrated these elements. Facsimiles were then threaded with a black twist-tie, and abdomens were formed over the body of the facsimile using black Newplast® brand Plasticine to allow beak marks and bite marks to be imprinted by avian predators.

Transect Arrangement and data collection: Within each study area (sympatric or allopatric), transects were composed of 100 individual sites with 20 facsimiles in each (5 of each of the four phenotypes: *A. californica* (unpalatable model)*, L. lorquini* (palatable mimic)*, J. coenia* (local palatable control)*, and L. weidemeyerii* (non-local novel control), for a total of 2,000 facsimiles per site, and a grand total of 4,000 facsimiles for the entire study. Each transect site was chosen based on available habitat, which often overlapped with the presence of the relevant butterfly species. Sites were separated on the transects by a minimum of 250m (as measured by a Garmin eTrex 10 GPS). This distance is a conservative estimate for the average home range size of potential butterfly predators in these areas, which we found to be approximately 213m (Table S1.3). The 20 models in each site were separated by approximately 2m and were attached to the nearest available branch. The haphazard perch selection favored low trees or bushes, but in some cases the facsimiles were hung on sturdy grasses or wildflowers. In all cases, care was taken to hang the facsimiles in a natural position, ordinarily with the dorsal side presented as with territorial and basking postures in the Limenitidini (Ledersouse 1993; Rosenberg and Enquist 1991; Willmott 2003).

Facsimiles were checked once during each 24-hour period over the course of 96

hours (four days) and repaired or replaced if attacked. The experiment was restricted to a four-day period in response to previous experiments of this type where predator learning affected the results after a few days of exposure to the facsimiles (Finkbeiner et al. 2012, 2017). When checked, facsimiles were visually inspected for signs of bird predation on the bodies or the wings and individual marks were photographed and recorded; because of the potential for ambiguity, attacks were photographed and evaluated by two researchers in the field, and then subsequently re-checked and permanently assigned to category based on the characteristics of the imprint left in the plasticine clay (bird attack/not bird attack/not attacked) using the field images (see Figure S1.2). Several different kinds of marks were observed during this study, including marks from birds, ants, grasshoppers, and rodents (Figure S1.2); only marks that could be described as "bird-like" were counted in the final data set. "Bird like" attacks resemble triangular bite marks or occasionally jagged puncture marks, whereas attacks from other animals reflect their particular anatomy. Note that in Idaho we observed several (n=7) bite marks that appeared to be from a rodent, leaving two rounded tooth marks in the clay bodies of the facsimiles (Figure S1.2 Panel B); these bites were occasionally difficult to distinguish from bird attacks when the damage to the body was extensive, so to be conservative any facsimiles that had rounded marks of any kind were counted as "not bird attack". Multiple bite marks on the same facsimile between days occurred only five times during the study and were counted as independent attacks.

Statistical Analysis: We used Maximum Likelihood to estimate probabilities that predators would attack each of the facsimile phenotypes (*A. californica* – putative model, *L. lorquini* – putative mimic, and *L. weidemeyerii* – novelty control) relative to the control species *J. coenia*, at each of the two geographic field locations. Attack probabilities (X_A) and their support limits were estimated using the technique described by Edwards (Edwards 1972). This technique estimates the probability ($Q_{A\,i\times ju}$) that avian predators in each site would attack a facsimile of type i relative to that of the *Junonia* control facsimile ju, by setting the attack rate on ju as a theoretical maximum such that $Q_{A\,i} = (X_{A\,i} / (X_{A\,ju} + X_{A\,i}))$. Thus, for predation between *Junonia* controls versus other species i facsimiles, the actual probabilities are $Q_{A\,i\times ju}/(Q_{A\,i\times ju} + 1)$ that predators attack i and $1/(Q_{A\,i\times ju} + 1)$ that they attack ju. The $\log_e$ likelihood for the experiment is:

$$\Sigma[X_{A\,i} * \log_e\{Q_{A\,i\times ju}/(Q_{A\,i\times ju} + 1)\} + X_{A\,ju} * \log_e\{1/(Q_{A\,i\times ju} + 1)\}]$$

where $X_{A\,i}$ is the number of attacks on species *i* and $X_{A\,ju}$ is the number of attacks on *Junonia coenia* models. A *G*-test was used to compare the $\log_e$ likelihood values between species comparisons, and the resulting *p*-values were adjusted by applying a Bonferroni correction to guard against false positives from multiple comparisons. Support limits, asymptotically equivalent to 95% confidence intervals (Edwards 1972), were estimated for each comparison by searching for values that decreased the $\log_e$ likelihood by two units, similar to similar work in the field searching for values that decreased the $\log_e$ likelihood by two units (Jiggins, Estrada, and Rodrigues 2004; Willmott et al. 2017)

Mark-recapture: Mark-recapture methods were used to estimate the average number of days in residence for *L. lorquini* and *A. californica* at two additional field sites in California with different relative frequencies of model and mimic, but within the geographic range of the model and mimic. These data are a second line of evidence evaluating the effectiveness of Batesian mimicry in given populations. The first location was at the Lodi Lake nature area in Lodi (San Joaquin Co., N038.14937, W121.29089, 20m elev.). The second location was Camp Ohlone Regional Park (Alameda Co., N037.48941, W121.74574, 382m elev.). Butterflies were collected with aerial nets or with bait traps. Trapping success varies based on species and bait type but has low overall success in our temperate-zone studies. The vast majority of captures is accomplished via hand-netting. Sampling occurred at both sites between late May and late August between 9:00 am and 5:00 pm at both locations; these dates overlap with the duration of the facsimile study. Transects were established between trap locations and traps were placed to sample equally among available habitats. In Lodi Lake, understory and canopy traps were baited with rotten-banana bait at each of 15 trap locations. Mean height of Lodi canopy traps was 6.1m (s.d. = 1.3) and understory was 1.1m (s.d. = 0.2). In Camp Ohlone there were a total of 32 trap locations, 16 rotten-banana baited traps were alternated with 16 rotten-shrimp traps, to attempt to compensate for very low trapping success with banana-baited traps. Canopy and understory traps were present at each location. Mean height of Camp Ohlone canopy traps was 9.4m (s.d. = 2.4m) and understory was 1.0m (s.d. = 0.3m). Bait was placed in the traps the first morning of each sampling week, shrimp bait was replaced every other day, and both bait types were supplemented as

necessary to keep bait moist. Bait was removed the last day each week. Butterflies were identified to species and sex and given a unique number with Sharpie™ brand fine-point marker on the base of ventral hindwing.

Estimates of residence time were obtained from recapture decay plots (Watt et al. 1977). The natural logarithm of all individuals recaptured days (d) or longer was plotted against the days in residence. Days in residence is defined as the number of days between recaptures, including the first day of capture (i.e., an individual captured and recaptured on the same day had an observed residence time of one day). The slope of the regression line is the natural logarithm of the daily residence rate, from which the average residence time was computed.

Assessing mimetic resemblance*:* To indirectly test the prediction that selection for mimetic traits should be relaxed in allopatry, wing measurements of the orange apical forewing patch (AFP) on *L. lorquini* were made for individuals sampled both in sympatry (California; n=7) and allopatry (Idaho; n=7) with the presumed model (*A. californica*). The size of the orange AFP was measured using a caliper across vein M1, from the marginal border of the wing to the most medial border of orange scales. This measurement is reported in ratio to wing size as measured from apical tip to base of attachment. Finally, to place these measurements within the broader context of natural variation observed for this species, we also included individuals (n=41) sampled from several sites within the "Humboldt" hybrid zone (Pine Forest range, NV; Santa Rosa Range, NV) between *L. lorquini* and *L. weidemeyerii* in the western Great Basin (Boyd et

al. 1999). ANOVA and subsequent Tukey post-hoc tests between sites were performed in R.

Results

Facsimile Construction: Just Noticeable Difference (JND) calculations for most facsimile-butterfly pairs and most colors indicated little-to-no discriminability with scores below the threshold value of one (1) JND. Most JND scores for color matching of A. californica (Orange: 1.04, White: 1.48, Brown: 0.71), L. lorquini (Orange: 0.46, White: 0.95, Brown: 0.46), L. weidemeyerii (White: 5.04, Brown: 0.62), and J. coenia (Orange: 0.49, White: 0.53, Brown: 0.59), indicate a good match. The exceptions are A. californica orange (1.04) and white (1.48), and L. weidemeyerii white (5.04).

Predation Experiments: Predation rates across both study areas were significantly lower than expected compared to similar experiments (Finkbeiner, Briscoe, and Mullen 2017). Using 2,000 facsimiles per study area (500 of each phenotype), we recorded 33 (1.65% attacked) bird attacks in California, and 56 attacks (~2.8% attacked) in Idaho. In California, the palatable control (*J. coenia*) facsimile received the most predation (13 of 33 attacks, ~39.4% of attacks), followed by the non-local, novel control (*L. weidemeyerii,* 10 of 34, ~30.0% of attacks), the putative Batesian mimic (*L. lorquini*, 6 of 33, ~18.2% of attacks), and finally the putative Batesian model (*A. californica,* 4 of 33, ~12.1% of attacks). In Idaho, the non-local control facsimile (*L. weidemeyerii*) was subject to the most predation (16 of 56, ~28.6% of attacks), palatable control (*J. coenia*) facsimile and the putative mimic (*L. lorquini*) facsimile received the same number of attacks (15 of 56, ~26.8% of attacks), and finally the putative Batesian model (*A. californica*) was attacked

the least (10 of 56, ~17.9% of attacks, Figure 1.2).

Attack probabilities, calculated as $Q_{A\,i} = (X_{A\,i} / (X_{A\,ju} + X_{A\,i}))$, and their support limits are presented in Table 1. In California, the probabilities of avian predators attacking *A. californica*, *L. lorquini*, and *L. weidemeyerii* butterfly facsimiles (relative to the control facsimile) were 0.24, 0.32, and 0.43, respectively. The attack rate on *A. californica* was significantly lower than *L. weidemeyerii* (G = 12.94 d.f. = 1, corrected p < 0.01), and also lower on *L. lorquini* than on *L. weidemeyerii* (G = 7.79, d.f. = 1, corrected $p = 0.047$). We did not find a significant difference in the $\log_e$ likelihood values between predator preference to attack *L. lorquini* and *A. californica* (G = 5.15, d.f. = 1, corrected $p = 0.21$).

In contrast, at our Idaho field location attack probabilities on *A. californica*, *L. lorquini*, and *L. weidemeyerii* (relative to the control facsimile), were 0.4, 0.5, and 0.52, respectively (Table 1). Although *L. lorquini* did not experience differences in relative attack probabilities from *L. weidemeyerii* (G = 1.35, d.f. = 1, corrected p = 0.73), we found that *A. californica* had a lower likelihood of attack than *L. lorquini* (G = 7.94, d.f. = 1, corrected p = 0.044) and *L. weidemeyerii* (G = 11.45, d.f. = 1, corrected p < 0.01). Comparisons of attack probabilities for the same phenotypes between Idaho and California indicated that all three experimental species: *L. weidemeyerii*, *L. lorquini*, and *A. californica* had a significantly higher relative risk of attack in Idaho than in California. *L. weidemeyerii* had a significantly higher risk of predation in Idaho than California (G = 11.451, d.f. = 1, corrected p < 0.01), as did *L. lorquini* (G = 17.890, d.f. = 1, $p < 0.01$), and *A. californica* (G = 15.10, d.f. = 1, corrected $p < 0.01$).

Survival, longevity, and mimetic resemblance: The relative frequency of the putative Batesian model to its presumptive mimic was found to have a statistically significant effect on longevity. We found that the average longevity of these recaptured individuals of the putative mimic species (*L. lorquini*) at the Camp Ohlone site, where the frequency of *A. californica* was relatively high (~80% of captures of the two species, 98 *L. lorquini* males captured/45 recaptured), had a significantly larger number of days in residence – 12.30 days (95% CI: 11.29-13.51) vs. 8.56 days (95% CI: 7.97-9.24)– than those found at the Lodi Lake site (~4% of captures *A. californica*, 117 *L. lorquini* males captured/48 recaptured) where *A. californica* is at a much lower frequency (Figure 1.3). In addition, an ANOVA comparing the size of the *L. lorquini* orange apical forewing patch (AFP) between different field sites (i.e., – sympatric with *A. californica*, allopatric with *A. californica*, or from the "Humboldt" hybrid zone, Figure 1.4) found a significant relationship between site type and AFP size ($F_{(2, 52)} = 8.5$, $p < 0.001$, Figure 1.5). Post hoc comparisons using the Tukey HSD test indicated a significant difference between the mean score for the hybrid (n=41)-sympatric (n=7) comparison, the sympatric-allopatric (n=7) comparison, but not for the allopatric-hybrid comparison ($p = 0.64$). In these comparisons, sympatric individuals had higher scores (indicating larger AFP-to-wing length ratios) than both hybrids ($p < 0.001$) and allopatric individuals ($p < 0.001$).

Reflectance spectra of the orange pigmentation are remarkably similar when compared between *A. californica* and *L. lorquini* (Figure S1.1), though *A. californica* has slightly more brightness in the blue to blue-green range (~400-500nm) and in the red range (~650nm). The mimetic species white bands are also quite similar, in contrast to

the white band of *L. weidemeyerii*, which had higher brightness overall and also reflects UV (Figure S1.1).

Discussion

The results of our predation and mark-recapture experiments, in combination with morphological data, strongly support the hypothesis that the phenotypic convergence between *A. californica* and *L.s lorquini* in areas of geographic overlap reflects predator-mediated natural selection for Batesian mimicry despite ongoing gene flow. Consistent with prior lab-based studies of avian predation (Prudic, Shapiro, and Clayton 2002), we found that *A. californica* and *L. lorquini* facsimiles experienced significantly fewer attacks in our study area in California, where both are common, relative to both the known palatable control (*Junonia coenia*), and a second, unknown novel control (*L. weidemeyerii*) (Figure 1.2, Table 1.2) than in our study area in Idaho where *A. californica* is absent. Since the protective benefit of effective mimicry is not extended to the same degree to facsimiles that resemble the model in other ways, as is the case with the *L. weidemeyerii* facsimiles, we can infer that the AFP is acting as a warning signal, and that bearing the mimetic phenotype is advantageous only when the model (*A. californica*) is present. This pattern is consistent with Batesian mimicry theory and with our prediction of differential attack rates based on Batesian model presence and confirms that *L. lorquini* is indeed a Batesian mimic of *A. californica.*

Our finding that predators did not avoid facsimiles of novel *L. weidemeyerii* to the same degree as palatable *L. lorquini* is interesting for three reasons. First, with the caveat that the facsimiles are stationary unlike live butterflies, this finding is not consistent with

either theories of predator avoidance of novel prey (e.g., diet conservatism or neophobia; (Lindström et al. 1999; Marples, Roper, and Harper 1998)) or disruptive coloration (Cott 1940; Cuthill et al. 2005; Seymoure and Aiello 2015; Silberglied, Aiello, and Windsor 1980). Second, because both species of *Limenitis* (*L. lorquini* and *L. weidemeyerii*) and *A. californica* used in this experiment possess similar transverse white medial bands, it suggests that predators primarily rely on the bright orange apical forewing patch (AFP) as the signal to discriminate between potentially palatable and unpalatable prey; chromatic elements (such as orange and red) in aposematic prey are more reliable as aposematic signals than achromatic elements (such as white), because white spectral reflectance is less consistent under variable light environments (Dell'Aglio, Stevens, and Jiggins 2016). Finally, because there is some variation in attack rates on *L. weidemeyerii* between sites, it is possible that the white medial band also has a role in predator avoidance. However, the white bands of *L. weidemeyerii* have very different reflectance profiles relative to *A. californica* and *L. lorquini* (Figure S1.2), suggesting that mimicry between these two species might also extend to their white coloration (Finkbeiner, Briscoe, and Mullen 2017), while the white band of *L. weidemeyerii* is maintained by other potential mechanisms (e.g., -mate recognition). Further work will be necessary to test this hypothesis because 1) the color accuracy of the white bands of *L. weidemeyerii* facsimiles proved difficult to reproduce, and 2) our support limit calculations suggest that larger sample sizes will be necessary to more accurately assess predation risk across all comparisons.

The results from our second experiment in allopatry demonstrate that protection

from predation for the mimic, *L. lorquini*, breaks down outside of the geographic range of its model, *A. californica*; which supports our predictions. Although there were differences in the absolute number of attacks among the four facsimile types, there was no significant differences in the probability of attack between the mimetic species, *L. lorquini,* or the novel control, *L. weidemeyerii,* relative to the palatable control, *J. coenia*. Surprisingly, however, facsimiles of the Batesian model, *A. californica*, experienced less predation than either *Limenitis* species, in relation to *Junonia*, despite the fact that the experiment was conducted several hundred miles outside the known geographic range of the model. Predator avoidance of the model in geographic regions where it does not occur might be explained by a variety of mechanisms (Pfennig and Mullen 2010), including: a) prior predator experience with the warning signal (AFP) within the geographic range of the model followed by predator migration, b) recent range contraction by the model, or c) biases in predator cognition such as innate avoidance (Coppinger 1970; Exnerová et al. 2015). However, further work will need to be done to differentiate among these possible explanations.

The hypothesis of Batesian mimicry is further supported by the results of our mark-recapture study, which shows that *L. lorquini* individuals have significantly longer residence times where *A. californica* is abundant relative to a site where it is rare (Figure 1.3). This frequency-dependent dynamic implies that individuals bearing a mimetic phenotype directly gain a longevity benefit when the cost of learning to discriminate the model and mimic is high, as when the unpalatable model is common relative to the mimic, which provides strong evidence for Batesian mimicry (Pfennig, Harcombe, and

Pfennig 2001; Ries and Mullen 2008).

Given this pattern of frequency-dependence in sympatry, the persistence of the *L. lorquini* orange apical forewing patch (AFP) coloration in the absence of the model would at first appear to be paradoxical (Pfennig and Mullen 2010; Ruxton, Sherratt, and Speed 2004). However, recent work suggests that the degree of spatial and temporal concordance between models and mimics may fluctuate more over ecological time than evolutionary time (Rabosky 2016). Therefore, the persistence of AFP coloration in allopatric *L. lorquini* populations may simply reflect an evolutionary lag between processes acting on contemporary vs. historical populations. This possibility is also supported by our data indicating that the accuracy of the mimicry varies significantly across the geographic distribution of *L. lorquini* (Figure 1.4, Figure 1.5). Specifically, we found that *L. lorquini* in allopatry had significantly smaller AFPs than those found in sympatry with the model (which had larger AFP's and very little variability), implying a possible selective disadvantage to bearing the AFP phenotype outside of the range of *A. californica* (Figure 1.5). If so, the persistence of the AFP in these areas may be due to other selective forces, such as sexual selection.

Hybrid Zone Dynamics: Although our primary goal was to investigate the adaptive significance of the convergent resemblance between *A. californica* and *L. lorquini* in this study, a secondary objective was to assess how selection and introgression interact across the phenotypic hybrid zone between *L. lorquini* and *L. weidemeyerii,* and to evaluate the potential role of Batesian mimicry in maintaining species boundaries. Previous genetic work suggests that there is significant gene flow between *L. lorquini* and *L. weidemeyerii*

(Porter 1990), which is corroborated by our observation of extensive phenotypic variation in the size and extent of the *L. lorquini* orange AFP for individuals sampled from hybrid populations relative to individuals sampled at our experimental sites (California and Idaho) where *L. weidemeyerii* is absent (Figure 1.5).

Interestingly, the geographic structure of the interactions between *L. lorquini* and *L. weidemeyerii* differ between the two hybrid zones (Boyd et al. 1999). Phenotypes abruptly transition across the southern hybrid zone (e.g., –the "Mono Lake" hybrid zone, see Figure 1.4 Panel B), which occurs in close proximity to the presence of the model. In contrast, in the upper Great Basin (e.g., – the "Humboldt" hybrid zone in western Nevada, Figure 1.4 panel B) the phenotypic transition between parental populations of *L. weidemeyerii* and *L. lorquini*, which occurs in the absence of the model, encompasses a larger physical distance, and hybrid populations show evidence of extensive mixing consistent with the formation of highly localized hybrid swarms (Boyd et al. 1999). Although geography likely leads to stronger physical isolation of parental populations and hybrid populations in the Humboldt hybrid zone, the persistence of large hybrid populations with large phenotypic variance suggests that selection for mimicry in this region is either relaxed due to the absence of the model or that selection is acting against the conspicuousness of the AFP. This latter conclusion is supported by well-known phenotypic data (Boyd et al. 1999), which indicates that there is an overall phenotypic bias in the Humboldt hybrid zone away from the *L. lorquini* phenotype.

While more work will be needed to definitively demonstrate that selection for mimicry maintains the species boundary between *L. lorquini* and *L. weidemeyerii*, the

sharper phenotypic clines observed near Mono Lake suggest a novel finding: that the relative geographic proximity of unpalatable *A. californica* (See Figure 1.1) results in stronger predator-mediated selection against introgression of non-mimetic wing pattern characters between these two species. This conclusion is supported by the observed bimodal distribution of phenotypes across the Mono lake hybrid zone, and the relative absence of phenotypic evidence for F1 hybrid females (Figure 1.4). Taken together with the results of our predation and mark-recapture studies, these findings suggest that selection for mimicry near Mono Lake results in a "tension" zone (Barton and Hewitt 1989) between these two hybridizing species that is maintained by a balance of dispersal from parental populations and selection against hybrid offspring.

Figures and Tables

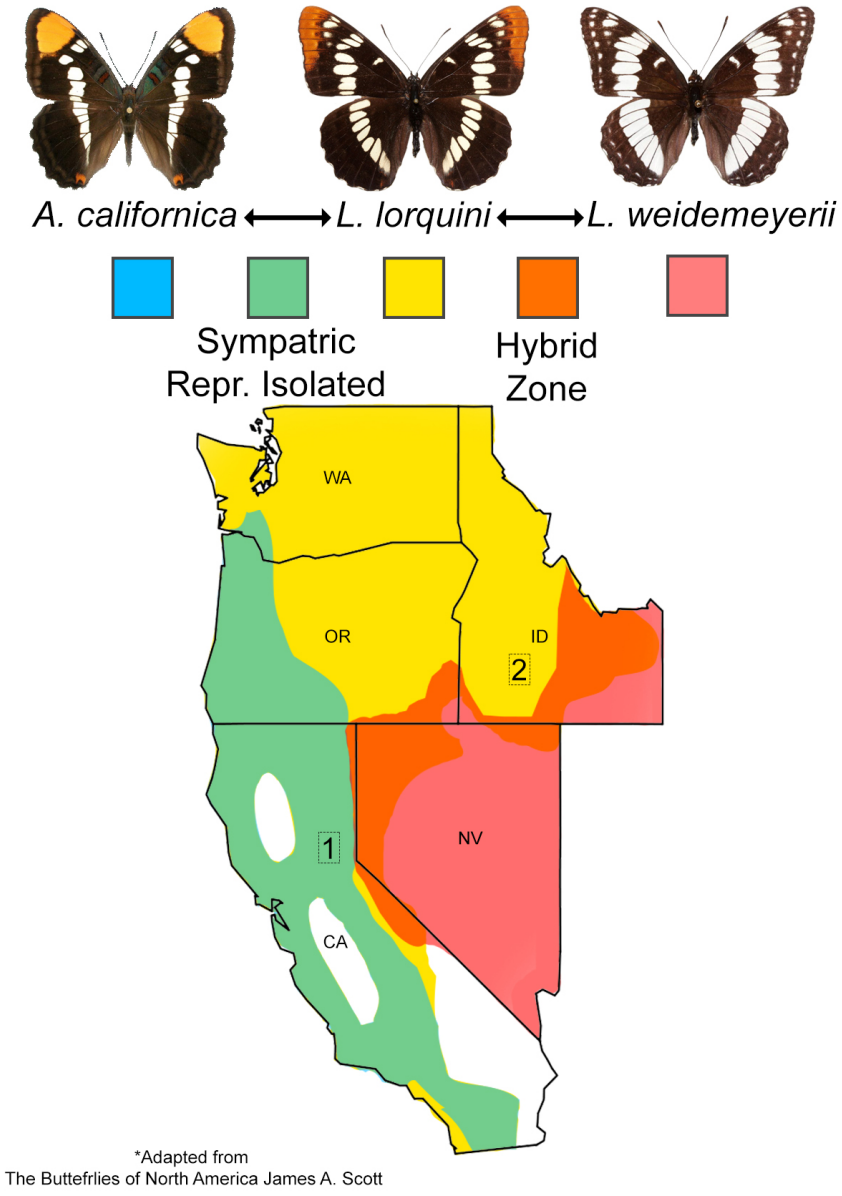

Figure 1.1 Approximate geographic ranges of the species of interest adapted from Scott (1992). The boxed numbers represent approximate locations of each study area for the facsimile experiments. Note that the range of *A. californica* is represented by blue but is sympatric *with L. lorquini* (yellow) throughout its entire range, so it is represented green.

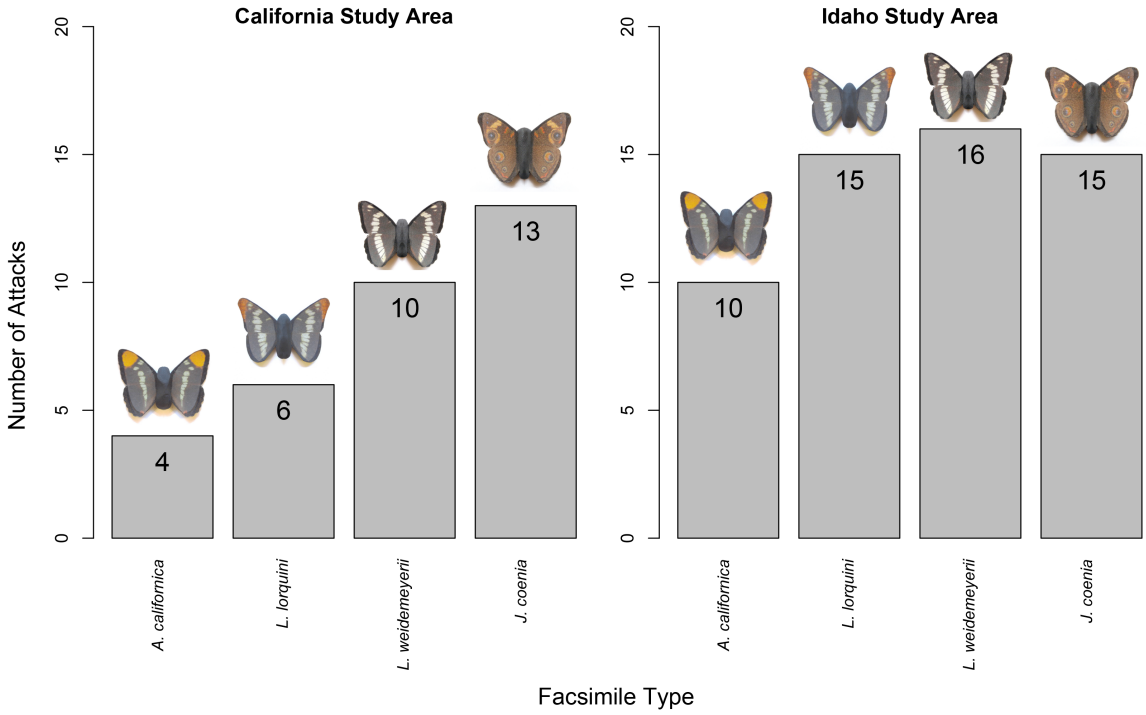

Figure 1.2 Number of attacks on each facsimile type in each field location. Each bar represents the cumulative number of attacks on each facsimile type. *A. californica* is the putative Batesian model, L. lorquini is the putative Batesian mimic (Prudic 2002). L. weidemeyerii was included as a "non-local control", meaning that predators should treat it as novel prey, similar to the control. Finally, J. coenia was included as a known palatable control. See Table 1 for probabilities and support limits, and Table 2 for G-tests and p-values.

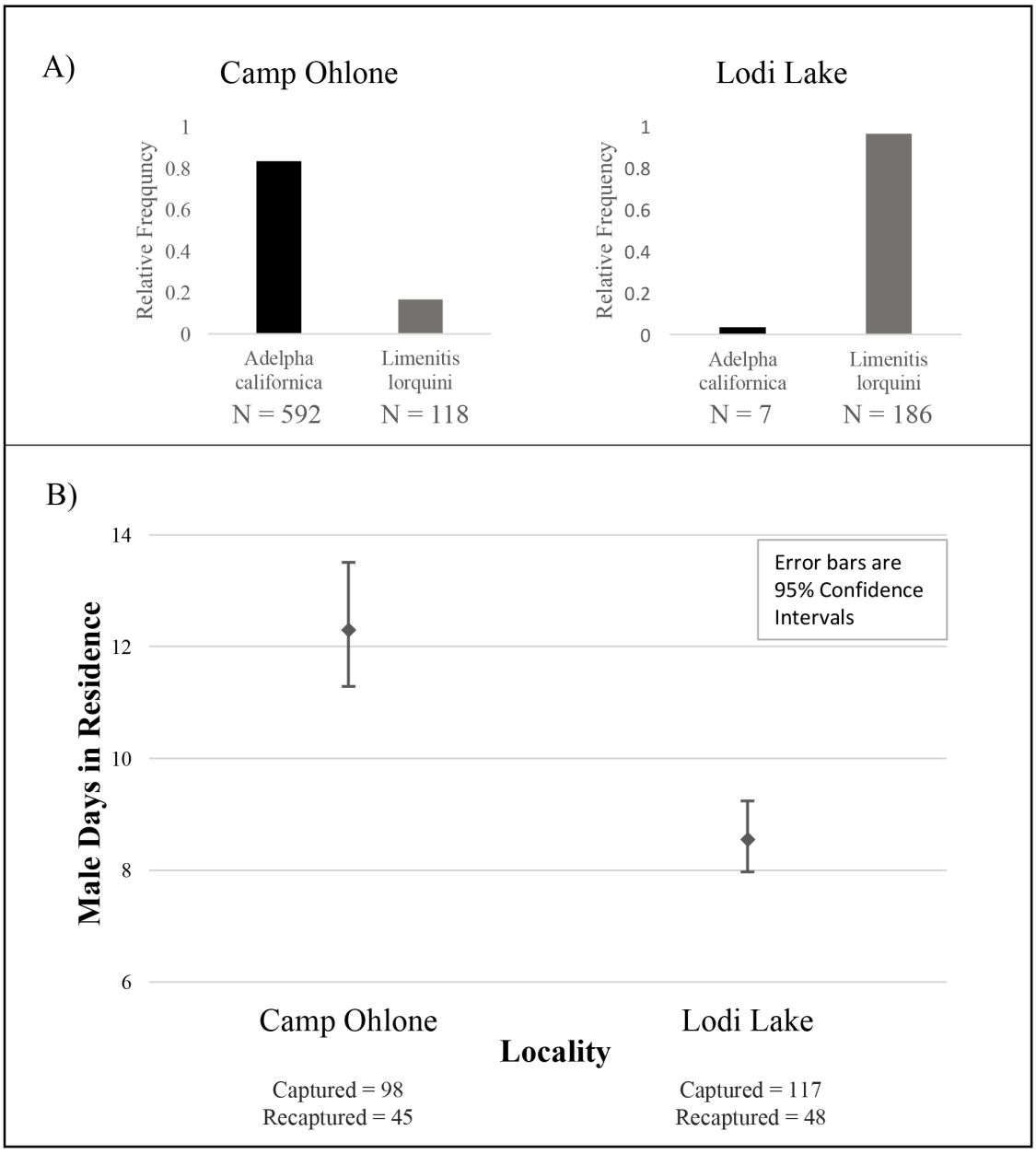

Figure 1.3 Mean time in residence as a function of model presence. A) the relative frequency of all *A. californica* and *L. lorquini* individuals encountered during the study are shown. The Camp Ohlone site has relatively high *A. californica* abundance, whereas Lodi Lake has relatively low *A. californica* abundance. B) The difference in mean residence time of *L. lorquini* males within each of these sites. Females were excluded from this analysis because of low capture rates. Error bars shown are 95% confidence intervals.

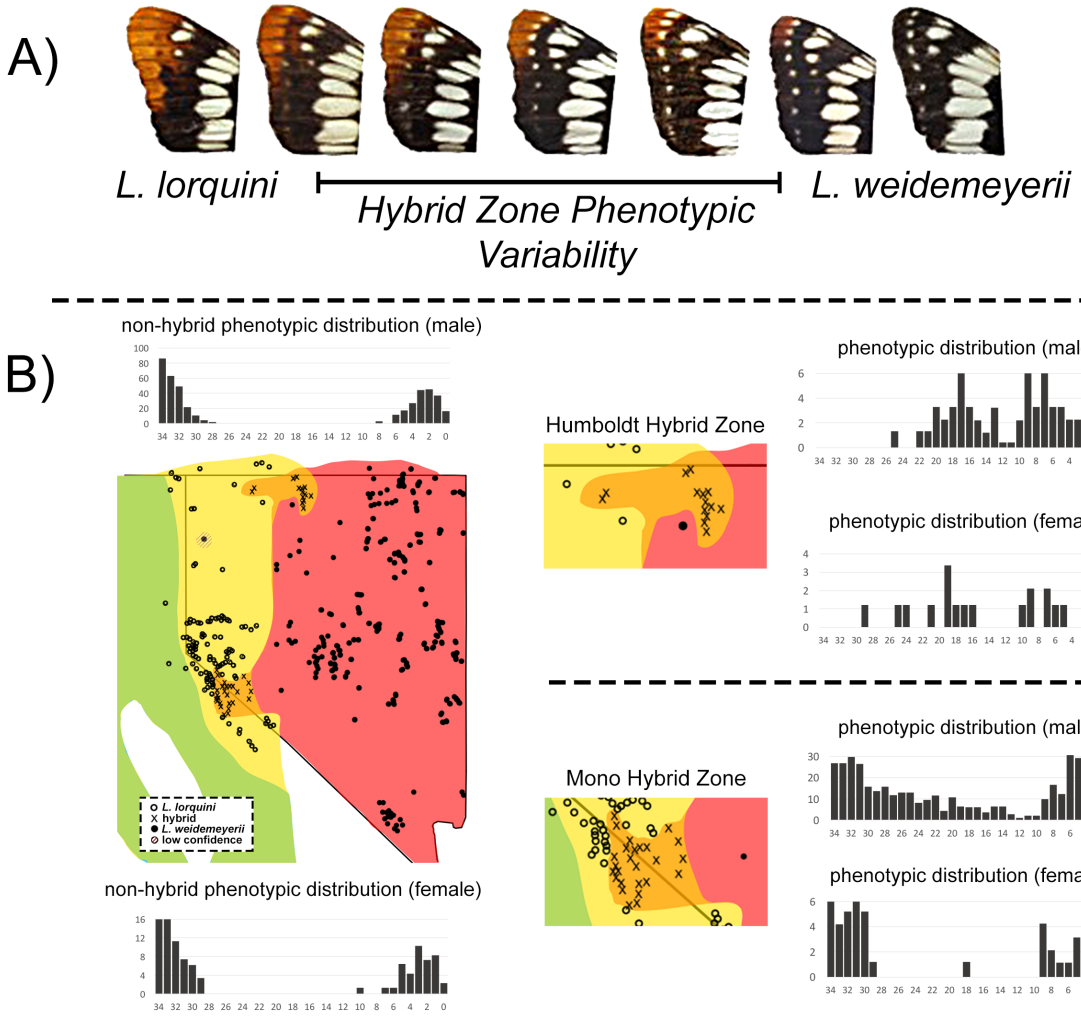

Figure 1.4 A) Panel A represents the extent of phenotypic variability in orange AFP at sample localities across the range of *L. lorquini* and *L. weidemeyerii* in the pictured states, including the hybrid zone (shown in orange). B) Panel B is a more detailed version of the map in Figure 1 to present the differential phenotypic distribution histograms at sample localities as reported in Boyd et al. (1999). The X-axes have been flipped (relative to Boyd et al. 1999) to reflect how phenotype changes with geography (West-to-East), with a value of 34 indicating *L. lorquini*-like, on the left, and 0 indicating *L. weidemeyerii*-like, on the right.

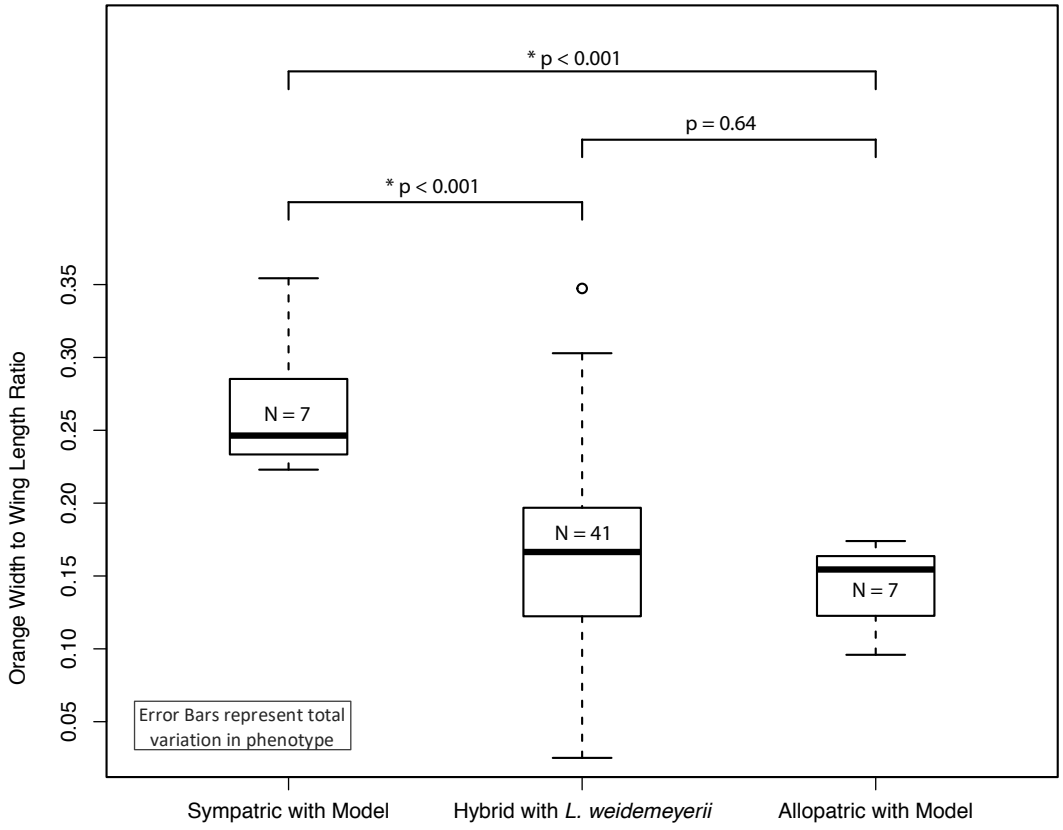

Figure 1.5 Variation in AFP size of *L. lorquini* associated with model presence. *L. lorquini* orange AFP differs significantly by locality (ANOVA $p < 0.001$). Tukey post-hoc tests indicate *L. lorquini* AFP is significantly larger in sympatry with the model compared to in the hybrid zone ($p < 0.001$), or in allopatry with the model ($p < 0.001$). Allopatric and hybrid populations did not differ ($p = 0.64$). Asterisks indicate a significant comparison of $p < 0.05$.

Table 1.1 Probability of attack relative to *J. coenia*. Parenthetical numbers are upper and lower support limits, equivalent to 95% confidence intervals.

Probability of attack relative to *J. coenia*	*A. californica*	*L. lorquini*	*L. weidemeyerii*
California Site	0.24 (0.08, 0.47)	0.32 (0.14, 0.54)	0.43 (0.24, 0.64)
Idaho Site	0.40 (0.22, 0.60)	0.5 (0.32, 0.68)	0.52 (0.34, 0.69)

Table 1.2 G-test for goodness of fit between attack rate comparisons. Each row is a comparison between the attack rates on two different butterfly facsimiles relative to the attack rate on *J. coenia*. In the last column, p-values have been adjusted using a Bonferroni correction for multiple comparisons**.**

	Comparison	G-score	p-value	Corrected p-value
California Comparisons	L. weid/A. calif (CA)	12.94	<0.001	0.003
	L. lorq/A. calif (CA)	5.15	0.023	0.209
	L. weid/L. lorq (CA)	7.79	0.005	0.047
Idaho Comparisons	L. weid/A. calif (ID)	9.29	0.002	0.021
	L. lorq/A. calif (ID)	7.94	0.005	0.044
	L. weid/L. lorq (ID)	1.35	0.245	0.730
Between-Site Comparisons	L. weid CA vs. ID	11.45	0.001	<0.001
	L. lorq CA vs. ID	17.89	<0.001	<0.001
	A. calif CA vs ID	15.10	<0.001	0.001

CHAPTER TWO:

Identifying the genomic basis of color pattern adaptation in *Limenitis lorquini*

Introduction

Understanding the mechanistic basis of the origin and maintenance of adaptive phenotypic diversity is a central goal of evolutionary biology. Mimetic phenotypes, convergent traits which reduce predation pressure on one or more individuals, are classic examples of adaptation because the individuals gain a direct and measurable benefit from bearing these traits when compared with individuals that do not (Bates 1862; Joron and Mallet 1998; Kapan 2001; 2001; Malcolm 1990; Mallet and Joron 1999; Pfennig, Harcombe, and Pfennig 2001; Pfennig and Mullen 2010; Ruxton, Sherratt, and Speed 2004; Speed and Turner 1999; J. R. G. Turner 1987; Vane-Wright 1980). This benefit predictably leads to differential success, sometimes through mechanisms like assortative mating, to restricted gene flow between wing-pattern races, and ultimately may lead to speciation (Jiggins and McMillan 1997; Jiggins et al. 2001; Mallet and Barton 1989; Naisbit, Jiggins, and Mallet 2003; Naisbit 2001; Pfennig, Akcali, and Kikuchi 2015). Therefore, understanding the genetic basis for these traits, sometimes called speciation phenotypes (Mullen and Shaw 2014; Shaw and Mullen 2011), is a key step in understanding the processes involved in the diversification of species.

Butterflies have long been used as model systems to study the relationship between coloration and selection. The reasons for this are manifold, but the most compelling is that the patterns of coloration on butterfly wings are conspicuous targets of multiple types of selection. Both predator mediated selection and sexual selection

influence the fitness consequences butterfly color patterns (J. V. Z. Brower 1958a; Mallet and Barton 1989; Mallet and Joron 1999; Ruxton, Sherratt, and Speed 2004). In addition, wing color patterns have physiological implications for fitness, such as heat retention, which is modulated by developmentally controlled phenotypic plasticity in some species (Nijhout 2001). These multiple processes contribute to an enormous diversity of conspicuous color patterns in butterflies, which combined with variation in the opportunities different species have to sequester host plant secondary compounds as a predator defense, has made interspecific mimicry a common phenomenon among butterflies. In fact, the evolution of wing pattern diversity in butterflies continues to be an important model system for evolutionary and developmental genetics, and speciation (Brakefield and French 1999; Gallant et al. 2014; Kunte et al. 2014; Martin et al. 2012; McMillan, Monteiro, and Kapan 2002; Reed et al. 2011; Reed and Serfas 2004).

Because selection acts on phenotypes that are determined by the underlying genomes, understanding the genetic and genomic basis of color pattern variation is critical to understanding the evolutionary processes responsible for the origin and maintenance of diversity. Several studies in the last decade have pursued using butterflies as a model system to explore the genetic and genomic basis of color pattern. This has led to the identification of many underlying the color pattern variation involved in mimicry, sexual selection, and speciation (Jiggins, Wallbank, and Hanly 2017). Based on these studies, it is clear that wing patterns in most butterflies have evolved through changes in, or changes in the regulation of, a small number of highly conserved genes even across very deep taxonomic history (Gallant et al. 2014; Martin and Orgogozo 2013; Martin et

al. 2012; Martin and Reed 2014; Papa, Martin, and Reed 2008); and even when the variation is in structural color rather than pigmentation (Thayer 2019). However, the bulk of our understanding of the genetic basis of adaptive phenotypic diversity is currently limited to a very small number of species emerging or established model species within *Heliconius, Manduca, Bombyx,* and *Papilio* (Kronforst and Papa 2015). Exploring the potentially divergent mechanisms underlying color pattern variation in a wider variety of organisms will lead to a better understanding of the evolutionary processes underlying the origins of novel and adaptive phenotypes.

Admiral butterflies in the genus *Limenitis* are an excellent system for examining questions related to the genomic basis of adaptation, specifically as it relates to the evolution of wing color patterns. Butterflies in the genus *Limenitis* have evolved mimetic phenotypes multiple times but have failed to evolve complete reproductive isolation (Fisher and Bennett 1930; Gunder 1932; Platt and Brower 1968; Porter 1989; 1990; Poulton 1909; Remington 1968). Historical studies of mimicry in *Limenitis* have been influential in the evolutionary literature, experimentally demonstrating the adaptive significance of mimicry (J. V. Z. Brower 1958a), contributing to the debate on species boundaries (Fisher and Bennett 1930; Mullen 2006; Mullen, Dopman, and Harrison 2008; Platt and Brower 1968; Remington 1968) and most recently contributing significantly to the literature on paradoxical imperfect mimicry (Ebel et al. 2015; Finkbeiner, Briscoe, and Mullen 2017; Finkbeiner et al. 2018; Kristiansen et al. 2018; Mullen et al. 2011).

There are three major mimetic relationships between *Limentis* and toxic model

species. The first, and most well-known, is between the Viceroy butterfly (*Limenitis archippus*) and the Monarch butterfly (*Danaus plexippus*). Mimicry between these two butterflies is well-studied, represents one of the first demonstrated examples of the "palatability spectrum" (Ritland and Brower 1991), and has been termed "quasi-Batesian" (Speed 1993) due to the high degree of variance in the relative palatability of these two butterflies throughout the full extent of their distribution. The second mimetic relationship in *Limenitis* is found in the *L. arthemis* species complex in the southeastern and southwestern United states. The subspecies of *L. arthemis* (*L. arthemis astyanax, L. arthemis arizonensis,* and *L. arthemis arthemis*) maintain two distinct phenotypes, one of which is considered to mimic the Pipevine Swallowtail (*Battus philenor*) (Platt, Coppinger, and Brower 1971). Despite their phenotypic differences between mimetic (*L. arthemis astyanax, L. arthemis arizonensis*) and non-mimetic (*L. arthemis arthemis*) the subspecies are interfertile, and the two northeastern subspecies (*L. arthemis astyanax, L. arthemis arthemis*) hybridize freely in a broad hybrid zone across much of the northeastern United States. Both of these examples of mimicry in *Limenitis* involve significant changes to the wing color pattern, which, as is fairly common in other butterfly species like *Heliconius* (Kronforst and Papa 2015), are the result of changes associated with as few as one color patterning gene, in this case *WntA* (Gallant et al. 2014; Martin and Reed 2014; Mazo-Vargas et al. 2017). The genetic basis of mimetic convergence remains unexplored in the third example of mimicry in the North American *Limenitis*, the apparent mimicry of the California Sister (*Adelpha californica*) by the Lorquin's Admiral (*L. lorquini*).

L. lorquini has long been thought to be a Batesian mimic of *A. californica*, which is a species of *Adelpha* butterfly found in California (Butler 1865). This inference has historically been supported by their similar appearance, broad overlap in range, and the existence of a *L. weidemeyerii,* a non-mimetic sister-species (Ebel et al. 2015; Mullen et al. 2011) to *L. lorquini* that can be found outside of the range of *L. weidemeyerii* (see Figure 1.1). Further evidence has been provided by palatability experiments demonstrating that naive Western Scrub Jays (*Aphelocoma californica*) held in captivity will avoid eating *L. lorquini* only if they have first been "trained" *on A. californica*, which the birds find distasteful (Prudic 2007). This supports the hypothesis that *L. lorquini* is co-opting the aposematic signal of *A. californica,* a finding that has since been demonstrated empirically in field study in natural habitats ((Kristiansen et al. 2018), Chapter 1). The most obvious mimetic component of *L. lorquini's* phenotype is the orange Apical Forewing Patch ("AFP"), which is absent in *L. weidemeyerii* and resembles a similar patch in *A. californica*. There may also be mimicry in the white medial bands, which do not reflect UV light in *L. lorquini* or in *A. californica* but do in *L. weidemeyerii* and many other *Adelpha* species (unpublished personal observation).

Despite a good understanding of the phenotypic and ecological aspect of mimicry in these butterflies, the genetic basis of the mimetic orange AFP color pattern element remains unexplored. However, given the conserved genetic basis of color formation in other butterfly species (Kronforst and Papa 2015), I hypothesize that the gene *optix* will be responsible for the presence/absence of the AFP. Here I present the results of a series of crossing experiments, a RAD-seq based linkage map, and a QTL association study

which aim to identify the genomic region(s) responsible for the presence or absence of the orange AFP in *L. lorquini*. Characterizing the relationships between genetics, genomics, and selectively advantageous traits is essential for a holistic understanding of how the evolution of such traits contributes to the divergence of species.

Methods

Rearing and mapping broods: To facilitate a QTL analysis of color pattern differences between *L. loquini* and *L. weidemeyerii,* a series of crossing experiments were performed (Fig 2.1). Wild-caught females of both species were captured and allowed to oviposit on willow saplings placed in mesh cages in the lab. Hatched larvae were allowed to develop, and offspring of true-breeding females were then crossed via hand-pairing and allowed to oviposit in the same way to produce F1 offspring. F1 offspring phenotypes were recorded after eclosure. F1 offspring were then mated to either an individual from the parental generation, their true-breeding offspring, or were full-sibling mated, to produce F2 offspring. Backcross and F2 offspring were then reared until eclosure, after which their phenotype was recorded, and the tissue preserved in 70% Ethanol at -20°C. A total of 142 offspring were produced, of which 89 were intercross offspring and 53 resulted from backcrosses. Phenotypes were scored as a simple presence/absence of an orange AFP.

Extraction and ddRAD-seq: 171 individual samples (including wild-caught, grandparents, parental, and F2/BC offspring) from our crossing experiment were genotyped using restriction-site associated DNA (RAD-seq) sequencing. Genomic DNA was extracted from thorax muscle, ground with a hand pestle, using Qiagen's DNeasy kit (Quiagen, Valencia CA) following the standard protocol with overnight incubation in the

lysis butter with 20uL of proteinase K. Final DNA concentrations were estimated using a NanoDrop® 2000 spectrophotometer. RAD-seq fragment libraries were prepared following the double-digest protocol in DaCosta and Sorenson (2014) with some minor modifications consistent with Stryjewsky and Sorenson (2017). Briefly, DNA samples were diluted to a standard 1μg concentration using ultrapure water before being digested with two restriction enzymes, *BfucI* and *SbfI* (New England Biolabs, Beverly, MA). Illumina sequencing adapters were then ligated to the digested DNA such that each sample had a unique barcode/index pair. After ligation, sample concentration was again quantified using qPCR (Kapa Library Quantification Kit, Kapa Biosystems, Wilmington, MA), and sets of 12 samples diluted to equimolar concentrations were pooled, reducing time and cost of downstream preparation steps. DNA fragments between 300-450bp in length were then size-selected using a PippinPrep® size selection protocol. Pooled libraries were then PCR amplified for 22 cycles using Phusion High-Fidelity DNA Polymerase (New England Biolabs, Beverly, MA) and quantified using qPCR as before. Finally, pools were combined in equimolar amounts for sequencing.

The pooled fragment libraries were sequenced on an Illumina® HiSeq2500 in RAPID mode with 150 base pair single-end reads. The entire library was sequenced on two sequencing lanes, one of which produced lower quality data, and a third lane of sequencing data was generated. High-quality data from all three lanes were integrated into the final dataset. An inline barcode and an index read were then used to assign sequencing reads to individual samples (see appendix for barcode sequences). The sequence data returned from the sequencing facility were demultiplexed for the index

read but not the inline barcode. To separate these data into one file for each individual in the dataset, the "process_radtags" program in the Stacks software package (Catchen et al. 2013) was used. This software uses a barcode file and the restriction enzyme recognition site adjacent to the barcode to demultiplex reads and to trim adapters.

Reads were then aligned to a custom version of the *L. arthemis* reference genome (Gallant et al. 2014, Mullen et al. 2019 (in prep)) using the Burrows-Wheeler Aligner and the bwa-mem algorithm (H. Li and Durbin 2009). This version of the reference genome includes additional sequence data when compared with earlier versions, but only contains those scaffolds which show protein synteny with the *H. melpomene* genome (Hmel 2.5). Aligned read data was piped into the Samtools package (H. Li et al. 2009) to produce BAM files, which were then analyzed in the Genome Analysis Tool Kit v3.7 (McKenna et al. 2010). Genotypes were called using the UnifiedGenotyper, and filtered using custom scripts and according to GATK best practices recommendations (DePristo et al. 2011). Finally, VCF files produced by GATK were filtered using the VCFtools software (Danecek et al. 2011) to generate a data set comprising highly confident SNP calls. Only biallelic SNPs with a per-sample sequencing depth of >10 were retained, samples with fewer than 10 reads were marked as “no call” at that SNP. SNPs were further filtered to include only those that were called for >85% of the individuals in our dataset.

Linkage Map Construction: The filtered SNP data were imported into the program LepMap3 (Rastas 2017), a memory-efficient linkage-mapping program which can make use of genotype likelihoods, along with a pedigree file. Incorporating genotype likelihoods gives this program the ability to work with lower read-depth sequencing data.

The pedigree file format mirrors the experimental crosses described earlier and can include grandparents/initial crosses (p), parents/first-generation offspring (f1) and offspring (f2 or Backcross). These individuals are then grouped by brood to reflect their familial relationships. However, because several grandparents in these crosses exhibited poor sequencing quality, no grandparents were ultimately included in the mapping pedigree. Some of the wild-caught individuals that generated the grandparents, and not used directly in the crosses, were included in sequencing but excluded from analysis. In all, 142 individuals were coded according to their brood identity in one of eight broods: five Intercross (F2) broods, and three backcross (BC) broods. Phenotype values were assigned as a binary state based on the presence or absence of any orange in the apical wing patch. LepMap3 was run following the standard workflow but with the LOD limit set to 6. Output files for QTL analysis were created from LepMap3 output files using custom python scripts. These output were used to create a VCF containing only linkage informative sites using VCFTools (Danecek et al. 2011). Linkage informative sites are defined as those sites which are inherited from at least one heterozygous parent (Rastas 2017). Final output files contained Linkage Group identity and centimorgan (cM) position from LepMap3, genotype from the GATK, and a marker name.

QTL Analysis: QTL analysis was conducted in the R statistical software (R Core Team 2016) using the r/qtl package (Broman et al. 2003) following the published guidelines (Broman and Sen 2009). Briefly, genotype data were imported from the VCF in "012" format data matrixes using base R. These data were then combined with Linkage information from LepMap3 and Phenotype information to produce a final analysis-ready

dataframe. This dataframe is then imported into r/qtl as a read.cross() object for qtl analysis and the data were checked for integrity. The function "jittermap()" was then used to separate overlapping loci by minute amounts to avoid known issues with the r/qtl software and analysis of co-occurring loci. The samples in the dataframe were then split into one of four groups: 1) All offspring, 2) All Intercross Offspring, 3) All Backcross Offspring, and 4) largest single brood. Each data set was analyzed separately as overlapping replicates. Splitting the data in this way allows for comparisons between the results of both overlapping (e.g. BC overlaps with All) and non-overlapping datasets (BC does not overlap with IC). QTL analysis proceeded by first estimating the recombination fraction and calculating the conditional genotype probabilities using the r/qtl Hidden Markov Model, which simultaneously accounts for genotyping errors, missing data, and dominant markers (Broman et al. 2003). Finally a QTL analysis with a single-QTL model (Broman and Sen 2009), was executed using the interval mapping algorithm "em" (Lander and Botstein 1989) as implemented in r/qtl. Other QTL estimation algorithms were tested but were found to produce either highly similar or less consistent results than the "em" algorithm, which is consistent with the findings of Broman and Sen (2009). Significance thresholds (alpha = 0.01, 0.001) were determined using permutation tests (n = 1000 per comparison;(Churchill and Doerge 1994)). Loci with LOD scores above the calculated significance threshold(s) were deemed to be "significantly associated" with the phenotype. Finally, results were visualized using a combination of base R graphics and the LinkageMapView package.

Loci that were found to be associated with the phenotype were the investigated by

aligning sequence data to the *Heliconius melpomene* genome using BLAST (Altschul et al. 1990). The *H. melpomene* genome (Hmel 2.5 (Davey et al. 2016)) was used because it is of higher quality and more fully annotated than the *L. arthemis* genome. To accomplish this, a 30kbp region around the SNP was extracted from the *Limenitis* reference genome using Samtools (H. Li et al. 2009). This region was then used as a query sequence in a Discontiguous Megablast (Altschul et al. 1990) against the most recent version of the *Heliconius melpomene* genome (Hmel 2.5). The quality of matches was then assessed, and their identities investigated using the genome exploration tools on the *Lepbase* website (https://www.lepbase.org).

Results

The breeding experiments revealed a broad range of variation in the AFP (Figure 2.2). Some individuals exhibited orange color pattern extending as far as the white stripe that occupies the central symmetry system in these butterflies, while the extent of orange on the wings of others was so minute that it was difficult to see unaided. However, when the presence/absence of orange was scored as a binary trait, and orange assumed to be dominant, the ratio of F2 intercross offspring with and without orange was approximately 3:1, as expected for a single-locus trait with orange dominant (Table 2.1). Similarly, the ratio of backcross offspring with and without orange was approximately 1:1 (Table 2.1). Three intercross broods were produced in 2011, and two additional intercross broods were produced in 2012. These broods contained a total of 89 offspring with a ratio of 63 orange to 26 black (X^2 test: X^2= 0.46, p ~0.50). A total of three backcross broods were produced, two in 2012 and one in 2013. There were 28 orange individuals and 25 black

individuals produced by the backcross broods (X^2 test: X^2= 0.085, p ~0.80). These results are consistent with a single locus determining the presence or absence of orange coloration in *Limenitis*, and that at this locus there is one dominant allele. However, the observed phenotypic variability suggests that more than one or more additional loci influence the extent of the orange phenotype.

A total of 222,133,770 reads were obtained from the three lanes of Illumina HiSeq2500 for the 172 sequenced individuals. Of those reads, 171,638,711 (~77%) were successfully demultiplexed by barcode in Stacks, assigned to individual samples, and retained for further analysis and filtering. There was substantial variation in the number of reads per sample, ranging from 66,968,846 to 4,022. The mean number of reads per sample was 1,003,735, and the median number was 843,920. After alignment, 917,698 SNPS were identified, of which a total of 13,391 high-quality bi-allelic SNPS were retained after stringent filtering.

LepMap3 identified 3935 SNPS as pedigree informative and retained these sites for linkage map construction. 188 linkage groups were recovered, but of these only a small number (~31) have appreciably high likelihood scores (< -100 lnL), and a smaller number (~16) have highly supported maps (< -5000), likely representing some combination of the 30 chromosomes found in *Limenitis* (or portions thereof). The largest linkage group (LG 1) was constructed from 193 SNPS on 22 scaffolds (Table 2.3). The 30 linkage groups with the highest statistical likelihood were constructed using an average of 109 SNPs, and from 20 scaffolds on average.

QTL analysis recovered only six linkage groups with contained loci that were

significantly associated with the presence of orange coloration in one or more of the analysed data sets (all offspring, backcross, intercross, largest brood), by crossing the threshold LOD set by the permutation tests (Figure 2.4). Among these linkage groups, roughly 10 loci were found to have associations (Table 2.4). The strength of the statistical association with phenotype carried among loci and many of these ten loci were not consistently recovered in every sub-comparison of the different sets of offspring. Only three loci had high LOD scores for both the intercross and backcross offspring. The first locus (hereafter "Locus 1"), which is also the most strongly associated, is found on LG 8 and has a LOD score of ~20 when all offspring are included, and roughly ~8 when only backcross offspring are considered (Figure 2.5). This locus corresponds to a SNP on scaffold00072 at bp 1,028,706 in the current iteration of the *Limenitis* genome. This is the highest LOD peak in every comparison. The second is found on LG 12 and has a LOD score of ~18 when all offspring are included, and ~6.7 when only backcross offspring are considered (Figure 2.5). This locus corresponds to a SNP on scaffold00065 at bp 680,925. Finally, the third potential QTL is also found on LG 8, with a score of ~17.7 when all offspring are included, and ~7.0 when only Backcross offspring are considered. Other QTL, their LOD score, and their genomic locations can be found in Table 2.3. Using only the intercross individuals results in a pattern that largely recapitulates the pattern found in the "All" and "Backcross" sub-comparisons (Figure 2.5).

Using NCBI's BLAST+ tool (Altschul et al. 1990), several candidate gene regions were identified in *Heliconius*. The first locus, found in LG 8 in the assembly, aligns to *H. melpomene* scaffold "Hmel218003o" around the 4Mbp region, and to the 5Mbp region of

Bombyx mori chromosome 23 (Yamamoto et al. 2008) (Table 2.4). Locus 2 is found on LG 12 in my assembly, but also mapped to *H. melpomene* scaffold "Hmel218003o" at around 5.7Mbp, and to the 7Mbp region of *B. mori* chromosome 23. Contrary to expectations based on an analysis of synteny (Table 2.5)Loci one and two therefore map to the same scaffolds/chromosomes in *Heliconius/Bombyx*, respectively, despite being found in different linkage groups in *Limenitis* (Table 2.6). Finally, locus 3 is found on LG 8 in my assembly, but maps to H. melpomene scaffold "Hmel209001o" at around 4Mbp, and to B. mori chromosome 14 around 12.2Mbp (Table 2.4). Locus 3 therefore maps to different scaffolds/chromosomes than loci one or two, despite being found on the same linkage group in my data (Table 2.6). Note that nine out of the ten loci that were found to have a significant association with phenotype map to *H. melpomene* scaffold "Hmel218003o". Remaining BLAST comparisons can be found in table 2.4.

The three loci with the most consistent associations to phenotype map to genomic regions that either contain or are proximate to several known proteins, imputed proteins and annotated domains (see: Table 2.7). Locus 1 is proximate to several toll-like receptor (TLR) genes, as well as an exportin-4 like protein sequence known as "HMEL017483". Locus 2 is also proximate to a toll-like receptor gene, as well as a sugar transporter gene, and an ortholog of the gene "Bursicon". The *H. melpomene* scaffold (Hmel208003o), to which most of my significant loci align, is also known to harbor the canonical color patterning gene "*optix*", which modulates the presence or absence of red color pattern elements in *Heliconius*, around 700Kbp from the beginning of the scaffold. Other proteins proximate to these BLAST results can be found in Table 2.7.

Discussion

The goal of any genetic mapping study is to identify gene regions that underlie the phenotypic variation among a group of individuals. To pursue this goal, I created a linkage map in an effort to localize the causal variant that is responsible for color pattern variation in western *Limenitis* butterflies. *Limenitis* butterflies were chosen for this study because they are closely related, and because they actively hybridize in the western Great Basin (Boyd et al. 1999), which should contribute to high genomic similarity and help distinguish the genomic signature of adaptation from genome-wide divergence. We originally hypothesized that *optix*, a color patterning gene that is causatively linked to red-orange color patterns *in Heliconius* (Martin et al. 2014), would be conserved Lepidoptera (Kronforst and Papa 2015), and therefore responsible for the orange AFP phenotype in *Limenitis*. Surprisingly, while the most strongly associated QTL aligns to a *Heliconius* scaffold that contains *optix,* it is not in close proximity to *optix* within that scaffold, nor do any of the statistically associated SNPs align to the *Limenitis* scaffold that contains *optix* (scaffold00223). This suggests two intriguing possibilities: 1) the QTL is in a region that contains a novel color patterning gene or 2) the QTL is in a region that contains a trans-acting element that modulates the expression of *optix.*

The linkage map was generated from 3935 linkage informative SNPS, and resolved into 250 linkage groups, of which ~30 well-supported linkage groups. While high likelihood values support these de-novo linkage groups, very little support can be drawn from comparison to a chromosomal assembly of a closely related butterfly species *Melitaea cinxia. Melitaea* is an ideal comparison because this species retains the ancestral

Nymphalid chromosomal arrangement, with 30 chromosomes rather than the 21 found in *Heliconius* (Ahola et al. 2014).The inferred linkage groups in *Limenitis* do not correspond well to the chromosomal arrangement of *Melitaea* based on comparisons of protein coding synteny at the scaffold level and based on BLAST comparisons of the QTL regions. In fact, most of the 10 SNPs from the QTL analysis align to chromosome 14 in *Melitaea,* to LG 18 in *H. melpomene*, and to chromosome 23 in *B. mori*, despite being found on different linkage groups in our map (Tables 2.5 and 2.6).

The most likely source of error in our linkage map construction is the relatively small scale of our crossing experiment. F2 brood sizes ranged from five to 39 (Table 2.1) and a total of only 142 individual offspring were included in the final analysis, making this a smaller study than generally expected for traditional linkage mapping methods (Beavis 1994; Lange and Boehnke 1982). Additionally, LepMap3 was created for whole-genome datasets (Rastas 2017), so it is possible that the lower density of markers reduced the effectiveness of joining linkage groups, though the effect of marker density on performance has not been explored. This is especially probable considering that most linkage groups exhibit low coverage at their extreme ends, possibly indicating poorly resolved linkage relationships between linkage groups. One way to overcome this issue in future experiments would be to reduce the stringency of filtering criteria for the SNP library. This should be possible in LepMap3, which can handle genotype likelihood data, allowing users to substantially increase the number of loci involved in an analysis (Rastas, 2017). However, I chose not to pursue this solution because of my lack of confidence in the sequence data quality for this dataset as a result of including the low-

quality lane of sequencing. Finally, our linkage map was constructed from broods that had undergone only a single generation of either backcrossing or intercrossing. There is no recombination between maternally inherited markers in Lepidoptera because there is no crossing over in females; this could result in much lower resolution of linkage relationships as linkage mapping is only possible if recombination polarizes the relationships between SNPs (Broman and Sen 2009). Spurious inference of linkage between physically unlinked SNPs perhaps produced poor synteny between this linkage map and the genomes of other Lepidoptera. Alternatively, lack of linkage information may have led to some linkage groups being split, when in reality they are contiguous. This latter interpretation is particularly likely given that BLAST alignments of the regions around the associated loci against the *Heliconius* genome do not overlap, but align to a relatively small region of a single scaffold (Figure 2.6).

Phenotypic inheritance patterns indicate that orange coloration in *Limenitis* is controlled by a single locus of large effect. Despite the quantitative variation in the extent of orange on the wing, this single-locus inference fulfilled our expectations based on the genetics of color pattern in other butterfly species (Kronforst and Papa 2015). Additionally, studies of the developmental genetics of butterfly wings have found that canonical morphogens such as *distal-less (dll), wingless,* and *engrailed* often exhibit complete dominance, which means that only one gene/gene region is required to produce a phenotypic change (Carroll et al. 1994). These genes are initially expressed in localized regions of the wing from which they diffuse to create gradients that activate developmental pathways to establish body segments and polarity (Lecuit et al. 1996;

Nellen et al. 1996; Neumann and Cohen 1997; Zecca, Basler, and Struhl 1996). These genes also have been found to function in the formation of wing patterning, such as establishing the locations of eyespots (Carroll et al. 1994). Further study has revealed a set of "developmental toolkit" genes that have been repurposed throughout the Lepidopteran evolutionary tree to generate a diversity of color patterns (Kronforst and Papa 2015). These genes include the signaling ligand *WntA* (black patterning (Gallant et al. 2014)), the cell-cycle regulatory protein *cortex* (yellow patterning (Nadeau et al. 2016)), and the transcription factor *optix* (red patterning (Kunte et al. 2014)). While our findings support this expected single-locus model, our QTL did not map to any of these three toolkit genes, instead mapping to a region roughly 4-7Mbp away from the color patterning gene *optix*. However, it is important to note that filtering removed SNPs that are associated directly with the *Limenitis* scaffold that contains the *optix* protein coding region, so it remains possible that *optix* is involved in generating the AFP.

QTL analysis returned 10 SNPs associated with the presence or absence of the orange AFP. Two pairs of these loci (Locus 4/7, and Locus 5/9) aligned to essentially the same position in *Heliconius*, and so they were considered to be the same locus, leaving eight putative color patterning loci. Locus 1 and Locus 2 stand out as particularly strongly associated with the phenotype, with LOD scores of 21.36 and 21.03, respectively. These loci, while mapping to different linkage groups in the *Limenitis* assembly, align to a roughly 2Mbp region on *Heliconius melpomene* scaffold "Hmel218003o", a scaffold which is known to harbor the color patterning gene *optix*. These loci, however, are not particularly close to *optix*, which demands explanation.

One intriguing possibility is that the gene regions near the QTL contain a novel color patterning gene. Of particular interest among our BLAST results is the gene *bursicon. Bursicon* is a neuropeptide first identified in *Drosophila* that is released into the hemolymph of insects shortly after emergence from the pupa (Loveall and Deitcher 2010). This protein interacts with a receptor called *Rickets* to instigate maturation of the wings, which happens after most other developmental processes are complete (Bilousov, Katanaev, and Kozeretska 2012). Since wing pigmentation is the final step in wing pattern development (Brakefield and French 1999) we would expect that the molecule responsible for a shift in wing pigment to be expressed rather late in the developmental timeline, but still prior to emergence. This separation in time between wing maturation and pigment deposition means that it is possible that *bursicon* could be used in both instances without signal confusion, similar to how other patterning genes operate (Carroll et al. 1994). Studies of *bursicon* expression during development are needed to test whether this gene is causatively associated with the AFP. If this association is causative we should expect to see evidence of *bursicon* expression significantly earlier than wing maturation if this gene is causatively associated with the orange AFP. The evidence of a QTL at this site in *Limenitis* makes *bursicon* an excellent candidate gene for further study.

Another possibility is that the QTL represents not a new color patterning gene, but rather a trans-acting element that interacts with *optix* to modulate the expression of red-orange color patterning. Trans-acting elements are typically genes that produce RNA or protein products, such as transcription factors, that interact with another gene (Sassone-

Corsi and Borrelli 1986). For example, *Dll* is a well-known trans-acting factor that has been implicated in the creation of color patterns, specifically eyespots, in Lepidoptera (Carroll et al. 1994). It is possible that one or more of the uncharacterized genes near the QTL we identified is such a trans-acting element. While further characterization of this region is necessary to fully elucidate its potential relationship with the orange AFP, one could speculate that it interacts with *optix* given they are located on the same linkage group in *Melitaea cinxia, Heliconius melpomene,* and *Bombyx mori, respectively* (table 2.4 and 2.5).

Further characterization of this gene region is necessary to fully elucidate its relationship with the orange AFP. RNA-i or CRISPR-CAS9 knockouts are exciting methods of establishing a functional relationship between the two; however, complete knockouts of *bursicon* may be too extreme because of its essential role in exoskeleton tanning and wing maturation in arthropods (Loveall and Deitcher 2010). It seems likely that individuals lacking *bursicon* or that have repressed expression would not be able to generate mature wings, which would be difficult to phenotype. As a result, in situ hybridization experiments may be the best way to demonstrate that certain gene products co-localize with the phenotype, as in previous work (Gallant et al. 2014) in *Limenitis*.

Though direct evidence of a functional relationship awaits further study, the current analysis localized several QTL associated with the presence or absence of the orange AFP to genomic regions in *Limenitis*. Comparisons among reference genomes suggest that most of the significantly associate SNPs are in fact the same region of the genome, though this region is not particularly close to any known color patterning genes,

suggesting that we have identified a new target of selection. While they remain untested, two hypotheses seem equally plausible: 1) the QTL we identified are associated with a trans-acting element that acts on *optix; or* 2) the QTL we identified are associated with a novel color patterning gene. Each possibility is intriguing and worthy of further study. Identifying the function of this gene will advance our knowledge of color pattern genetics and development of adaptive color patterns. These results highlight the value of evolutionary dynamics across a variety of different species to gain a fuller picture of the evolution of divergent adaptive phenotypes.

Figures

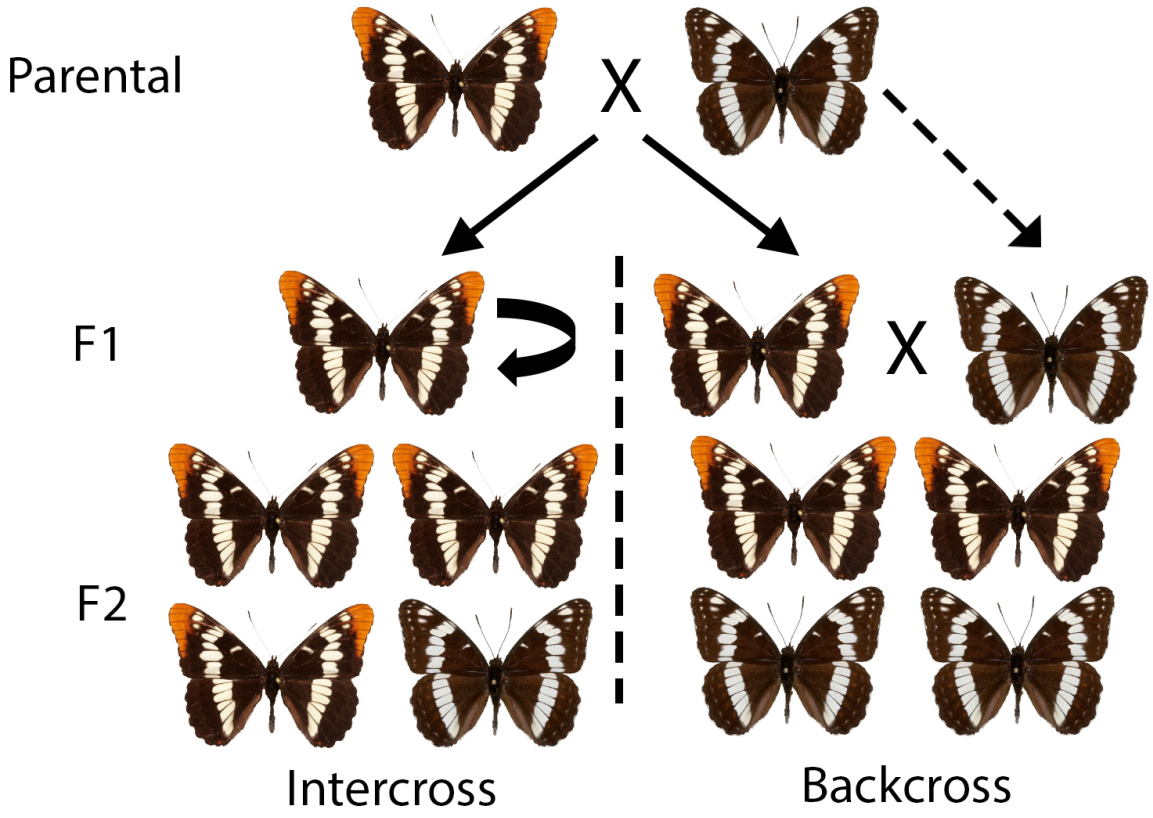

Figure 2.1 A representation of the two types of hybrid crosses and expected phenotypic proportions of offspring produced during this experiment, assuming that orange coloration is a dominant Mendelian trait. The left panel depicts an Intercross, whereby F1 hybrid offspring are mated to a full sibling to produce F2 hybrids with an expected phenotypic ratio of 3:1 orange:non-orange. The right panel depicts a backcross, whereby F1 hybrid offspring are mated to a member of the parental population that does not exhibit the phenotype of interest, producing a 1:1 expected phenotypic ratio in the F2 generation.

Figure 2.2 A depiction of the range of phenotypic diversity observed in the F2 hybrid offspring in the crossing experiments. Note the variation in extent of orange color patterning. Despite this high degree of variability, offspring ratios from the mating experiment are consistent with a simple two-allele Mendelian trait.

Figure 2.3 The 30 largest linkage groups produced from the LepMap3 analysis. Loci indicated with the color red represent loci that have higher LOD scores than the significance threshold calculated using a 1000-iteration permutation test. Note that locus density is highly variable, particularly when comparing linkage group centers and tips, and when comparing smaller chromosomes to larger ones.

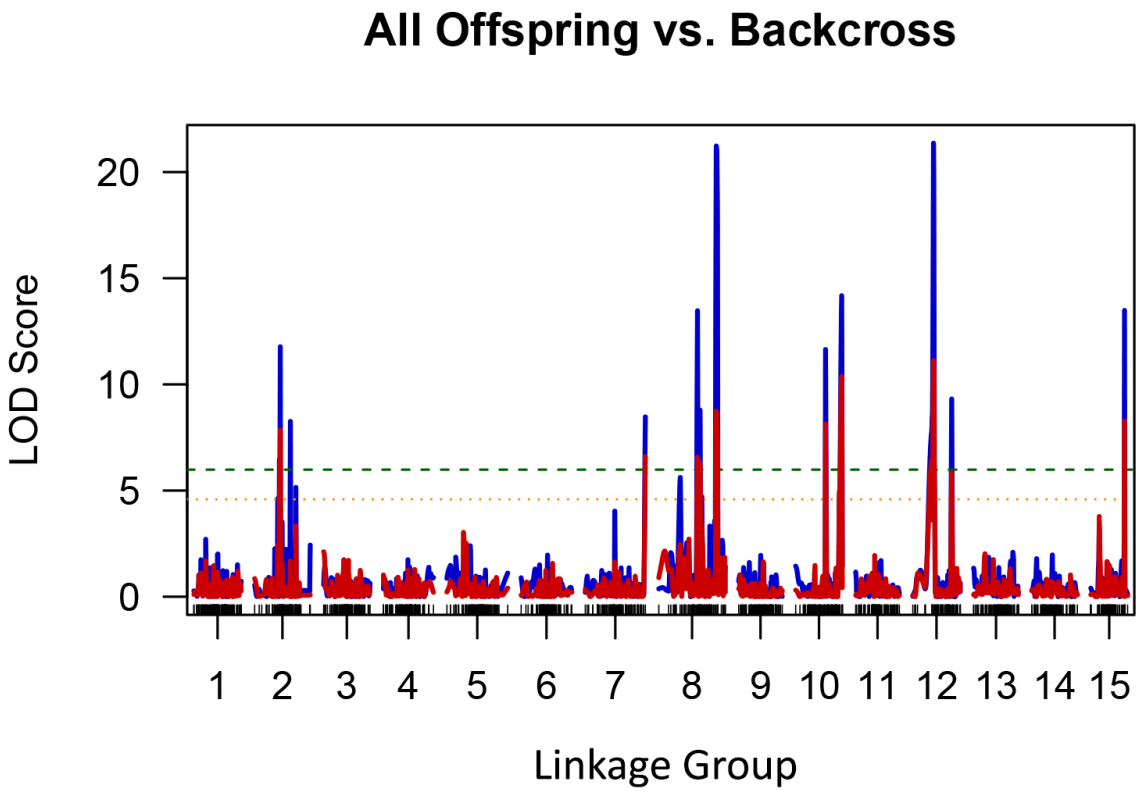

Figure 2.4 LOD scores for SNPs on each of the first 15 linkage groups. The dotted orange and dashed green line represent significance thresholds ($p < 0.01$, $p < 0.001$) gathered from a permutation test utilizing 1000 permutations. Blue lines represent LOD scores from the "all offspring" comparison, whereas the red line represents backcrossed offspring. Significant associations with orange AFP color patterning are found on LGs 2, 7, 8, 10, and 12, with the highest peaks found on LG 8 and LG 12.

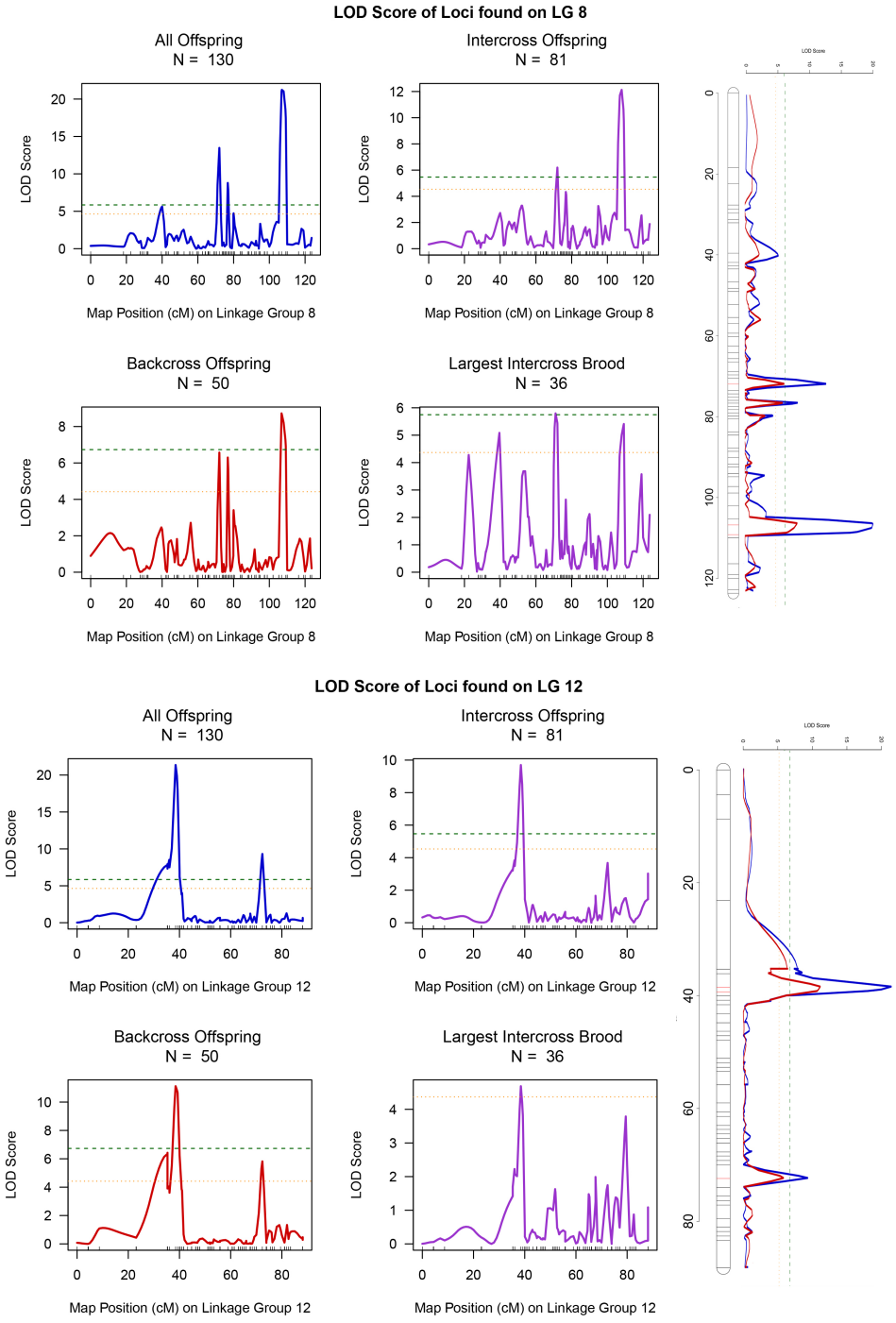

Figure 2.5 LOD score distributions across the two linkage groups with the highest LOD peaks. Each of the small panels on the left shows the LOD scores in the respective linkage group for each QTL analysis. The panels on the right graph combine the "All Offspring" LOD scores and the "Backcross Offspring" LOD scores to show concordance between the two comparisons.

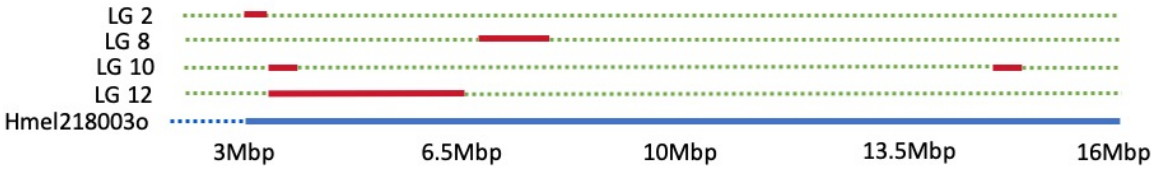

Figure 2.6 A schematic representation of the BLAST alignments of 2kbp queries drawn from around the QTL.

Tables

Table 2.1 The results of the crossing experiments presented in each year that offspring were produced. In each case, individuals from each species were mated to produce hybrid offspring, which were then mated either to their siblings (intercross) or to a member of the parental generation (backcross) to produce second generation broods. The third row shows the number of broods and offspring produced in each year. Finally, in the bottom row, phenotypic ratios are tested for departure from the expected 3:1 (intercross) or 1:1 (backcross) ratio using a chi-squared test.

<table>
<tr><th></th><th colspan="3">2011</th><th colspan="3">2012</th><th colspan="3">2013</th></tr>
<tr><td>Parental</td><td colspan="3">Wild Caught Individuals
L. lorquini x L. weidemeyerii</td><td colspan="3">Wild Caught Individuals
L. lorquini x L. weidemeyerii</td><td colspan="3">Wild Caught Individuals
L. lorquini x L. weidemeyerii</td></tr>
<tr><td>Number of Families</td><td colspan="3">3 Full-sibling mate pair families</td><td colspan="3">2 Full-sibling mate pair families
2 Backcrossing mate pair families</td><td colspan="3">1 Backcrossing mate pair family</td></tr>
<tr><td>Resulting Number of Offspring</td><td colspan="2">Intercross 1:
Intercross 2:
Intercross 3:</td><td>5
24
7</td><td colspan="2">Intercross 4:
Intercross 5:
Backcross 1:
Backcross 2:</td><td>39
14
9
32</td><td colspan="2">Backcross 3:</td><td>12</td></tr>
<tr><td rowspan="2">Statistics</td><td colspan="4">Intercrosses</td><td colspan="5">Backcrosses</td></tr>
<tr><td><u>Observed:</u>
63 Orange
26 Black</td><td colspan="2"><u>Expected (3:1):</u>
67.75 Orange
22.25 Black</td><td>X^2: p ~ 0.50</td><td><u>Observed:</u>
28 Orange
25 Black</td><td colspan="2"><u>Expected (1:1):</u>
26.5 Orange
26.5 Black</td><td>X^2: p ~ 0.80</td></tr>
</table>

Table 2.2 The number of linked SNPS used to construct linkage groups.

Linked SNPS	All LG's	30 Largest LG's
Total	3930	3265
Average	15.53	108.83
Median	3	103
Min	2	17
Max	193	193

Table 2.3. The Number of scaffolds that were used to construct the top 30 linkage groups. Note that these scaffolds are not necessarily unique, a scaffold included in LG1 could also be included in LG2. SNPs from many scaffolds were assigned to multiple linkage groups.

LG Number	**1**	**2**	**3**	**4**	**5**	**6**	**7**	**8**	**9**	**10**	MAX	37 (LG 10)
Scaffolds in LG	22	32	28	33	20	19	35	23	20	37	MIN	5 (LG 30)
LG Number	**11**	**12**	**13**	**14**	**15**	**16**	**17**	**18**	**19**	**20**	AVG	23.87
Scaffolds in LG	19	18	22	21	16	27	14	17	14	17	MED	19
LG Number	**21**	**22**	**23**	**24**	**25**	**26**	**27**	**28**	**29**	**30**		
Scaffolds in LG	19	18	31	15	13	12	16	8	6	5		

Table 2.4 QTL analysis results are presented with their corresponding LOD scores. LOD scores passing the permutation threshold are shaded. A 15Kbp region around each marker was aligned using BLAST to the *Heliconius* genome (Hmel2.5), and the resulting alignment is presented by scaffold and position. Linkage groups 2, 8, 10 and 12 all align to the *Heliconius* scaffold known to contain the coding region of *optix*

Locus Number	Marker Name	LG	cM position (ALL)	Scaffold in *Limenitis* Genome	Position	Scaffold in *Heliconius* Genome	*Heliconius* Location	LOD ALL	LOD BC	LOD IC
Locus 1:	marker2015	12	38.48	scaffold00065	1029739	Hmel218003o	4033413-4035060	21.36	11.12	9.70
Locus 2:	marker1407	8	106.83	scaffold00072	1028706	Hmel218003o	6861771-6862621	21.03	8.72	11.29
Locus 3:	marker2004	12	39.26	scaffold00065	680925	Hmel218003o	5705260-5706470	17.96	10.66	7.17
Locus 4:	marker1517	8	109.21	scaffold00053	1115470	Hmel218003o	7932759-7932637	17.45	6.92	9.73
Locus 5:	marker1716	10	85.56	scaffold00092	243048	Hmel218003o	16238630-16242079	14.18	10.37	4.79
Locus 6:	marker2317	15	62.67	scaffold00048	1410884	Hmel212001o	13497000-13496633	13.48	8.27	5.36
Locus 7:	marker1515	8	72.04	scaffold00053	1115455	Hmel218003o	7932759-7932637	13.43	6.56	6.19
Locus 8:	marker422	2	47.63	scaffold00010	1383768	Hmel218003o	3104692-3105952	11.77	7.86	4.24
Locus 9:	marker1714	10	55.51	scaffold00092	243044	Hmel218003o	4335635-4336056	11.64	8.14	6.02
Locus 10:	marker2012	12	72.38	scaffold00065	955620	Hmel218003o	3976436-3976673	9.31	5.82	3.68

Table 2.5 Inferred linkage group correspondence to chromosome-level genome assemblies in three species of Lepidoptera using a comparison of protein synteny. Note that results for synteny and BLAST alignments (Table 2.6) are often inconsistent.

Locus #	*Limenitis* Scaffold	Linkage Group (*Limenitis*)	Linkage Group (*H. melpomene*)	Chromosome (*M. cinxia*)	Chromosome (*B. mori*)
Locus 1:	scaffold00065	12	18	14	23
Locus 2:	scaffold00072	8	18	14	23
Locus 3:	scaffold00065	12	18	14	23
Locus 4:	scaffold00053	8	18	14	23
Locus 5:	scaffold00092	10	Z	1	1
Locus 6:	scaffold00048	15	13	26	14
Locus 7:	scaffold00053	8	18	14	23
Locus 8:	scaffold00010	2	18	14	23
Locus 9:	scaffold00092	10	Z	1	1
Locus 10:	scaffold00065	8	13	26	14

Table 2.6 Linkage group correspondence to chromosome-level genome assemblies in three species of Lepidoptera using BLAST alignment. Note that results for synteny (Table 2.5) and BLAST alignments are often inconsistent.

Locus #	*Limenitis* Scaffold	Linkage Group (*Limenitis*)	Linkage Group (*H. melpomene*)	Chromosome (*M. cinxia*)	Chromosome (*B. mori*)
Locus 1:	scaffold00065	12	18	14	23
Locus 2:	scaffold00072	8	18	14	23
Locus 3:	scaffold00065	12	18	14	23
Locus 4:	scaffold00053	8	18	14	23
Locus 5:	scaffold00092	10	18	14	23
Locus 6:	scaffold00048	15	7	28	2
Locus 7:	scaffold00053	8	18	14	23
Locus 8:	scaffold00010	2	18	14	23
Locus 9:	scaffold00092	10	18	14	23
Locus 10:	scaffold00065	8	18	14	23

Table 2.7 Genes found near the *Limenitis* QTL based BLAST alignment to the *Heliconius* genome.

Locus #	*Heliconius* scaffold: position	Protein Hit 1	Protein Hit 2	Protein Hit 3	Protein Hit 4
Locus 1:	Hmel218003o: 4033413-4035060	HMEL034295 (Cullin - 5)	HMEL006496 (ETIF 2 Sub. 3)	HMEL006499 (uncharacterized)	HMEL006495 (ATP synthase)
Locus 2:	Hmel218003o: 6861771-6862621	HMEL017483 (exportin 4-like)	HMEL017487 (TLR-J)	HMEL017479 (TLR-I)	HMEL034352 (uncharacterized)
Locus 3:	Hmel218003o: 5705260-5706470	HMEL034331 (Bursicon)	HMEL034332 (histone demethylase)	HMEL005787 (sugar transporter)	HMEL011010 (TLR-F)
Locus 4/7:	Hmel218003o: 7932759-7932637	HMEL034380 (nucleic-acid-bind.)	HMEL034379 (uncharacterized)	HMEL016208 (translation init. factor)	HMEL009488 (carboxylate synthase)
Locus 5:	Hmel218003o: 16238630-16242079	HMEL017112 (Uncharacterized)	HMEL034535 (Uncharacterized)	HMEL034536 (Uncharacterized)	HMEL006492 (Kelch-Like Protein)
Locus 6:	Hmel205001o: 352933-353461	HMEL036595 (zinc finger)	HMEL036596 (uncharacterized)	HMEL036594 (adenosine receptor)	HMEL036593 (uncharacterized)
Locus 8:	Hmel218003o: 3104692-3105952	HMEL014940 (phosphatase)	HMEL014937 (uncharacterized)	HMEL014936 (repressor expression-enhancing protein)	HMEL034262 (uncharacterized)
Locus 9:	Hmel218003o: 4335635-4336056	HMEL034293 (Uncharacterized)	HMEL034292 (Uncharacterized)	HMEL006491 (Uncharacterized)	HMEL034537 (Uncharacterized)
Locus 10:	Hmel218003o: 3976436-3976673	HMEL034293 (uncharacterized)	HMEL006491 (uncharacterized)	HMEL034292 (uncharacterized)	HMEL006492 (kelch-like protein)

CHAPTER THREE

Identifying Variants Underlying Adaptation in *Limenitis lorquini*

Introduction

A central goal of evolutionary biology is to understand how the phenotypes of organisms are linked to genetics and gene function. The diversity of butterfly wing coloration and the myriad ways in which color patterns influence the fitness makes them a favored subject for this type of study. Over the last decade, rapid progress has been made in identifying the genetic basis of color pattern in a variety of species, including butterflies (Kronforst et al. 2012). Much of this progress has come from painstaking crossing experiments using individuals from different species to generate large recombinant mapping broods, allowing researchers to identify linkage blocks associated with a phenotype of interest (Broman and Sen 2009). Laboratory crosses reduce potential environmental variation and therefore increase mapping power and the ability to identify genetic variants with a relatively small number of genetic markers (Hoekstra et al. 2006; Reed et al. 2011). For example, using this approach, Reed et al. (2011) demonstrated that phenotypic variation in patterns of red pigmentation among different geographic races of *Heliconius* butterflies was associated with the genomic region encompassing a well-known transcription factor *optix*.

Interestingly the *optix* gene was originally described in *Drosophila* as a developmental precursor to eye development (Toy et al. 1998), which suggests that its function in red-orange color patterning in *Heliconius* represents a co-option of this function. The finding that that developmental genes are often re-purposed in other

developmental contexts aligns with one the most surprising findings in the field of evolutionary developmental biology (evo-devo), that of the "developmental toolkit". The developmental toolkit comprises a set of genes that are highly conserved even among deeply diverged taxa (Carrol 2008), the discovery of which has broad implications for understanding the relationship between genes and phenotypes. As a consequence, the focus of evo-devo research has shifted from finding new genes to identifying new regulatory mechanisms, and investigating how regulatory evolution determines the spatial and temporal control of gene expression during development (Pearson, Lemons, and McGinnis 2005; Ronshaugen, McGinnis, and McGinnis 2002). This has led to the discovery of developmental genes that are not only conserved across distantly related taxa, but that are also involved in different aspects of development within the individual organism (Carroll et al. 1994).

Many of the loci underlying color have been identified in recent years including *cortex* (yellow), *optix* (red), and *WntA* (black), across a small handful of butterfly species (Gallant et al. 2014; Jiggins and McMillan 1997; Martin and Orgogozo 2013; Martin et al. 2012; Naisbit, Jiggins, and Mallet 2003; Papa, Martin, and Reed 2008; Reed et al. 2011; Sheppard et al. 1985b). The conserved function of developmental genes, when combined with the modularity of wing pattern development (Nijhout 2001), and with the finding that evolution of color pattern is generally due to regulatory changes as associated with mutations in evolutionary "hotspots" (Martin and Orgogozo 2013), provides a plausible mechanism for diversification of butterfly color patterns. However, there is a need to study additional species to examine the scope of the phenomenon in a

comparative evolutionary framework. Despite the power of classic genetic crossing experiments, they are expensive, time intensive, and lab stocks are difficult to maintain. In addition to these drawbacks, laboratory studies are also necessarily narrow in scope, often addressing only Mendelian genes and discrete characters (Hoekstra et al. 2006; Reed et al. 2011), leading to questions about their generalizability (Sansom and Brandon 2007). However, with the advent of next generation sequencing we are no longer restricted to the laboratory and can take full advantage of variation that exists in natural populations.

Investigations of genotype-to-phenotype relationships in natural populations are a logical companion for QTL experiments. Until recently, whole genome analyses have been largely inaccessible for use in natural populations because of sample size and cost, with notable exceptions in medicine (Ozaki et al. 2002; Visscher et al. 2017) and agriculture (Huang and Han 2014; Korte and Farlow 2013; Liu and Yan 2019). However, as the cost of generating robust whole-genome sequence data declines, natural populations can now be sampled, sequenced, and scrutinized with minimal effort and cost. Datasets composed of densely distributed markers can then be used in genotype-to-phenotype genome wide association studies (GWAS) to identify causal variants. These types of studies rely on linkage disequilibrium between adjacent markers to identify regions of interest, and with enough recombination between the focal species, can identify causal variants (Korte and Farlow 2013). As a result, GWAS studies have emerged as an expedient way to identify genetic variants associated with phenotypic variability, even in natural populations.

One example of the successful deployment of this model is the identification of the causal variants underlying the variation in lateral plate count and opercle shape in natural populations of sticklebacks (Alligood 2017). However, natural populations also present challenges associated with population structure, unknown relationships among samples, and genotype-by-environment effects. One way to compensate for these variables is to use extremely large sample sizes, as exemplified in studies seeking to identify genes underlying disease risk in human populations (Ozaki et al. 2002; Visscher et al. 2017). A more realistic way to compensate for these confounding variables for organismal biologists is to focus on hybrid populations, in which population structure is likely to be minimal and in which genetic variation across most of the genome is broadly shared between individuals of different phenotype (Harrison 1993). When used in this way, hybrid zones become natural laboratories in which crossing has been occurring for multiple generations in concert with ongoing selection, resulting in an ideal system in which to identify causal variants for divergent phenotypes.

One such hybrid zone occurs between two admiral butterflies in the western United States. The Lorquin's Admiral (*Limenitis lorquini*) and the Weidemeyer's Admiral (*Limenitis weidemeyerii*) hybridize extensively in a pair of hybrid zones formed where their geographic distributions meet (Boyd et al. 1999). Hybridization between these two groups has been documented since at least the early 20th century (Edwards 1972), and has been well described (Boyd et al. 1999). The most obvious phenotypic difference between these two species is the presence or absence of an orange apical forewing patch (AFP) found in *L. lorquini* individuals as well as in many hybrid

individuals. In the previous two chapters, I demonstrated the adaptive significance of this phenotypic variation, and I used a traditional linkage mapping approach to identify the genomic region associated with the presence or absence of AFP. However, the causal variants associated with this phenotype have yet to be identified. Here I present the results of a GWAS using whole-genome sequences for a sample of 52 *Limenitis* individuals that tests the three following competing hypotheses about the mechanisms underlying adaptive phenotypic variation in AFP among western *Limenitis*:

1. The Canonical color patterning gene *optix* is responsible for variation in AFP patterning between *L. lorquini* and *L. weidemeyerii.*
2. A previously undescribed gene, or a trans-acting element of optix, is responsible for the variation
3. Genome mis-assembly of the *Limenitis arthemis* genome is leading to spurious results in low-power analyses as seen in the linkage analysis in Chapter 2

Methods

Sample Collection and Preparation: Genomic DNA was extracted from wild-caught *L. lorquini* (n = 20), *L. weidemeyerii* (n = 20), and individuals with the orange AFP phenotype from the hybrid zone (n = 12). Hybrid samples were selected which showed variation in the extent of orange coloration as judged by eye. The sample spanned individuals where orange was weakly present (n = 4), intermediately present (n = 4), and strongly present (n = 4). Sampling localities (Table 3.1) covered 4 states (CA, OR, NV, CO) to get a representative sample of the genotypic variation within these two species, which are potentially isolated by distance; geographic sampling localities are displayed in

Figure 3.1. In total, geographic sampling included 20 *L. lorquini*, 20 *L. weidemeyerii,* and 12 putatively hybrid individuals. Of the *L. lorquini,* 12 were collected from the San Francisco Bay Area (N39.29, W122.92) and 8 from Josephine county in Oregon (N42.60, W123.36). The *L. weidemeyerii* (n = 20) were primarily collected from Mono county California (n = 10, N38.12, W119.10) and Pershing county Nevada (n = 7, GPS: N40.84, W117.67), but a small sample of individuals (n = 3) from Delta county (n = 38.94, W107.36) in Colorado were also included. Finally, putatively hybrid individuals (n = 12) were collected from sites in Mono County (N38.43, W119.21, n = 3) and Humboldt county in Nevada (N41.78, W118.60, n = 10). Adults were collected using hand-nets, their wings were removed and placed in glassine envelopes with paper vouchers, and bodies were then preserved in either RNALater (Thermo Fisher, Waltham MA) solution or a 70% Ethanol solution. DNA was extracted from ~25 mg of thoracic flight muscle using a DNeasy kit (Quiagen, Valencia CA) following standard protocol and including 20uL of proteinase K. To increase the likelihood of complete lysis, the lysis mixture was allowed to incubate overnight. Final DNA concentrations were determined using a NanoDrop® 2000 spectrophotometer.

Library preparation and Sequencing: Genomic DNA quality was first assessed using an Agilent® (Santa Clara, CA) TapeStation system. Samples that passed quality assessments were prepared for sequencing by ligating Illumina® (San Diego, CA) Nextera PCR primers and indexed adapters, allowing unique identification of each sample. Sequencing was conducted on two separate pools of samples, hereafter called fragment libraries. The first set of libraries included only *L. lorquini* (n = 10) and *L. weidemeyerii* (n = 10)

individuals, originally generated for a separate project (Mullen et al. 2019, in prep), whereas the second included *L. lorquini* (n = 10), *L. weidemeyerii* (n = 10), and putative hybrids (n = 12). Both sequencing runs were conducted on Illumina® HiSeq2500 machines in RAPID mode with 150 bp paired-end reads. The first sequencing run, originally containing four *Limenitis* species (n= 40) including *L. lorquini* (n = 10) and *L. weidemeyerii* (n = 10) was sequenced on three lanes whereas the second library, containing *L. lorquini* (n = 10), *L. weidemeyerii* (n = 10), and Hybrids (n = 12), was sequenced on two. Raw sequence data, including sequence quality, was returned from the sequencing facility demultiplexed by sample. Custom bash scripts were used to check for adapter sequences and, if present, were removed from the data using the Cutadapt (v1.8) software with default parameters and the Illumina adapter sequence as the search template.

Sequence Alignment and Initial Filtering: The Burrows-Wheeler Aligner (H. Li and Durbin 2009) and the bwa-mem algorithm (Heng Li 2013) were used to align sequence reads to the *Limenitis* reference genome (Mullen et al., in prep), which comprises 306.3 megabases (Mb) in 4,786 scaffolds (N_{50} 2.16 Mb), with the longest scaffold approaching 32 Mb. For the analyses presented here, I focused on a reduced set of *Limenitis* scaffolds (n = 236), which had been previously mapped and ordered relative to the *Heliconius melpomene* genome (Davey et al. 2016). Aligned output from BWA was piped directly into the Samtools software (H. Li et al. 2009) to produce binary alignment map (BAM) files for each sample and each lane in our dataset. This is done so that libraries can be assigned unique read group ID's based on sequencing lane. The resulting BAM files were

then merged by sample before being deduplicated and coordinate sorted using Picard (v2.18.11). The resulting merged files were then analyzed using the Genome Analysis Tool Kit v3.7 (McKenna et al. 2010).

Genotypes were called with respect to our reference genome using the UnifiedGenotyper, and hard-filtered using custom scripts and according to GATK best practices recommendations (DePristo et al. 2011). Briefly, custom python scripts were used to generate plots of several variant quality statistics including: Quality by Depth (QD), Fisher Strand (FS, the phred scaled probability of strand bias at a given site), Strand Odd Ratio (SOR), RMS Mapping Quality (MQ), Mapping Quality Rank Sum Test (MQRankSum), and Read Positive Rank Sum (ReadPosRankSum). Each of these plots was compared to their expected distributions for high-quality data to inform the choice of filtering parameters that were applied to the raw variants. Final filters were: "QD < 5", "FS > 60", "SOR > 2", "MQ < 40", "MQRS < -12.5", and "RPRS < -8.0". In each case, variants satisfying any of these criteria were removed from the dataset.

Final Filtering: Finally, variant call files (VCFs) produced by GATK were filtered using the VCFtools software (Danecek et al. 2011) to generate a final data set confident SNP calls. Only biallelic SNPS of high quality (QUAL >30) and with a sequencing depth of 5 or greater per individual were selected. SNPs were further filtered to remove those that deviate significantly from null expectations of Hardy Weinberg equilibrium, to remove SNPs with a minor allele frequency of less than 0.01, and to include only those SNPs that were called for >75% of the individuals in our dataset (Purcell 2007, Alligood 2015).

GWAS: To perform association tests with the SNP data, I first used the software PLINK (v1.9) (Purcell et al. 2007) to produce binary files, and to perform a Principal Components Analysis (PCA) to test for population structure in the data. I then used the binary files, which are compatible with the software suite GEMMA (genome-wide efficient mixed-model association, v0.98), to perform association tests by implementing univariate mixed models (Zhou and Stephens 2012) to test for genotype-phenotype association. These were implemented by fitting a univariate linear model using the "-lm" flag. Tests statistics and p-values were estimated using the Wald test, the likelihood ratio test, and the score test. This analysis was completed twice: once with unfiltered biallelic data (n = 20,609,607 SNPS), and once with filtered highly confident SNP calls (n = 197,575 SNPS). In both cases, GEMMA was set to exclude sites based on minor allele frequency (MAF), missingness (MISS), and deviation from hardy weinberg equilibrium (HWE), however parameters were adjusted (Table 2.3) from their standard values. Results were visualized using custom scripts in conjunction with the "qqman" (S. D. Turner 2018) package in R (R Core Team 2016).

BLAST: Finally, to test the hypothesis of genome mis-assembly, genomic regions with SNP loci showing evidence of significant association to the AFP phenotype were compared to the *Heliconius melpomene* genome (Hmel 2.5) using BLAST (Altschul et al. 1990). This comparison was made because an earlier analysis of synteny between protein coding regions in *limenitis* and *Heliconius* indicated possible mis-assembly of the genome (see Chapter 2). Therefore, to check for concordance between the results of our QTL analysis and those of the GWAS, a 2kbp region around each significant SNP was

extracted from the *Limenitis* reference genome using Samtools. The resulting file was then used to query the *Heliconius melpomene* genome in a Discontiguous Megablast (BLAST+ v2.7.1) search with default settings. Resulting matches were sorted by bit score and by length and were recorded if they spanned more than 10% of the query sequence (i.e., they were more than 200bp in length).

Results

Sequencing: To produce sequence data for the 52 samples included in this dataset, two separate sequencing runs were used. In the first sequencing run, we sequenced 20 individuals across two separate lanes of HiSeq2500 sequencing, which returned a total of ~860 million reads, and an average of 42 million unmapped reads per sample. Average mapping rate was roughly 86%, likely due to the fact that I analyzed a subset of all scaffolds in the full genome sequence of *L. arthemis* (see Methods). However, the variance in mapping rate was high at the extreme ends, with mapping success only 6.7% for one sample due to significant read mispairing. If this sample is excluded, mapping rate increases to 91%. As a result, this sample was excluded from all further analyses. In the second sequencing run, 32 individuals were sequenced across two lanes of HiSeq2500 and returned ~590million reads and an average of 18 million reads per sample. Mapping rate was higher in the second run, with ~93% of reads mapped to the genome, an average of 17 million reads per sample. There was also variation in sequencing depth among samples, with a maximum of 29.8 million reads and a minimum of 10.8 million reads assigned to single samples. See Table 3.1 for more information about sequencing results.

Raw data set statistics: Sequences were filtered according to GATK best practices which produced a file containing 32 million unfiltered variants. Summary statistics were generated from this dataset using VCFTools (v0.1.16). The mean read depth per individual for the set of 32M variants was 10.6 which was very similar to mean read-depth-per-sample of 10.03. However, this global average obscures the differences between the two libraries. Library 1, containing only *L. weidemeyerii* and *L. lorquini* had an average read depth of 14.4, whereas Library 2 had roughly half as many reads with 7.6. This results in an average missingness in Library 2 (31%) that is much higher than the missingness in Library 1 (0.06%) when the individual with poor alignment results is excluded. This difference in missingness between runs impacts the later filtering, as excluding sites that are not present in more than 70% of individuals would exclude a significant proportion of the sites found in Library 1 that are not also found in Library 2. Call quality was high, with an average QUAL score of 1810.69 in the full dataset and only 1.8 million sites (0.6%) with a QUAL score less than 30.

Following a second round of filtering to retain only high-quality SNPs, the mean depth-by-site for this dataset was higher at 14.56, but the mean depth by individual is lower, at 13.78. When calculated separately for each sequencing run, the source of this variance becomes clear. Library 1 has a higher average read depth-by-individual than in the initial dataset that was only filtered by quality using GATK. The new read depth-by-individual increases to 19.99 from 14.4 following the second round of filtering in library one, whereas library two only increases to 10.3 from 7.6. Library one has an average missingness of 7% in whereas Library 2 still has high missingness after final filtering,

with an average 28%. Average quality is much higher in the filtered dataset (QUAL = 3863.3) and, as expected after filtering, none of the sites have a quality score of less than 30. Overall, the filtered dataset clearly contains SNPs of higher quality than the unfiltered and initially filtered datasets, but it loses a very significant number of SNPS (~32 million vs ~22 million).

Principal Components Analysis: To scrutinize patterns of genetic structure among our samples, we performed a principal components analysis in PLINK (v1.9). Based on the first two principal component axes, the samples are separated into four distinct clusters (Figure 3.2), corresponding to geography and phenotype, indicating that there is population structure in this dataset. Two of these clusters represent, respectively, *L. lorquini* individuals from Oregon and the San Francisco Bay area, and hybrid individuals from Nevada. The two remaining clusters comprise individuals that phenotypically resemble pure *L. weidemeyerii* and lack any apparent orange forewing coloration. Surprisingly, these two phenotypically similar clusters do not overlap in the PCA, but are instead separated largely by the second principal component axis, which explains ~2.5% of the variation in the data. These two clusters comprise individuals from the first and second dataset, which are also separated geographically. Library 1 *L. weidemeyerii* were all collected from a single site (GPS: N38.12, W119.08) where individuals with orange AFPs were also collected, whereas Library 2 was composed of individuals from sites in Mono county California (GPS:), Pershing county Nevada (GPS: N40.84, W117.67), and Gunnison county Colorado (GPS: 38.94, W107.30). The geographical distribution of these samples may account for the differences in position along the second principal

component.

GWAS: To identify potentially causative SNPs, I performed a genome-wide association analysis employing a univariate linear model and estimated the significance of the association between individual SNPs and the orange AFP phenotype. This same procedure was repeated twice, once each for a larger (unfiltered, n SNPs = ~22 million) and smaller (filtered, n SNPs = ~207 thousand) SNP datasets (see details in methods, Table 3.3). The GWAS using the larger, unfiltered, SNP dataset found statistically significant evidence for an association between 13 SNPs and the AFP phenotype, with each of these SNPs having a p-value of $1.0x10^{-30}$ or smaller when calculated utilizing a likelihood ratio test (Table 3.3). In contrast, analysis of the smaller filtered SNP dataset yielded a slightly larger number of associated SNPs (24), with p-values of $1.0x10^{-17}$ or smaller based on likelihood ratio tests (Table 3.4). Surprisingly, no SNP is found to be significantly associated in both analyses. However, three scaffolds (scaffold00006, scaffold 00035, and scaffold00176) included significantly associated SNPs in both analyses, although none of these associated scaffolds included a SNP that has significant association in both analyses. This is likely due to the variable effects of filtering on effective sample size and statistical power at individual SNPs. In contrast to our hypotheses, none of the scaffolds on which these associated SNPs were found were predicted to be syntenic with the scaffold in *Heliconius* that contains *optix* (see supplemental data).

Finally, one of the associated SNPs identified in the smaller dataset is located within the *Limenitis* scaffold that contains the *optix* protein coding domain. This SNP,

called “Locus 20” in this analysis, is found on *Limenitis* scaffold “scaffold00223”, at position 57,614 bp. This is quite close to the *optix* coding region, which is begins roughly 14Kbp away at position 43,397 bp. The location of the optix coding region in the *Limenitis* genome was determined by a BLAST alignment of both the nucleotide sequence and protein sequence from *Heliconius*. Both alignments identified the region around 43Kbp within “scaffold00223” as the location of the *optix* protein.

BLAST alignment: A 2Kbp sequence surrounding each of the associated SNPs from the large and small datasets was used as a query sequence in a BLAST search against the *Heliconius melpomene* genome (Hmel2.5). The regions encompassing seven of the 13 significant SNPs from the large dataset generated alignments that exceeded 200bp in length (Table 3.4). These seven alignments matched four different *Heliconius* scaffolds with scaffolds “Hmel 206001o” and "Hmel216002o" appearing three times each. In both of these cases, these BLAST alignments are not unique, but rather the result closely linked significant SNPs falling within virtually identical 2Kbp regions that align to the same genomic regions. The most highly associated SNPs are equally associated and have p-values (designated "Locus 1" and “Locus 2” in this analysis), which have a p-value three orders of magnitude smaller than the next-most associated SNPs. Only one of these two, “Locus 1”, aligned to the *Heliconius* genome, and it aligned to a scaffold that contains the protein coding region of *optix* (i.e., "Hmel218003o"), but aligned to ~7.5Mbp region, whereas *optix* is found at ~700Kbp. This alignment is at odds with an overall analysis of synteny between *Limenitis* and *Heliconius,* in which *Limenitis* “scaffold00021” was found to be most similar to the *Heliconius* scaffold

“Hmel204001o”. However, this result accords with the results of the QTL analysis (see Chapter 2), in which a region between 6.8 and 7.9Mbp was found to be associated with the phenotype. Both "Locus 2" and "Locus 4/7" from the QTL analysis are found on linkage group 8 and aligned to the 6.8-7.9Mbp region of the same *Heliconius* scaffold as the alignment from this highly associated SNP on “scaffold00021”. In the linkage analysis, these two QTL loci were adjacent, and both showed an association with the phenotype. Genes in this QTL region were identified as Orthologs of Toll-Like Receptor (TLR) proteins, as nucleotide binding proteins, and as translation initiation factors. TLR’s are a class of membrane-bound ligand-binding proteins well known for their role in innate immune responses (Botos, Segal, and Davies 2011), whereas the other two protein types bind nucleotides and initiate translation, respectively.

Among the 23 SNPs identified as significant in the small dataset, 13 produced sequence alignments longer than 200bp. These 13 SNPs mapped to nine different *Heliconius* scaffolds with three aligning to "Hmel218003o" and three others to "Hmel206001o". It should be noted that all three of the alignments to "Hmel206001o" are from the same region of the *Limenitis* scaffold "scaffold00006" and so the query sequences generated from this set of SNPs overlap considerably and identify a single small region of the genome. The same cannot be said of the three loci that align to "Hmel218003o", each of which all come from different *Limenitis* scaffolds. "Locus 6" in this analysis aligns to this region of the *Heliconius* chromosome at roughly 7.6Mbp. Despite being found on a different *Limenitis* scaffold from the SNP in the large analysis, this alignment is again found between 6.9 and 8.5Mbp, which is consistent with the

results of the QTL analysis. Finally, "Locus 15" from the filtered analysis also aligns to the *Heliconius* "Hmel218003o" scaffold, but outside of the region found to be most strongly associated in the QTL analysis.

Discussion

In this study, I have attempted to identify SNPs associated with the orange AFP phenotype in *L. lorquini* by analyzing whole-genome sequencing data from both parental and hybrid populations of *Limenitis* found in western North America. Samples were drawn from a variety of populations spanning four states and included 52 individuals in total. Based on experiments and analyses completed in Chapters 1 and 2, I expected to find at least one genomic region with one or more highly associated SNPs that map to one of the *Limenitis* scaffolds that was also found to harbor a QTL. I also expected to find that associated SNPs would align to the *Heliconius* genome in the same regions as those covered by the QTLs. Alternatively, I expected to find SNPs that were associated directly with *optix* (Martin et al. 2014; Reed et al. 2011). This latter hypothesis, though not supported by the results of my QTL mapping experiment, continues to be relevant because all of the RAD-seq loci from the *Limenitis* scaffold that contains the *optix* protein (i.e., "scaffold00223") were filtered out of the final QTL data set (see Chapter 2). This means that it was impossible to find a direct association with *optix* in that experiment. Given prior evidence from other butterfly species, notably *Heliconius* (Martin et al. 2014; Reed et al. 2011), that *optix* influences multiple aspects of color pattern variation and is responsible for adaptive differences in patterns of red pigmentation, it was a logical putative candidate gene in *Limenitis*. It is also possible that apparent genomic distance

between *optix* and the RAD-seq QTL as well as some of the significant SNPs from the GWAS, which mapped to similar locations in *Heliconius,* is an artifact of either genome mis-assembly, incomplete assembly and/or chromosomal rearrangements between *Heliconius* and *Limenitis.* The GWAS analysis found evidence for a small handful of significantly associated SNPs that map to a variety of scaffolds in the *Limenitis* genome assembly. Intriguingly, in both analyses, a pair of strongly associated SNP loci map to the same general region of the *Limenitis* genome identified in chapter 2. While this result seems to support the hypothesis of a novel color patterning locus or trans-acting factor influencing *optix* expression, additional experiments will be necessary to confidently rule out concerns about the quality of genome assembly.

GWAS analysis of both unfiltered and filtered genotype data supports the hypothesis of a causative relationship between gene regions that align to *Heliconius* scaffold "Hmel218003o" and the AFP phenotype (Figure 3.5). In each association analysis, SNPs aligning to this scaffold were significantly associated with the variation in the presence or absence of AFP. This is particularly convincing in the analysis of the larger SNP dataset, in which one of the two most strongly associated SNPs (both $p = 2.75E^{-35}$) was found to align to this scaffold. When the region around this SNP is aligned to the *Heliconius* genome, it aligns to a region of "Hmel218003o" at roughly 7.5Mbp, which is within a region flanked by two RAD-seq QTL (see Chapter 2). "Locus 6" in the filtered analysis also aligns to the same region of the same *Heliconius* scaffold at roughly 7.6Mbp, despite being found on a different *Limenitis* scaffold. Finally, "Locus 14" from the filtered analysis aligns to the same region, but further downstream, at roughly

8.5Mbp. Taken together, the results of both my RAD-seq QTL mapping experiment and GWAS analysis support a putatively causal association between this genomic region, comprising QTL linkage group 8, and the AFP phenotype.

Finding SNPs that align to the *optix*-containing *Heliconius* scaffold and that are associated with the presence or absence of AFP in *Limenitis* in two different, independent experiments is consistent with the *a priori* hypothesis that this well-known color-patterning gene may control or influence the expression of this trait in this system. However, these SNPS do not align to the region of the *Heliconius* scaffold that produces the protein *optix* (~700 kbp). Rather, they align significantly upstream of this region, between 6.8 Mbp and 7.9 Mbp. When the protein coding genes in this region of the *Heliconius* genome were investigated, several putative proteins were found. Particularly compelling were a pair of proteins called "HMEL034380" and "HMEL016208," which were found near the alignments of QTL Loci 4 and 7. These two proteins code for a "nucleic acid binding protein" and a "translation initiation factor," respectively. Given that *optix* itself is a transcription factor regulating red-orange color in *Heliconius* (Reed et al. 2011), it is possible that these genes are transcription factors that regulate red-orange color patterning in *Limenitis*. Another possibility is that these genes, or another gene nearby, regulate the function of *optix* as trans-acting elements, as suggested in Chapter 2. However, this conclusion is premature without either a functional demonstration of the link between one of these genes and the phenotype, or evidence of reduced gene flow between *L. lorquini* and *L. weidemeyerii* in this region of the genome.

Interestingly, I also found a SNP ("Locus 20") significantly associated with the

phenotype on *Limenitis* scaffold "scaffold00223". This scaffold, which is only 91 Kbp in length, contains the protein coding region of *optix* in the *Limenitis* assembly. While not the strongest association in the dataset based on statistical significance, its presence represents intriguing evidence for a possible role of *optix* in regulating red-orange color pattern in *Limenitis*. Importantly, this associated SNP is not within the coding region of *optix* based on a BLAST alignment with the *Heliconius* genome. This sequence aligns to the 690 Kbp region of the *Heliconius* scaffold "Hmel218003o", whereas the *optix* gene itself is found at ~706 Kbp. It is possible that this SNP represents a cis-regulatory mutation that affects the expression of this gene in *L. lorquini*, similar to findings of *optix* regulation in *Heliconius* (Reed et al. 2011). Thus, it is possible that color pattern variation, including the presence, absence and/or extent of orange pigmentation on the forewings of *Limenitis*, may be the result of both cis- and trans-acting factors influencing spatial patterns of *optix* expression.

While this hypothesis is intriguing, the GWAS also found significant associations at a number of other loci spread across the genome (Tables 3 and 4). These other loci appear to have no relationship to the strongest QTL based on BLAST alignments to the *Heliconius* genome. Although these may be true associations, confidence in their veracity is lower because of the lack of corroborating evidence from the QTL mapping experiment. This concern is reinforced by the limited overlap in the identity of SNPs found in the two different GWAS datasets (unfiltered and filtered). For example, the most strongly associated marker in the smaller dataset, found on *Limenitis* scaffold "scaffold000061", is unique among the top SNPs from either dataset in aligning to

Heliconius scaffold "Hmel209001," but this scaffold is not identified in the QTL analysis. It is difficult to assess whether any individual SNP represents a spurious association. Clearly, however, more functional and population genetic work must be completed to confirm or rule out any of these associations. This is particularly true of loci such as the two "Locus 9" from the filtered and unfiltered analysis, respectively, which align to *Heliconius* scaffold "Hmel206001o" within ~300bp of one another. "Locus 14" from the unfiltered dataset also aligns to this scaffold, albeit 1 Mbp away, suggest that these associations may be genuine despite the lack of concordance with the RAD-seq QTL results.

As mentioned, the discordance between the associations found in the large and small datasets suggests that these results be viewed with caution. However, the way that SNPs were filtered to produce the smaller dataset may partially explain these differences. The final SNP variant calls were derived from a combination of sequencing data from two separate sequencing libraries and runs, generated for different purposes and at different times, resulting in substantial variation in the quality (see Results, specifically discussion of quality scores) and mean depth of the data between libraries. One example of this average number of reads per individual. Sequencing Library 1, which contained only *L. lorquini* and *L. weidemeyerii* individuals from a dataset generated for a different project (Mullen et al. 2019, in prep) had 37 million mapped reads per individual on average, whereas Library 2 had only 17 million mapped reads per individual (Table 3.2). This inequality results in a substantial difference in variant-site-missingness, where individual samples in Library 2 are missing 28% of variants on average. This means that

Library 2 has fewer detected variants than Library 1, which is problematic because Library 2 contains the hybrid individuals and is should therefore more informative for our analysis because the set of shared alleles between orange hybrids and *L. lorquini* that also do not occur in *L. weidemeyerii* should be smaller than when comparing *L. lorquini* to *L. weidemeyerii* directly. Additionally, filtering for SNPS that occur at high confidence in at least 75% of individuals (Alligood 2017; Purcell et al. 2007) results in low SNP retention. Finally, it is possible that removing SNPs using a HWE threshold filter may have skewed the results of the final analyses. Using HWE-based filtering criteria is a common practice in NGS data handling, even when dealing with case-control studies (Wang and Shete 2012; Hosking et al. 2004; Xu et al. 2002), to remove spurious SNP calls resulting from sequencing error. However, there has been some recent discussion about parsing types deviations from HWE to avoid filtering out informative data (Chen, Cole, and Grond-Ginsbach 2017). It is possible that the HWE filter applied in this study negatively impacted the analysis by removing biologically informative deviations from HWE (Chen, Cole, and Grond-Ginsbach 2017). However, selective sweeps of linked markers should lead to a regional increase in genomic signatures of selection around the selected SNP. As a result, selection can be detected by looking for these regional increases, even in instances where a HWE filter removes the causative SNP.

It is important to note that, even when high-quality SNP data are used, GWAS studies have several sources of error, some of which cannot be eliminated from this data. Although GWAS studies of hybrid populations potentially allow for a much longer history of recombination than laboratory crossing experiments, they rely on identifying

populations that vary based in the trait of interest, but which do not exhibit strong genome-wide divergence or population structure (Pallares et al. 2014). To avoid spurious associations, GWAS requires eliminating or at least controlling for allele frequency differences that result from population structure (Astle and Balding 2009; Flint and Eskin 2012; Purcell et al. 2007). Therefore, the relatively large number of associations found throughout the genome in these analyses is not surprising when considering the results of the PCA (Figure 3.2). The PCA showed clear signatures of population structure, particularly along PC1, which accounts for 15.4% of the variance in the data. It is therefore expected that some of the associations found by GEMMA may be spurious. However, because the data from the QTL experiment were generated independently of these data, any concordance between the two is less likely to be the result of spurious association. Denser sampling, particularly from both *L. lorquini*-like and *L. weidemeyerii*-like individuals in the hybrid zone(s) is likely to improve the signal-to-noise ratio in this data (Pallares et al. 2014) and would dramatically increase confidence in these findings.

A further source of error in this dataset is the incomplete assembly and possibility of mis-assembly in the current iteration of the *Limenitis* genome. This possibility is particularly evident in the QTL analysis, in which variants from a given *Limenitis* scaffold are assigned to multiple well-supported linkage groups. In addition, loci found to be associated with the AFP phenotype in both the QTL and GWAS analyses align to similar regions in the *Heliconius* genome within scaffold "Hmel218003o" despite being from a number of different *Limenitis* scaffolds. The *Limenitis* reference was generated

using multiple outbred individuals resulting in high levels of heterozygosity and poor N50 assembly statistics (Mullen pers. comm.). To overcome this challenge, the genome assembly was refined using the software pipeline REDUNDANS (Pryszcz and Gabaldón 2016). REDUNDANS is designed to reduce heterozygosity in genome assemblies, but the resulting scaffolds are a chimeric mixture of multiple haplotypes in the original set of scaffolds (Pryszcz and Gabaldón 2016). If there are assembly errors in the original *Limenitis* genome as a result of high heterozygosity, it is possible that these assembly errors were carried forward into the current analysis and this may be an explanation for the scattered distribution of significantly associated SNPs in the *Limenitis* genome.

Despite these challenges, a subset of the associations presented here agree with the findings of the QTL experiment and analysis presented in Chapter 2, suggesting that a new gene or trans-acting factor is responsible for orange color patterning in *Limenitis* butterflies. This finding is surprising given that other developmental pathways controlling color pattern appear to rely on a small set of highly conserved "developmental toolkit" genes across a variety of phylogenetic depths (Mallet and Barton 1989; Martin and Orgogozo 2013; Martin et al. 2012; Papa, Martin, and Reed 2008; Reed et al. 2011; Sheppard et al. 1985b). This observed conservatism in color pattern genetics calls for a similarly conservative interpretation of these data. Further study, including association studies using larger sample sizes, should be conducted to test these hypotheses. The relationship between color pattern variation and species divergence is well supported in the literature (Mallet and Barton 1989; Jiggins et al. 2001), and the underlying genetic variation largely reflects these differences (Mallet et al. 1990). Therefore, studies that

demonstrate variation in the rates of introgression at these SNPs would further support their causative role in pattern formation while simultaneously casting significant light on the role of these SNPs in maintaining the species boundary between *L. lorquini* and *L. weidemeyerii*.

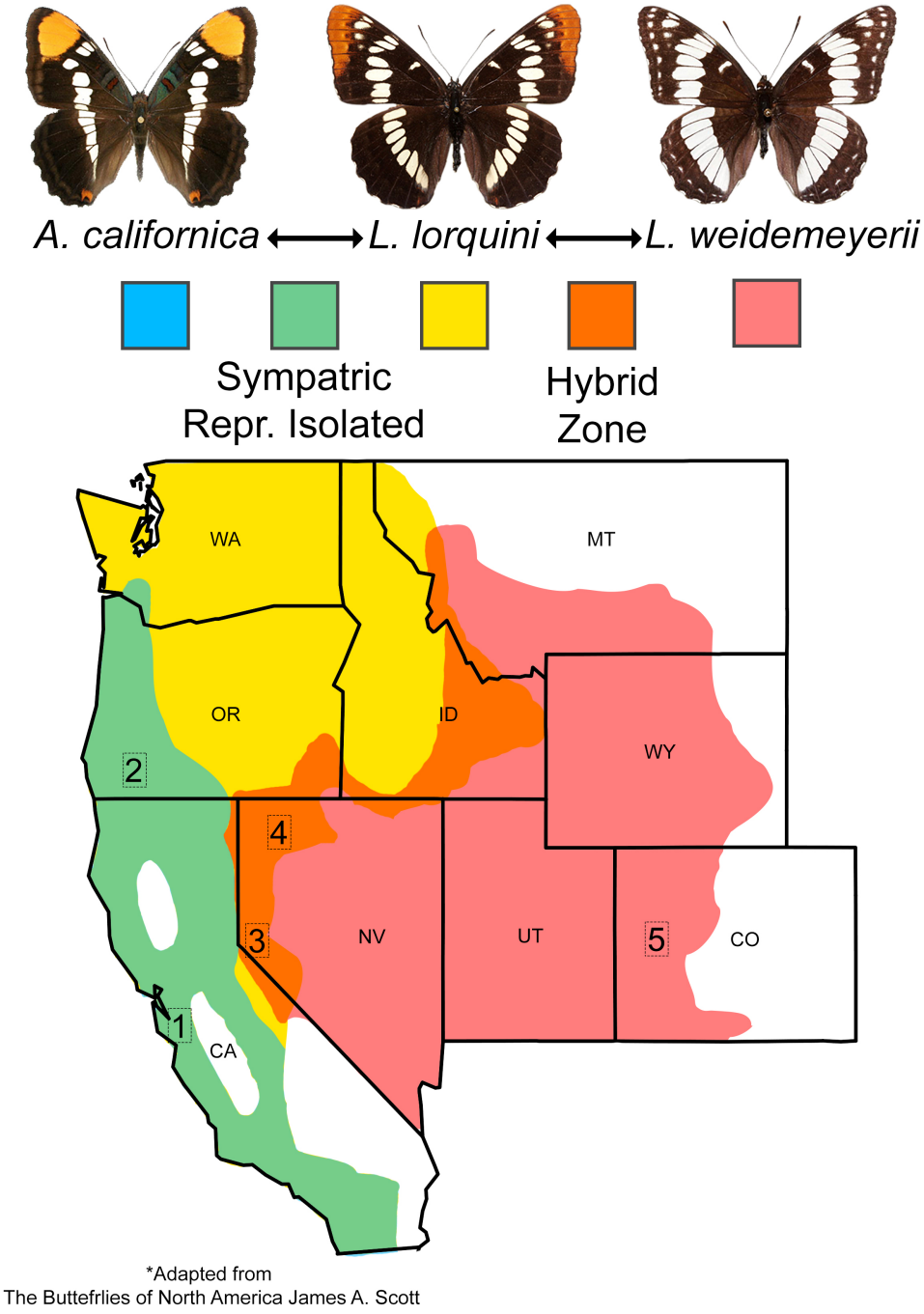

Figure 3.1 Approximate geographic ranges of the species of interest adapted from Scott (1992). The boxed numbers represent approximate locations of each sample locality for the GWAS experiment: 1) Bay Area, 2) Oregon, 3) Mono, 4) Humboldt (individuals were also collected in nearby Pershing county), and 5) Colorado. Note that the range of *A. californica* is represented by blue but is sympatric *with L. lorquini* (yellow) throughout its entire range, so it is represented green.

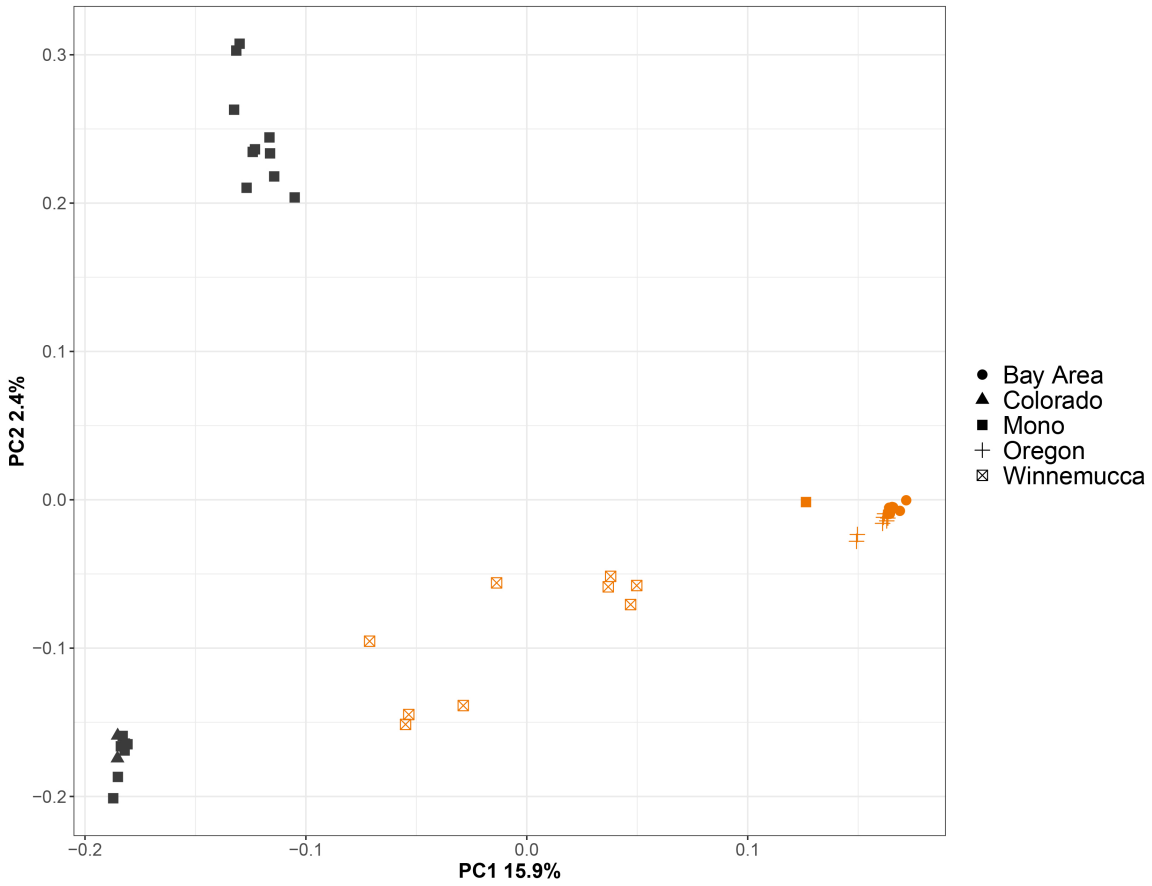

Figure 3.2 Population structure in the unfiltered dataset as represented by plotting samples along the first two principal components. Note that PC1 accounts for ~16% of the variation in the data as compared to just 2.5% for PC2. Colors correspond to phenotype, with orange representing samples that are *L. lorquini*-like and black representing samples that are *L. weidemeyerii*-like. The shape of the points corresponds to their sample locality. Note that the Humboldt hybrid zone (Winnemucca) are intermediate with respect to pure *L. lorquini* and pure *L. weidemeyerii*. The cluster of points above 0.2 on the PC2 axis are all taken from Mono county, and sequenced in Library 1.

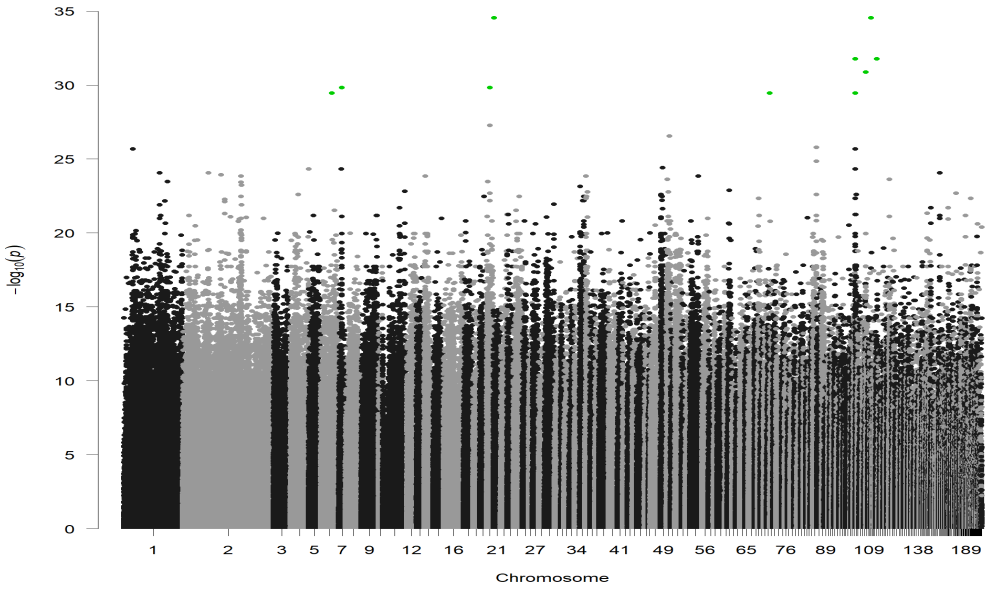

Figure 3.3 GWAS results for the unfiltered dataset. This graph was produced by randomly sampling the 2 million data points without eliminating the top 13 SNPS. The x-axis represents *Limenitis* scaffolds. Green SNPS most strongly associated.

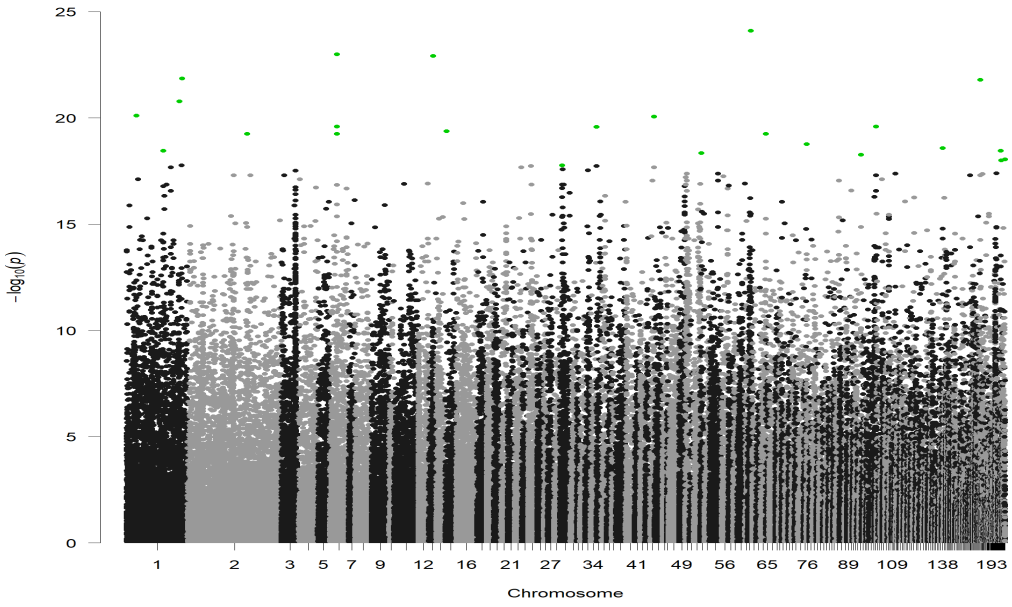

Figure 3.4 GWAS results for the filtered dataset. The x-axis represents *Limenitis* scaffolds. Green SNPS most strongly associated.

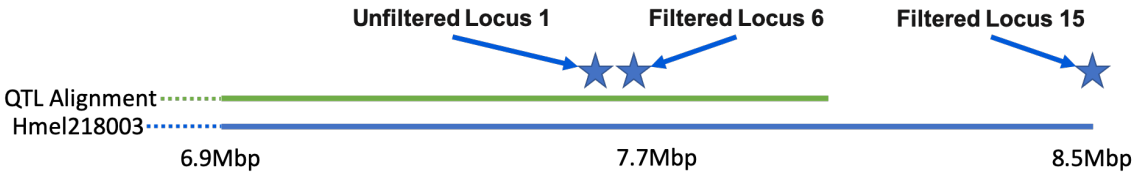

Figure 3.5 A Schematic Representation of the BLAST alignments of selected *Limenitis* loci against the *Heliconius* genome. The green line represents the span across which quantitative trait loci from chapter 2 align to the *Heliconius* genome, and stars represent the location of BLAST alignments for 2 kbp regions around three SNPs.

Tables

Table 3.1 Sample localities of the individual samples used for whole-genome sequencing. Sample names were taken from field labels.

Locality Name	County	State	Approximate GPS	Samples
Winnemucca	Humboldt	Nevada	41.775, -118.603	Hybrid *Limenitis* (N = 10)
Mono	Mono	California	38.425, -119.207	Hybrid *Limenitis* (N = 2) *L. weidemeyerii* (N = 17)
Bay Area	Monterey	California	36.478, -121.740	*L. lorquini* (N = 12)
Oregon	Josephine	Oregon	42.603, -123.359	*L. lorquini* (N = 8)
Colorado	Gunnison	Colorado	38.954, -107.276	*L. weidemeyerii* (N = 3)

Table 3.2 Sequencing results by library.

Sequencing Library	# of Samples	Mapped Reads (mapping %)	Reads Per Sample	Unfiltered Variants Detected
Library 1	*L. lorquini* (n = 10) *L. weidemeyerii* (n = 10)	743,633,877 (86.5%)	**Avg:** 37,181,693 **Max:** 78,137,308 **Min:** 1,985,233	32,314,357
Library 2	*L. lorquini* (n = 10) Putative hybrids (n = 12) *L. weidemeyerii* (n = 10)	549,394,308 (92.9%)	**Avg**:17,168,572 **Max:** 29,751,073 **Min:** 10,823,226	

Table 3.3 Filtering parameters used for each program in the GWAS pipeline.

GATK	BCFTOOLS/VCFTOOLS	GEMMA (Large Data Set)	GEMMA (Small Data Set)
QD < 5	Max Alleles = 2	Hardy Weinberg Equilibrium = 0	Hardy Weinberg Equilibrium = 0
FS > 60	Min Alleles = 2	Minor Allele Frequency = 0.001	Minor Allele Frequency = 0.001
SOR > 2	Skip/Remove Indels	Missingness 0.50	Missingness 0.75
MQ < 40	Output Variant Sites		
MQRS < -12.5	Minimum Depth = 5 (small data set only)		
RPRS < -8.0	Minimum Quality = 30 (small data set only)		
HaplotypeScore > 13.0	Max Missingness = 75% (small data set only)		
Resulting Variants: **32,314,357**	Resulting SNPS: **22,640,612 (large) 207,802 (small)**	Resulting SNPS: **20,609,607**	Resulting SNPS: **197,575**

Table 3.4 The most highly associated SNPS in the GWAS of the unfiltered dataset. This analysis was based on 20 million SNPS.

Locus #	Scaffold	BP	P-value (LRT)	BLAST RESULT	BP	Size of hit	Sequence Identity
Locus 1	scaffold00021	257810	2.75E-35	Hmel218003o	7556121-7556629	518	68.533
Locus 2	scaffold00111	115697	2.75E-35	No major hits			
Locus 3	scaffold00103	56713	1.64E-32	Hmel216002o	4925001-4924801	204	83.33
Locus 4	scaffold00116	340966	1.64E-32	No major hits			
Locus 5	scaffold00108	1945	1.30E-31	No major hits			
Locus 6	scaffold00007	1026855	1.45E-30	No major hits			
Locus 7	scaffold00020	1097933	1.45E-30	No major hits			
Locus 8	scaffold00006	3921118	3.42E-30	No major hits			
Locus 9	scaffold00071	1014192	3.42E-30	Hmel206001o	13735184-13733998	1219	68.499
Locus 10	scaffold00071	1014209	3.42E-30	Overlaps with Locus 9 and 11			
Locus 11	scaffold00071	1014219	3.42E-30	Overlaps with locus 9 and 10			
Locus 12	scaffold00103	18857	3.42E-30	Hmel216002o	4961332-4961128	205	88.293
Locus 13	scaffold00103	18862	3.42E-30	Overlaps with Locus 12			

Table 3.5 Filtered SNPS GWAS. Two BLAST hits have been included despite not being 200bp in length.

Locus #	Scaffold	BP	P-value (LRT)	BLAST RESULT	BP	Size of Alignment	Sequence Identity
Locus 1	scaffold00061	989094	7.84E-25	No major hit			
Locus 2	scaffold00006	2478920	1.08E-22	Hmel206001o	12793690-12793032	682	68.328
Locus 3	scaffold00013	1496886	1.27E-22	No major hit			
Locus 4	scaffold00001	18410329	1.30E-21	Hmel220003o	305088-305321	247	75.304
Locus 5	scaffold00176	29840	1.49E-21	No major hit			
Locus 6	scaffold00001	17432294	1.39E-20	Hmel218003o	7675286-7675494	209	81.818
Locus 7	scaffold00001	3212569	6.12E-20	Hmel202001o	2774232-2774599	373	69.169
Locus 8	scaffold00044	1354467	6.77E-20	No major hit			
Locus 9	scaffold00006	2478304	1.93E-19	Hmel206001o	12793397-12793690	312	68.59
Locus 10	scaffold00101	630073	1.93E-19	Hmel204001o	9343219-9342822	398	71.106
Locus 11	scaffold00035	33036	1.96E-19	Hmel217001o	4942065-4942609	580	71.207
Locus 12	scaffold00015	341694	3.08E-19	Hmel201001o	5218466-5219016	554	75.271
Locus 13	scaffold00002	19660042	4.09E-19	No major hit			
Locus 14	scaffold00006	2480141	4.09E-19	Hmel206001o	12793032-12793460	434	70.507
Locus 15	scaffold00064	1793090	4.09E-19	Hmel218003o	8533881-8534931	1064	64.986
Locus 16	scaffold00076	92261	1.15E-18	No major hit			
Locus 17	scaffold00138	411452	1.78E-18	No major hit			
Locus 18	scaffold00001	12242527	2.33E-18	Hmel210001o	9823668-9823900	233	84.979
Locus 19	scaffold00001	12242541	2.33E-18	overlaps with locus 18			
Locus 20	scaffold00223	57614	2.35E-18	Hmel218003o	693217-693329	114	88.596
Locus 21	scaffold00053	277310	2.92E-18	No major hit			
Locus 22	scaffold00094	643364	3.56E-18	No major hit			
Locus 23	scaffold00628	12914	5.72E-18	No major hit			
Locus 24	scaffold00224	89842	6.27E-18	Hmel205001o	9837424-9837946	527	70.019

Table 3.6 Associated loci from the QTL analysis presented in Chapter 2. Query sequences for BLAST alignments are taken from flanking regions around each associated SNP. Each query sequence is 2kbp in size.

QTL Locus	*Limenitis* scaffold	Linkage Group	Heliconius scaffold	BLAST Start	BLAST End
Locus 1	scaffold00065	12	Hmel218003o	4035060	4033413
Locus 2	scaffold00072	8	Hmel218003o	6861771	6862621
Locus 3	scaffold00065	12	Hmel218003o	5705260	5706470
Locus 4	Scaffold00053	8	Hmel218003o	7932759	7932637
Locus 5	scaffold00092	10	Hmel218003o	4335635	4336056
Locus 7	scaffold00053	8	Hmel218003o	7932759	7932637
Locus 8	scaffold00010	2	Hmel218003o	3104692	3105952
Locus 9	scaffold00092	10	Hmel218003o	4335635	4336056
Locus 10	scaffold00065	12	Hmel218003o	3976436	3976673

Table 3.7 Similarity between the GWAS results and the QTL results based on BLAST alignments of 2kbp flanking sequences.

GWAS SNP Name	Analysis	*Limenitis* scaffold	Heliconius scaffold	BLAST Start	BLAST End	Similar to QTL Locus #
Locus 1	Unfiltered	scaffold00021	Hmel218003o	7556121	7556629	Locus 2/4/7
Locus 1	Filtered	Scaffold00061	Hmel209001o	4085036	4085125	*None*
Locus 6	Filtered	scaffold00001	Hmel218003o	7675286	7675494	Locus 2/4/7
Locus 15	Filtered	scaffold00064	Hmel218003o	8533881	8534931	*None*
Locus 20	Filtered	scaffold00223	Hmel218003o	693217	693329	*None*

CONCLUSION

All of the results of my experimental field work indicate that *L. lorquini* is a Batesian mimic of *A. californica*, and that this the presence or absence of the orange AFP is under selection. While more work will be needed to definitively demonstrate that the AFP is a "speciation phenotype" that maintains the species boundary between *L. lorquini* and *L. weidemeyerii*, there is clear evidence that predator-mediated selection of an adaptive mendelian trait plays a key role in driving the maintenance of biological diversity in the *Limenitis*. Despite analytical challenges in both chapter two and chapter three, I have identified a strong association between the orange AFP phenotype and a region of the *Heliconius* genome (Hmel 2.5) on the same scaffold as the *optix* protein. This conclusion was reached in two independent analyses based on independent datasets and biological samples. Strongly associated SNPS from the GWAS analysis align to a region of the *Heliconius* genome which overlaps the region that was implicated as causative in the QTL analysis, increasing my confidence in these results. These results suggest that a new gene or trans-acting factor is responsible for orange color patterning in *Limenitis* butterflies. Fully characterizing the relationship between this genomic region and the presence of the orange AFP will require additional demonstrations of a functional connection between the genotype and the phenotype. Identifying the function of this gene will advance the field of color pattern genetics and development, give us further insights into the evolution of adaptive color patterns, and allow us to scrutinize the species boundary continuum for traits which predictably lead to the divergence of species.

APPENDIX

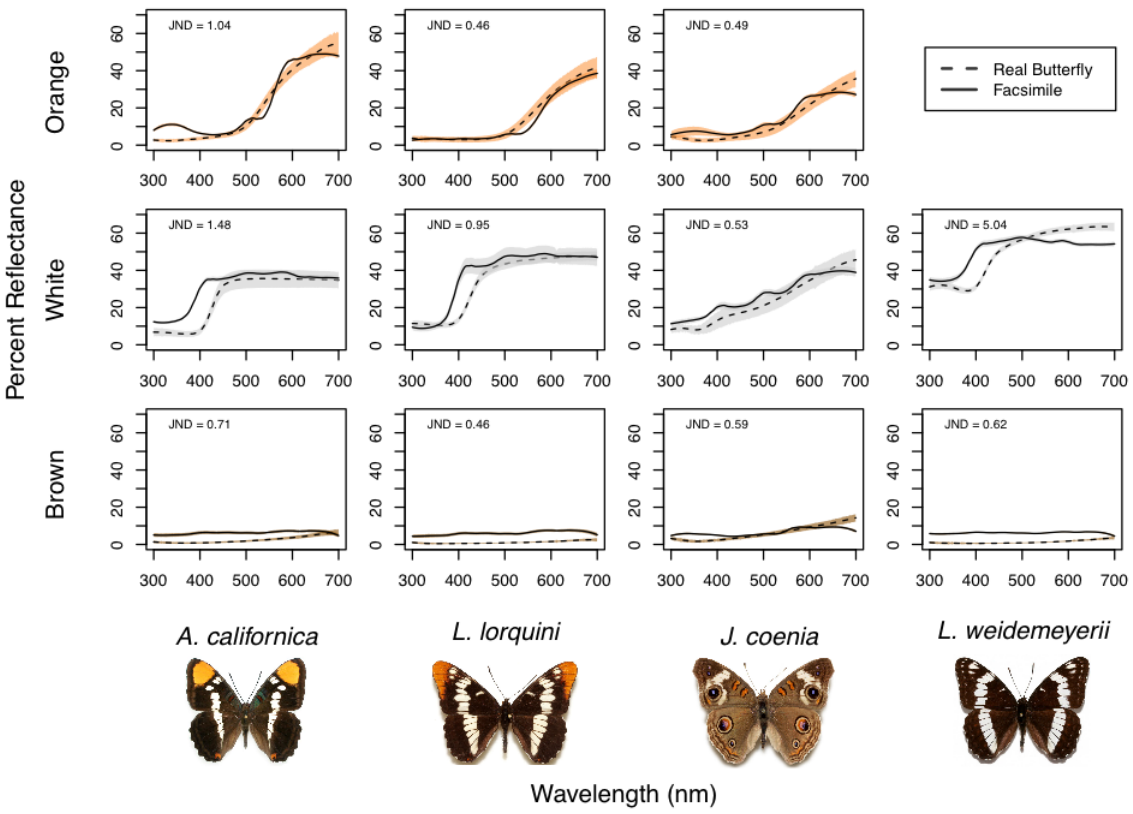

Figure S1 Comparison of the mean spectral reflectance (lines) and 99% confidence intervals (shadow) of real and facsimile color pattern elements. Each line represents a grand mean of three sampling events from each wing of three individuals. L. weidemeyerii does not have orange color-pattern elements, and so was not measured for this color. The solid lines overlain on these graphs represent the reflectance profiles of the artificially constructed facsimile butterflies. Note the similarities between the spectra of the facsimiles with the real wings. A quantitative measure of similarity calculated using the "Blue Tit" visual system is presented in "Just noticeable differences" (JND) above the legend in each graph. The magnitude of these differences appears to be consistent with the differences found in Finkbeiner et al. (2012, 2014, and 2017), with one major exception in L. weidemeyerii white. A JND above 1 is generally considered discriminable in ideal conditions.

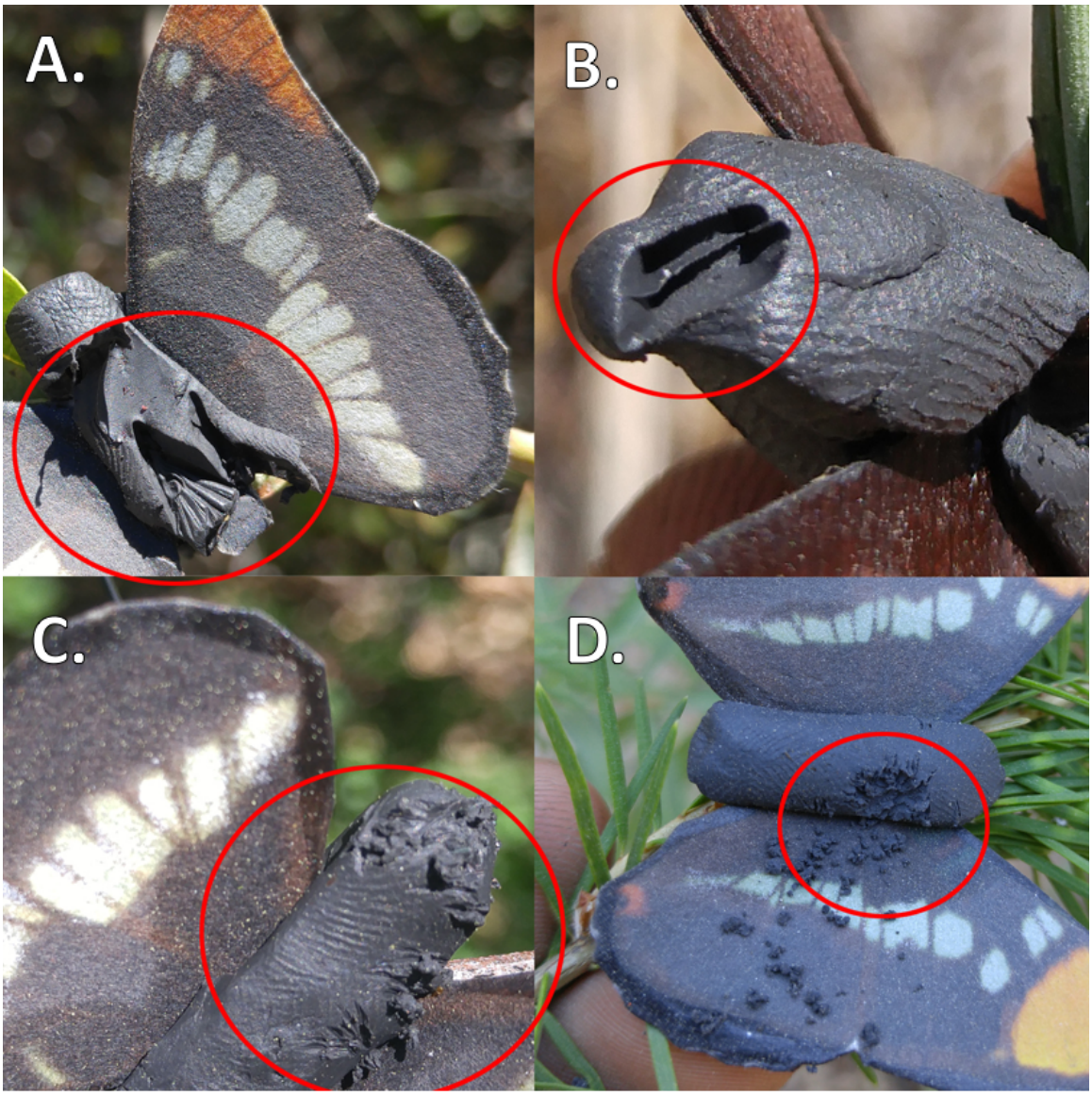

Figure S2 Attack types A) Bird attack B) Rodent attack C) Grasshopper or similar attack D) ant or other hymenopteran. Only attacks that were similar to those in panel A were included in our analysis as a "hit" or "attack". Attacks that were so destructive that it was difficult to determine the type of attack were also excluded.

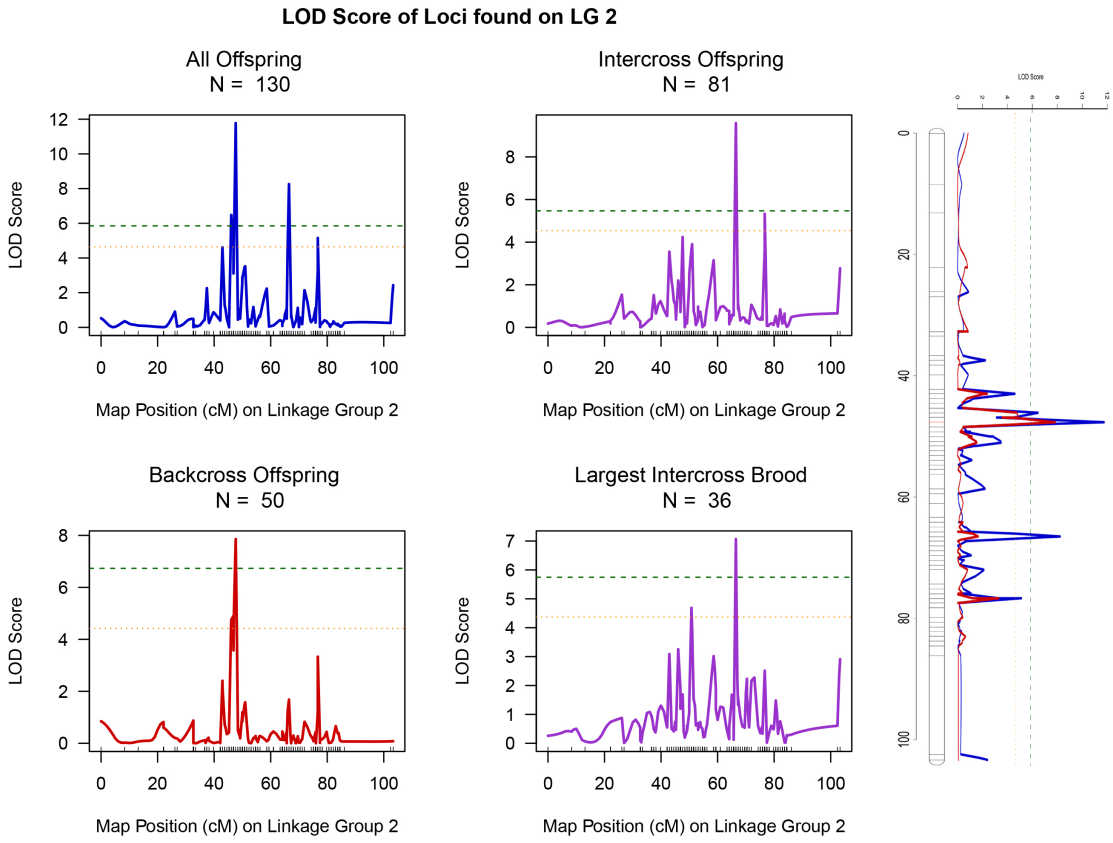

Figure S3 LOD score distributions across the linkage group 2. Each of the small panels on the left shows the LOD scores in the respective linkage group for each QTL analysis. The panels on the right graph combine the "All Offspring" LOD scores and the "Backcross Offspring".

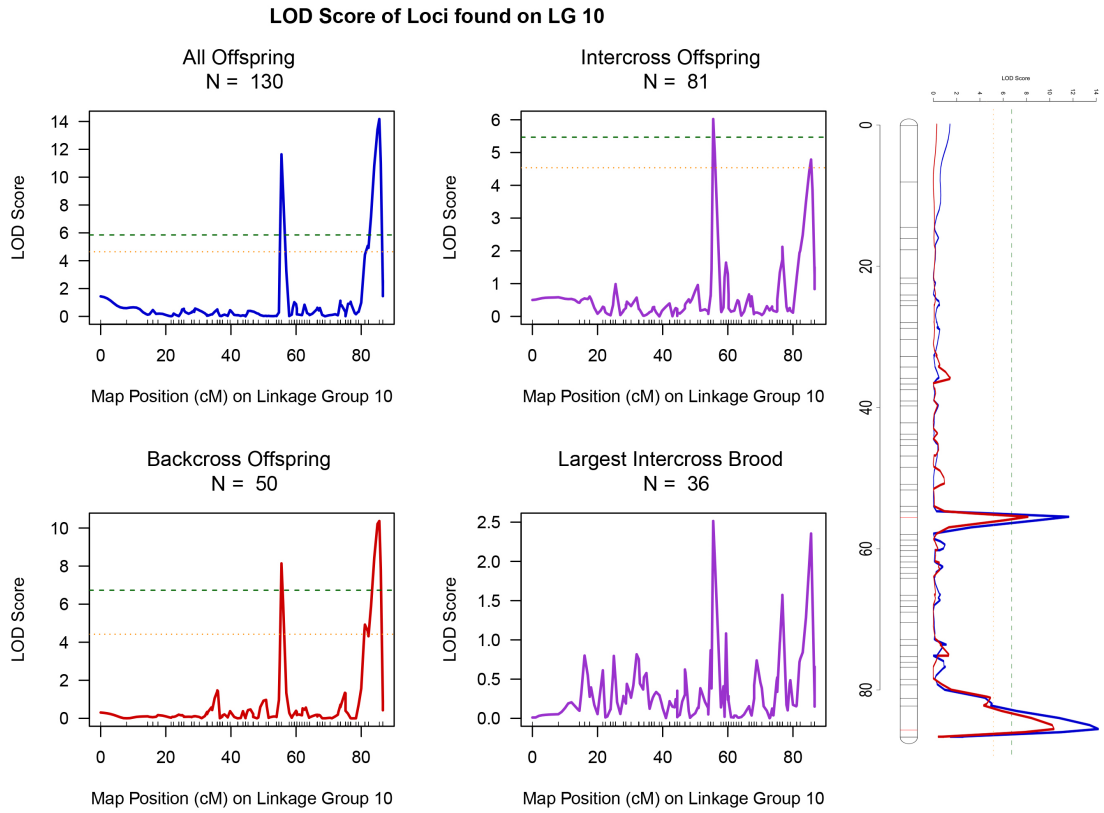

Figure S4 LOD score distributions across the linkage group 10. Each of the small panels on the left shows the LOD scores in the respective linkage group for each QTL analysis. The panels on the right graph combine the "All Offspring" LOD scores and the "Backcross Offspring".

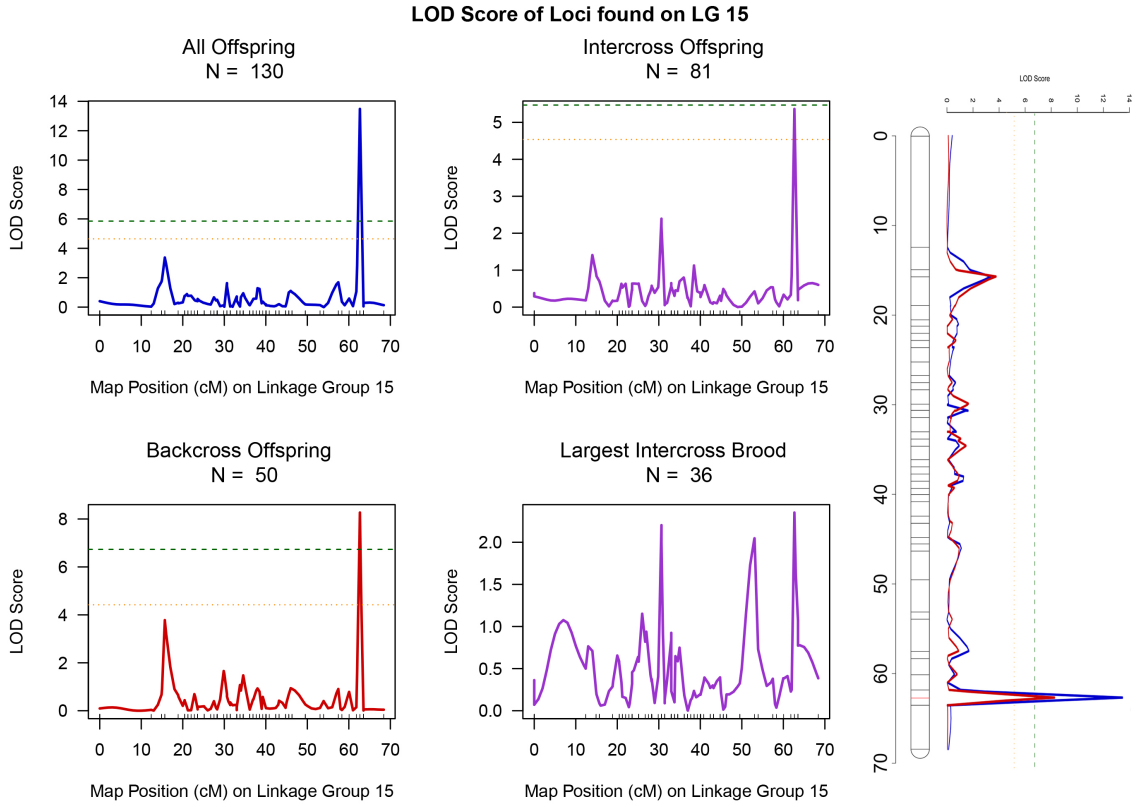

Figure S5 LOD score distributions across the linkage group 15. Each of the small panels on the left shows the LOD scores in the respective linkage group for each QTL analysis. The panels on the right graph combine the "All Offspring" LOD scores and the "Backcross Offspring".

Table S2 GPS coordinates for numbered transects for facsimile placement within the California study area. Each numbered transect contained 20 butterfly facsimiles, five of each species.

California Sites							
Site	Latitude	Longitude	Elevation (m)	Site	Latitude	Longitude	Elevation (m)
1	43.88	-116.18	880	51	43.89	-116.01	1531
2	43.88	-116.18	907	52	43.89	-116.01	1488
3	43.88	-116.17	934	53	43.90	-116.00	1445
4	43.88	-116.18	934	54	43.90	-116.00	1412
5	43.88	-116.17	943	55	43.90	-116.00	1406
6	43.87	-116.17	956	56	43.90	-115.99	1401
7	43.87	-116.17	958	57	43.90	-115.99	1380
8	43.87	-116.17	974	58	43.90	-115.98	1349
9	43.87	-116.16	977	59	43.90	-115.98	1334
10	43.87	-116.16	989	60	43.91	-115.98	1316
11	43.87	-116.16	1000	61	43.91	-115.97	1302
12	43.87	-116.15	1023	62	43.88	-115.91	1252
13	43.87	-116.15	1027	62	43.88	-115.91	1254
14	43.87	-116.14	1047	64	43.88	-115.92	1256
15	43.87	-116.14	1047	65	43.87	-115.91	1257
16	43.87	-116.14	1061	66	43.87	-115.91	1256
17	43.87	-116.13	1071	67	43.87	-115.91	1247
18	43.87	-116.13	1079	68	43.87	-115.91	1245
19	43.87	-116.13	1087	69	43.86	-115.92	1242
20	43.87	-116.12	1093	70	43.86	-115.92	1248
21	43.87	-116.12	1101	71	43.86	-115.92	1279
22	43.87	-116.11	1122	72	43.86	-115.92	1277
23	43.87	-116.11	1126	73	43.85	-115.92	1266
24	43.87	-116.11	1149	74	43.85	-115.93	1228
25	43.88	-116.10	1161	75	43.85	-115.93	1223
26	43.88	-116.10	1168	76	43.85	-115.93	1211
27	43.88	-116.09	1172	77	43.85	-115.92	1235
28	43.88	-116.09	1193	78	43.84	-115.92	1237
29	43.88	-116.09	1203	79	43.84	-115.93	1232
30	43.88	-116.08	1215	80	43.84	-115.93	1225

31	43.88	-116.08	1232	81	43.84	-115.93	1237
32	43.88	-116.08	1254	82	43.84	-115.93	1194
33	43.88	-116.07	1258	83	43.83	-115.94	1190
34	43.88	-116.07	1277	84	43.83	-115.94	1185
35	43.88	-116.07	1279	85	43.83	-115.94	1182
36	43.88	-116.06	1287	86	43.83	-115.94	1173
37	43.88	-116.06	1313	87	43.83	-115.95	1183
38	43.88	-116.06	1306	88	43.82	-115.95	1160
39	43.88	-116.05	1338	89	43.82	-115.95	1154
40	43.88	-116.05	1345	90	43.82	-115.96	1149
41	43.88	-116.05	1360	91	43.81	-115.96	1144
42	43.88	-116.04	1389	92	43.81	-115.96	1149
43	43.88	-116.04	1421	93	43.81	-115.96	1137
44	43.88	-116.03	1442	94	43.80	-115.96	1135
45	43.89	-116.03	1461	95	43.80	-115.96	1124
46	43.89	-116.02	1519	96	43.79	-115.96	1121
47	43.89	-116.02	1517	97	43.79	-115.96	1116
48	43.89	-116.02	1531	98	43.79	-115.96	1109
49	43.90	-116.02	1545	99	43.79	-115.97	1128
50	43.89	-116.02	1583	100	43.78	-115.97	1107

Table S3 GPS coordinates for numbered transects for facsimile placement within the Idaho study area. Each numbered transect contained 20 butterfly facsimiles, five of each species. Note that the 101st transect was a replacement for one of the transects which was destroyed overnight. Data were not counted for this site (Site 60), and were replaced with data from site 101.

Idaho Sites							
Site	Latitude	Longitude	Elevation (m)	Transect	Latitude	Longitude	Elevation (m)
1	39.31	-120.67	1415	51	39.26	-120.68	1548
2	39.31	-120.67	1413	52	39.26	-120.68	1540
3	39.31	-120.66	1417	53	39.26	-120.68	1531
4	39.31	-120.66	1423	54	39.26	-120.68	1539
5	39.31	-120.66	1417	55	39.26	-120.69	1541
6	39.32	-120.66	1390	56	39.26	-120.69	1520
7	39.32	-120.66	1379	57	39.26	-120.69	1521
8	39.33	-120.65	1445	58	39.27	-120.69	1522
9	39.33	-120.65	1518	59	39.27	-120.69	1506
10	39.34	-120.65	1547	61	39.28	-120.68	1511
11	39.34	-120.65	1592	62	39.28	-120.68	1477
12	39.35	-120.65	1665	63	39.28	-120.68	1484
13	39.31	-120.68	1389	64	39.28	-120.68	1495
14	39.31	-120.68	1389	65	39.28	-120.68	1490
15	39.34	-120.65	1613	66	39.29	-120.68	1500
16	39.32	-120.79	1407	67	39.29	-120.67	1505
17	39.32	-120.78	1368	68	39.29	-120.67	1541
18	39.32	-120.78	1353	69	39.29	-120.67	1556
19	39.32	-120.78	1346	70	39.30	-120.67	1566
20	39.31	-120.78	1349	71	39.30	-120.60	1743
21	39.32	-120.77	1358	72	39.30	-120.60	1739
22	39.31	-120.77	1350	73	39.30	-120.61	1744
23	39.32	-120.77	1350	74	39.30	-120.60	1757
24	39.32	-120.77	1371	75	39.30	-120.60	1779
25	39.32	-120.76	1360	76	39.30	-120.60	1784
26	39.32	-120.76	1367	77	39.30	-120.59	1785
27	39.32	-120.76	1338	78	39.30	-120.59	1812
28	39.32	-120.76	1348	79	39.30	-120.59	1791
29	39.32	-120.75	1344	80	39.30	-120.58	1793

30	39.33	-120.75	1345	81	39.30	-120.58	1777
31	39.33	-120.75	1345	82	39.30	-120.58	1782
32	39.33	-120.75	1370	83	39.30	-120.58	1781
33	39.33	-120.75	1364	84	39.30	-120.57	1787
34	39.33	-120.74	1353	85	39.30	-120.57	1789
35	39.33	-120.74	1399	86	39.29	-120.57	1783
36	39.33	-120.74	1389	87	39.29	-120.57	1779
37	39.33	-120.73	1398	88	39.29	-120.56	1797
38	39.33	-120.73	1405	89	39.29	-120.56	1825
39	39.33	-120.72	1382	90	39.29	-120.56	1856
40	39.33	-120.72	1363	91	39.30	-120.61	1753
41	39.27	-120.66	1474	92	39.31	-120.61	1737
42	39.27	-120.66	1468	93	39.31	-120.61	1736
43	39.27	-120.67	1490	94	39.31	-120.61	1738
44	39.27	-120.67	1513	95	39.31	-120.61	1756
45	39.26	-120.67	1503	96	39.31	-120.61	1762
46	39.26	-120.67	1508	97	39.32	-120.61	1780
47	39.26	-120.67	1532	98	39.32	-120.61	1783
48	39.26	-120.67	1558	99	39.32	-120.61	1768
49	39.26	-120.68	1571	100	39.32	-120.61	1762
50	39.25	-120.68	1594	101	43.782	-115.974	1092

Table S4 Linear Distance Diameter estimates of home range size for several putative butterfly predators with known geographic ranges that overlap our study areas. Information was compiled from the Cornell lab of Ornithology website after identifying possible predators of adult Lepidoptera found in our study areas.

Species Name	Common Name	HR Diameter Estimate (m)	Source/Citation
Cyanocitta stelleri	Steller's jay	120	Brown, J. L. 1963a. Aggressiveness, dominance and social organization in the Steller Jay. Condor no. 65:460-484.
Aphelocoma californica	California Scrub Jay	185	Carmen, W. J. 1988. Behavioral ecology of the California Scrub Jay (*Aphelocoma coerulescens*. Phd Thesis, Univ. of California, Berkeley.
Sialia mexicana	Western Bluebird	87	Colestock, K. L. 2006. Landscape scale assessment of contaminant effects on insectivorous birds. Master's Thesis. Utah State Univ. Logan.
Contopus sordidulus	Western Wood Pewee	160	Eckhardt, R. C. 1979. The adaptive syndromes of two guilds of insectivorous birds in the Colorado Rocky Mountains. Ecol. Monogr. 49:129-149.
Empidonax traillii	Willow Flycatcher	160	
Empidonax oberholseri	Dusky Flycatc her	160	
Geothlypis trichas	Common Yellowthroat	167	
Setophaga petechia	Yellow Warbler	155	
Cardellina pusilla	Wilsons Warbler	64	
Geothlypis trichas	Common Yellowthroat	167	
Tyrannus verticalis	Western Kingbird	285	Goldberg, N. H. 1979. Behavior flexibility and foraging strategies in Cassin's and Western kingbirds (*Tyrannus vociferans* and *T. verticalis*) breeding sympatrically in riparian habitats in central Arizona. Phd Thesis. Univ. of Illinois, Champaign-Urbana.
Tyrannus vociferans	Cassin's Kingbird	285	
Sayornis nigricans	Black Phoebe	374	Irwin, K. 1985. Foraging ecology and reproduction of the Black Phoebe in Humboldt County. Master's Thesis. California State Univ., Humboldt.
Turdus migratorius	American Robin	200	Wheelwright, N. T. 1986. The diet of American Robins. Auk 103:710-725. Pitts, T. D. 1984. Description of American Robin territories in northwest Tennessee. Migrant 55:1-6.
Contopus cooperi	Olive Sided Flycatcher	625	Wright, J.M. 1997. Preliminary study of olive-sided flycatchers in central Alaska, 1994-1996. Alaska Department of Fish and Game. Final Report, Juneau, AK
	Average	212.93	

Table S5 Analysis of protein synteny between *Limenitis arthemis* and *Heliconius melpomene. Abbreviations: "Lim.* Scaf #" = *Limenitis* scaffold number, "# of Prot" = number of proteins identified as syntenic.

Lim. Scaf #	Scaffold Length	*Heliconius* Scaffold Name	# of Prot.	*Lim. Scaf* #	Scaf. Len.	*Heliconius* Scaffold Name	# of Prot.
1	20238534	Hmel220003o	281	**120**	634469	Hmel206001o	17
2	31042543	Hmel212001o	204	**121**	517063	Hmel213001o	17
3	5752760	Hmel211001o	102	**122**	650105	Hmel203003o	34
4	6271485	Hmel218003o	228	**123**	1076252	Hmel217001o	27
5	4019797	Hmel212001o	79	**124**	508241	Hmel221001o	19
6	6267820	Hmel213001o	233	**125**	658746	Hmel213001o	8
7	2269647	Hmel210001o	48	**126**	1140381	Hmel202001o	37
8	5386796	Hmel206001o	180	**127**	712281	Hmel219001o	3
9	5858054	Hmel211001o	179	**128**	495129	Hmel210001o	25
10	1458867	Hmel218003o	30	**129**	492438	Hmel201001o	19
11	8233769	Hmel201001o	150	**130**	928579	Hmel202001o	18
12	3355357	Hmel212001o	140	**131**	521612	Hmel217001o	27
13	2556729	Hmel213001o	88	**132**	604839	Hmel212001o	13
14	3162699	Hmel202001o	107	**133**	482309	Hmel219001o	5
15	3547134	Hmel205001o	88	**134**	506823	Hmel201001o	14
16	6875015	Hmel212001o	111	**135**	487974	Hmel201001o	6
17	3171799	Hmel210001o	69	**136**	699878	Hmel213001o	4
18	2322194	Hmel206001o	40	**137**	536548	Hmel212001o	39
19	2371282	Hmel219001o	103	**138**	637629	Hmel214004o	37
20	2288290	Hmel216002o	113	**139**	779874	Hmel210001o	29
21	2455649	Hmel204001o	92	**140**	408467	Hmel213001o	34
22	2270746	Hmel215003o	133	**141**	324269	Hmel206001o	25
23	2139955	Hmel213001o	64	**142**	393696	Hmel201001o	17
24	3062685	Hmel213001o	102	**143**	391830	Hmel207001o	35
25	2109006	Hmel204001o	63	**144**	451884	Hmel217001o	12
26	1355308	Hmel209001o	52	**145**	386701	Hmel221001o	8
27	2069120	Hmel210001o	109	**146**	394660	Hmel201001o	19
28	1999080	Hmel219001o	82	**147**	398823	Hmel203003o	37
29	3454437	Hmel201001o	66	**148**	665096	Hmel206001o	8
30	2163551	Hmel215003o	40	**149**	372466	Hmel216002o	5
31	1054230	Hmel219001o	50	**150**	371301	Hmel212001o	3
32	1837516	Hmel203003o	56	**151**	412550	Hmel210001o	30
33	1745787	Hmel208001o	44	**152**	281590	Hmel217001o	13
34	1866854	Hmel203003o	24	**154**	649692	Hmel202001o	30
35	1723720	Hmel217001o	106	**155**	370870	Hmel215003o	35
36	1735816	Hmel217001o	54	**156**	353604	Hmel220003o	11
37	1716978	Hmel213001o	62	**157**	399799	Hmel217001o	18
38	1320673	Hmel206001o	31	**158**	344322	Hmel214004o	4
39	3276309	Hmel219001o	123	**159**	372444	Hmel207001o	29
40	3066127	Hmel203003o	31	**160**	342822	Hmel209001o	5

41	1831651	Hmel212001o	46	**161**	338576	Hmel213001o	16
42	1614452	Hmel220003o	37	**162**	344360	Hmel202001o	19
43	1678709	Hmel217001o	30	**163**	342532	Hmel210001o	13
44	1517139	Hmel211001o	61	**165**	168079	Hmel219001o	16
45	2628552	Hmel210001o	36	**166**	337719	Hmel212001o	31
46	1378669	Hmel210001o	31	**169**	320377	Hmel215003o	24
47	610524	Hmel205001o	38	**170**	459249	Hmel217001o	29
48	3499841	Hmel207001o	77	**171**	306156	Hmel206001o	15
49	2040198	Hmel216002o	43	**172**	488861	Hmel205001o	18
50	1445474	Hmel211001o	124	**173**	303080	Hmel205001o	14
51	1440006	Hmel216002o	22	**175**	320485	Hmel209001o	12
52	2168477	Hmel221001o	67	**176**	289353	Hmel202001o	7
53	1413128	Hmel214004o	28	**177**	288783	Hmel214004o	4
54	1586677	Hmel213001o	26	**178**	281322	Hmel207001o	15
55	4084496	Hmel201001o	111	**179**	281876	Hmel203003o	23
56	2191474	Hmel210001o	83	**180**	133575	Hmel211001o	13
57	1683119	Hmel208001o	32	**181**	434571	Hmel205001o	10
58	1317330	Hmel219001o	44	**182**	274572	Hmel212001o	20
59	2542647	Hmel201001o	49	**183**	259040	Hmel206001o	5
60	974303	Hmel219001o	20	**184**	264442	Hmel219001o	6
61	1511179	Hmel201001o	77	**185**	253629	Hmel220003o	12
62	1344480	Hmel207001o	27	**186**	237815	Hmel206001o	6
63	1322859	Hmel208001o	61	**187**	238860	Hmel217001o	11
64	1813461	Hmel221001o	28	**188**	216656	Hmel207001o	8
65	1148056	Hmel218003o	44	**189**	213577	Hmel210001o	10
66	2080429	Hmel213001o	42	**190**	221364	Hmel213001o	15
67	1143972	Hmel207001o	113	**193**	254744	Hmel212001o	17
68	914461	Hmel201001o	73	**194**	222002	Hmel220003o	9
69	1120661	Hmel212001o	36	**195**	56798	Hmel212001o	3
70	1086740	Hmel215003o	38	**196**	179439	Hmel217001o	5
71	1088571	Hmel202001o	97	**197**	191896	Hmel212001o	15
72	1050973	Hmel218003o	39	**198**	173172	Hmel203003o	14
73	1046807	Hmel205001o	54	**200**	128885	Hmel220003o	5
74	1917438	Hmel218003o	50	**201**	154764	Hmel217001o	11
75	984617	Hmel215003o	35	**202**	154555	Hmel206001o	3
76	990633	Hmel220003o	62	**205**	150948	Hmel219001o	4
77	978423	Hmel210001o	28	**206**	111925	Hmel218002o	16
78	1289600	Hmel211001o	30	**207**	283271	Hmel217001o	9
79	934792	Hmel219001o	21	**208**	147723	Hmel210001o	9
80	1284799	Hmel211001o	38	**209**	137936	Hmel220003o	12
81	898778	Hmel221001o	49	**210**	137550	Hmel211001o	3
82	890065	Hmel207001o	26	**213**	124546	Hmel208001o	12
83	886375	Hmel215003o	18	**214**	122775	Hmel219001o	11
84	693725	Hmel216002o	13	**216**	123525	Hmel206001o	3
85	839693	Hmel219001o	12	**218**	111700	Hmel221001o	3
86	1409511	Hmel220003o	57	**219**	106543	Hmel218003o	7
87	1603973	Hmel204001o	28	**220**	177456	Hmel202001o	14
88	831753	Hmel211001o	60	**222**	93419	Hmel221001o	5

89	1298327	Hmel207001o	60	**223**	89856	Hmel218003o	2
90	589493	Hmel212001o	17	**224**	176355	Hmel206001o	6
91	782829	Hmel212001o	64	**225**	86696	Hmel213001o	7
92	748645	Hmel219001o	17	**226**	85065	Hmel206001o	5
93	737146	Hmel213001o	14	**229**	79155	Hmel208001o	19
94	906023	Hmel213001o	10	**230**	76750	Hmel217001o	3
95	1040559	Hmel201001o	29	**232**	128780	Hmel218003o	4
96	449767	Hmel201001o	7	**233**	94209	Hmel215003o	3
97	689049	Hmel209001o	28	**237**	65826	Hmel209001o	16
98	222385	Hmel213001o	4	**241**	60570	Hmel212001o	5
99	1526722	Hmel214004o	39	**244**	60836	Hmel208001o	6
100	305432	Hmel220003o	9	**246**	67049	Hmel217001o	3
101	730068	Hmel207001o	40	**248**	56480	Hmel211001o	6
102	671946	Hmel216002o	16	**252**	59267	Hmel217001o	3
103	666662	Hmel216002o	25	**254**	66988	Hmel213001o	3
104	654021	Hmel206001o	32	**256**	46318	Hmel214004o	3
105	955798	Hmel203003o	17	**260**	89940	Hmel206001o	3
106	679534	Hmel217001o	16	**262**	44516	Hmel218003o	3
107	664861	Hmel207001o	21	**274**	77017	Hmel202001o	4
108	638297	Hmel221001o	18	**304**	28574	Hmel204001o	4
109	755462	Hmel208001o	12	**330**	40155	Hmel217001o	3
110	221094	Hmel221001o	4	**362**	21152	Hmel215003o	3
111	496480	Hmel208001o	9	**371**	20344	Hmel210001o	3
112	590229	Hmel205001o	26	**450**	15176	Hmel219001o	4
113	81032	Hmel221001o	7	**454**	14971	Hmel207001o	13
115	596199	Hmel214004o	25	**489**	13937	Hmel205001o	4
116	785840	Hmel221001o	15	**611**	11418	Hmel206001o	3
117	549297	Hmel213001o	19	**628**	14703	Hmel218003o	4
118	715126	Hmel219001o	37	**650**	10843	Hmel202001o	3
119	554589	Hmel205001o	7	**AC Scaf**	171321	Hmel210001o	8

BIBLIOGRAPHY

Ahola, Virpi, Rainer Lehtonen, Panu Somervuo, Leena Salmela, Patrik Koskinen, Pasi Rastas, Niko Välimäki, et al. 2014. "The Glanville Fritillary Genome Retains an Ancient Karyotype and Reveals Selective Chromosomal Fusions in Lepidoptera." *Nature Communications* 5 (September): 4737. https://doi.org/10.1038/ncomms5737.

Alligood, Kristin S. 2017. "Using Natural Populations of Threespine Stickleback to Identify the Genomic Basis of Skeletal Variation." Ph.D., United States -- Oregon: University of Oregon. http://search.proquest.com/docview/1899144663/abstract/E2483C2101BE4C91PQ/1.

Altschul, Stephen F., Warren Gish, Webb Miller, Eugene W. Myers, and David J. Lipman. 1990. "Basic Local Alignment Search Tool." *Journal of Molecular Biology* 215 (3): 403–10. https://doi.org/10.1016/S0022-2836(05)80360-2.

Aristotle. 350BC. *On the Parts of Animals*.

Astle, William, and David J. Balding. 2009. "Population Structure and Cryptic Relatedness in Genetic Association Studies." *Statistical Science* 24 (4): 451–71. https://doi.org/10.1214/09-STS307.

Austin, George T., and Dennis D. Murphy. 1987. "Zoogeography of Great Basin Butterflies: Patterns of Distribution and Differentiation." *Great Basin Naturalist* 47 (2): 186–201.

Bates, H. W. 1862. "Contributions to an Insect Fauna of the Amazon Valley (Lepidoptera:Heliconinae)." *Journal of the Proceedings of the Linnean Society of London. Zoology* 6 (22): 73–77. https://doi.org/10.1111/j.1096-3642.1862.tb00932.x.

———. 1879. "Reservations on Müllerian Mimicry." *Transactions of the Entomological Society of London*, xxviii–xxix.

Beavis, WD. 1994. "The Power and Deceit of QTL Experiments: Lessons from Comparative QTL Studies." In *Proceedings of the Forty-Ninth Annual Corn and Sorghum Industry Research Conference*, 250–266. Washington, DC.

Bilousov, O. O., V. L. Katanaev, and I. A. Kozeretska. 2012. "Miniature as a Hypothetical Regulatory Protein of the Bursicon/Rickets Signaling Cascade in the Wing Epithelia of Drosophila Melanogaster." *Biopolymers and Cell* 28 (4): 288–91. https://doi.org/10.7124/bc.000060.

Botos, Istvan, David M. Segal, and David R. Davies. 2011. "The Structural Biology of Toll-Like Receptors." *Structure (London, England : 1993)* 19 (4): 447–59. https://doi.org/10.1016/j.str.2011.02.004.

Boyd, Bret M, Bruce M Boyd, George T Austin, and Dennis D Murphy. 1999. "Hybridization of Limenitis in the Western Great Basin (Lepidoptera: Nymphalidae)." *Holarctic Lepidoptera* 6 (2): 37–74.

Brakefield, Paul M., and Vernon French. 1999. "Butterfly Wings: The Evolution of Development of Colour Patterns." *BioEssays* 21 (5): 391–401. https://doi.org/10.1002/(SICI)1521-1878(199905)21:5<391::AID-BIES6>3.0.CO;2-Q.

Brock, J P, and K Kaufman. 2003. *Kaufman Field Guide to Butterflies of North America*. Kaufman Field Guides. Houghton Mifflin. https://books.google.com/books?id=kxH-6rPPGpEC.

Broman, Karl W., and Saunak Sen. 2009. *A Guide to QTL Mapping with R/Qtl*. 2009 edition. Dordrecht: Springer.

Broman, Karl W., Hao Wu, Saunak Sen, and Gary A. Churchill. 2003. "R/Qtl: QTL Mapping in Experimental Crosses." *Bioinformatics* 19 (7): 889–90. https://doi.org/10.1093/bioinformatics/btg112.

Brower, Jane Van Zandt. 1958a. "Experimental Studies of Mimicry in Some North American Butterflies: Part I. The Monarch (Danaus Plexippus), and Viceroy (Limenitis Archippus)." *Evolution* 12 (1): 32–47.

———. 1958b. "Experimental Studies of Mimicry in Some North American Butterflies. Part III. Danaus Gilippus Berenice and Limenitis Archippus Floridensis." *Evolution* 12 (3): 273–285.

Brower, Lincoln P. 1984. "Chemical Defence in Butterflies." In *The Biology of Butterflies*, edited by R. I. Vane-Wright and P. R. Ackery, 109–133. London: Academic Press.

Brunetti, Craig R, Jayne E Selegue, Antonia Monteiro, Vernon French, Paul M Brakefield, and Sean B Carroll. 2001. "The Generation and Diversification of Butterfly Eyespot Color Patterns." *Current Biology* 11 (20): 1578–85. https://doi.org/10.1016/S0960-9822(01)00502-4.

Butler, A.G. 1865. "Descriptions of the Characters of Six New Species of Rhopalocerous Lepidoptera in the Collection of the British Museum, With Notes on the Allied Species." In *Proceedings of the Zoological Society of London.*, 1865:485–87. London : Academic Press, [etc.],. https://www.biodiversitylibrary.org/item/90412.

Carpenter, Geoffrey Douglass Hale, and Edmund Brisco Ford. 1933. *Mimicry*. London: Methuen.

Carroll, S., J Gates, D. Keys, S. Paddock, G. Panganiban, J. Selegue, and J. Williams. 1994. "Pattern Formation and Eyespot Determination in Butterfly Wings." *Science* 265 (5168): 109–14. https://doi.org/10.1126/science.7912449.

Catchen, Julian, Paul A. Hohenlohe, Susan Bassham, Angel Amores, and William A. Cresko. 2013. "Stacks: An Analysis Tool Set for Population Genomics." *Molecular Ecology* 22 (11): 3124–40. https://doi.org/10.1111/mec.12354.

Chen, Bowang, John W. Cole, and Caspar Grond-Ginsbach. 2017. "Departure from Hardy Weinberg Equilibrium and Genotyping Error." *Frontiers in Genetics* 8 (October). https://doi.org/10.3389/fgene.2017.00167.

Churchill, G. A., and R. W. Doerge. 1994. "Empirical Threshold Values for Quantitative Trait Mapping." *Genetics* 138 (3): 963–71.

Coppinger, Raymond P. 1970. "The Effect of Experience and Novelty on Avian Feeding Behavior with Reference to the Evolution of Warning Coloration in Butterflies. II. Reactions of Naive Birds to Novel Insects." *The American Naturalist* 104 (938): 323–35. https://doi.org/10.1086/282666.

Cott, Hugh B. 1940. *Adaptive Coloration in Animals*. Methuen & Company, Limited. https://books.google.com/books?id=Mlipx90CC8YC.

Coyne, Jerry A, and Allen H Orr. 2004. *Speciation*. Edited by H Allen Orr. Sunderland, Mass.: Sunderland, Mass. : Sinauer Associates.

Cruickshank, Tami E., and Matthew W. Hahn. 2014. "Reanalysis Suggests That Genomic Islands of Speciation Are Due to Reduced Diversity, Not Reduced Gene Flow." *Molecular Ecology* 23 (13): 3133–3157. https://doi.org/10.1111/mec.12796.

Cuthill, Innes C., Martin Stevens, Jenna Sheppard, Tracey Maddocks, C. Alejandro Párraga, and Tom S. Troscianko. 2005. "Disruptive Coloration and Background Pattern Matching." *Nature* 434 (7029): 72. https://doi.org/10.1038/nature03312.

DaCosta, Jeffrey M., and Michael D. Sorenson. 2014. "Amplification Biases and Consistent Recovery of Loci in a Double-Digest RAD-Seq Protocol." *PLoS ONE* 9 (9): e106713. https://doi.org/10.1371/journal.pone.0106713.

Danecek, P., A. Auton, G. Abecasis, C. A. Albers, E. Banks, M. A. DePristo, R. E. Handsaker, et al. 2011. "The Variant Call Format and VCFtools." *Bioinformatics* 27 (15): 2156–58. https://doi.org/10.1093/bioinformatics/btr330.

Darst, Catherine R., and Molly E. Cummings. 2006. “Predator Learning Favours Mimicry of a Less-Toxic Model in Poison Frogs.” *Nature* 440 (7081): 208–211. https://doi.org/10.1038/nature04297.

Davey, John W, Mathieu Chouteau, Sarah L Barker, Luana Maroja, and Simon W Baxter. 2016. “Major Improvements to the Heliconius Melpomene Genome Assembly Used to Confirm 10 Chromosome Fusion Events in 6 Million Years of Butterfly Evolution.” *G3: Genes, Genomes, Genetics* 6 (March): 695–708. https://doi.org/10.5061/dryad.3s795.

Dell’Aglio, Denise, Martin Stevens, and Chris D. Jiggins. 2016. “Avoidance of an Aposematically Coloured Butterfly by Wild Birds in a Tropical Forest.” *Ecological Entomology* 41 (5): 627–632. https://doi.org/10.1111/een.12335.

DePristo, Mark A, Eric Banks, Ryan Poplin, Kiran V Garimella, Jared R Maguire, Christopher Hartl, Anthony A Philippakis, et al. 2011. “A Framework for Variation Discovery and Genotyping Using Next-Generation DNA Sequencing Data.” *Nature Genetics* 43 (5): 491–98. https://doi.org/10.1038/ng.806.

Ebel, Emily R., Jeffrey M. Dacosta, Michael D. Sorenson, Ryan I. Hill, Adriana D. Briscoe, Keith R. Willmott, and Sean P. Mullen. 2015. “Rapid Diversification Associated with Ecological Specialization in Neotropical Adelpha Butterflies.” *Molecular Ecology* 24 (10): 2392–2405. https://doi.org/10.1111/mec.13168.

Edwards, A W F. 1972. *Likelihood*. Cambridge University Press. https://books.google.com/books?id=8eMIAQAAIAAJ.

Exnerová, Alice, Dana Ježová, Pavel Štys, Lucia Doktorovová, Bibiana Rojas, and Johanna Mappes. 2015. “Different Reactions to Aposematic Prey in 2 Geographically Distant Populations of Great Tits.” *Behavioral Ecology* 26 (5): 1361–1370. https://doi.org/10.1093/beheco/arv086.

Finkbeiner, Susan D., Adriana D. Briscoe, and Sean P. Mullen. 2017. “Complex Dynamics Underlie the Evolution of Imperfect Wing Pattern Convergence in Butterflies.” *Evolution*, 1–11. https://doi.org/10.1111/evo.13165.

Finkbeiner, Susan D., Adriana D. Briscoe, and Robert D. Reed. 2012. “The Benefit of Being a Social Butterfly: Communal Roosting Deters Predation.” *Proceedings of the Royal Society B* 279 (March): 2769–2776. https://doi.org/10.1098/rspb.2012.0203.

Finkbeiner, Susan D, Patricio A Salazar, Sofía Nogales, Cassidi E Rush, Adriana D Briscoe, Ryan I Hill, Marcus R Kronforst, Keith R Willmott, and Sean P Mullen. 2018. “Frequency Dependence Shapes the Adaptive Landscape of Imperfect Batesian Mimicry.” *Proceedings of the Royal Society B: Biological Sciences* 285

(1876). http://rspb.royalsocietypublishing.org/content/285/1876/20172786.abstract.

Fisher, R A, and J H Bennett. 1930. *The Genetical Theory of Natural Selection: A Complete Variorum Edition*. OUP Oxford.

Flint, Jonathan, and Eleazar Eskin. 2012. "Genome-Wide Association Studies in Mice." *Nature Reviews Genetics* 13 (11): 807–17. https://doi.org/10.1038/nrg3335.

Gallant, Jason R, Vance E Imhoff, Arnaud Martin, Wesley K Savage, Nicola L Chamberlain, Ben L Pote, Chelsea Peterson, et al. 2014. "Ancient Homology Underlies Adaptive Mimetic Diversity across Butterflies." *Nature Communications* 5: 4817. https://doi.org/10.1038/ncomms5817.

Gross, Joshua B., Richard Borowsky, and Clifford J. Tabin. 2009. "A Novel Role for Mc1r in the Parallel Evolution of Depigmentation in Independent Populations of the Cavefish Astyanax Mexicanus." *PLOS Genetics* 5 (1): e1000326. https://doi.org/10.1371/journal.pgen.1000326.

Gunder, J. D. 1932. "NEW RHOPALOCERA (LEPIDOPTERA)." *The Canadian Entomologist* 64 (12): 276–84. https://doi.org/10.4039/Ent64276-12.

Harper, George R, and David W. Pfennig. 2007. "Mimicry on the Edge: Why Do Mimics Vary in Resemblance to Their Model in Different Parts of Their Geographical Range?" *Proceedings. Biological Sciences / The Royal Society* 274 (1621): 1955–61. https://doi.org/10.1098/rspb.2007.0558.

Harrison, Richard G. 1993. *Hybrid Zones and the Evolutionary Process*. New York: New York : Oxford University Press. http://books.google.com/books?hl=en&lr=&id=aFJFkVKskYIC&pgis=1.

Hart, N. S., J. C. Partridge, I. C. Cuthill, and A. T. D. Bennett. 2000. "Visual Pigments, Oil Droplets, Ocular Media and Cone Photoreceptor Distribution in Two Species of Passerine Bird: The Blue Tit (Parus Caeruleus L.) and the Blackbird (Turdus Merula L.)." *Journal of Comparative Physiology A: Sensory, Neural, and Behavioral Physiology* 186 (4): 375–387. https://doi.org/10.1007/s003590050437.

Hetz, Martin, and C. N. Slobodchikoff. 1988. "Predation Pressure on an Imperfect Batesian Mimicry Complex in the Presence of Alternative Prey." *Oecologia* 76 (4): 570–573. https://doi.org/10.1007/BF00397872.

Hoekstra, Hopi E., Rachel J. Hirschmann, Richard A. Bundey, Paul A. Insel, and Janet P. Crossland. 2006. "A Single Amino Acid Mutation Contributes to Adaptive Beach Mouse Color Pattern." *Science* 313 (5783): 101–4. https://doi.org/10.1126/science.1126121.

Hosking, Louise, Sheena Lumsden, Karen Lewis, Astrid Yeo, Linda McCarthy, Aruna Bansal, John Riley, Ian Purvis, and Chun-Fang Xu. 2004. "Detection of Genotyping Errors by Hardy–Weinberg Equilibrium Testing." *European Journal of Human Genetics* 12 (5): 395–99. https://doi.org/10.1038/sj.ejhg.5201164.

Howarth, B, M Edmunds, and F Gilbert. 2004. "Does The Abundance Of Hoverfly (Syrphidae) Mimics Depend On The Numbers Of Their Hymenopteran Models?" *Evolution* 58 (2): 367–375. https://doi.org/10.1111/j.0014-3820.2004.tb01652.x.

Huang, Xuehui, and Bin Han. 2014. "Natural Variations and Genome-Wide Association Studies in Crop Plants." *Annual Review of Plant Biology* 65 (1): 531–51. https://doi.org/10.1146/annurev-arplant-050213-035715.

Huheey, James E. 1980. "Batesian and Mullerian Mimicry: Semantic and Substantive Differences of Opinion." *Evolution* 34 (6): 1212–1215.

Jeffords, M. R., J. G. Sternburg, and G. P. Waldbauer. 1979. "Batesian Mimicry : Field Demonstration of the Survival Value of Pipevine Swallowtail and Monarch Color Patterns." *Evolution* 33 (1): 275–286.

Jiggins, Chris D., C. Estrada, and A. Rodrigues. 2004. "Mimicry and the Evolution of Premating Isolation in Heliconlus Melpomene Linnaeus." *Journal of Evolutionary Biology* 17 (3): 680–691. https://doi.org/10.1111/j.1420-9101.2004.00675.x.

Jiggins, Chris D., and W. Owen McMillan. 1997. "The Genetic Basis of an Adaptive Radiation: Warning Colour in Two *Heliconius* Species." *Proceedings of the Royal Society of London. Series B: Biological Sciences* 264 (1385): 1167–75. https://doi.org/10.1098/rspb.1997.0161.

Jiggins, Chris D., Russell Naisbit, Rebecca L. Coe, and James Mallet. 2001. "Reproductive Isolation Caused by Colour Pattern Mimicry." *Nature* 411 (6835): 302–305. https://doi.org/10.1038/35077075.

Jiggins, Chris D., Camilo Salazar, Mauricio Linares, Jesus Mavarez, and Phil Trans R Soc B. 2008. "Review. Hybrid Trait Speciation and Heliconius Butterflies." *Philosophical Transactions of the Royal Society of London. Series B, Biological Sciences* 363 (1506): 3047–3054. https://doi.org/10.1098/rstb.2008.0065.

Jiggins, Chris D., Richard W. R. Wallbank, and Joseph J. Hanly. 2017. "Waiting in the Wings: What Can We Learn about Gene Co-Option from the Diversification of Butterfly Wing Patterns?" *Philosophical Transactions of the Royal Society B: Biological Sciences* 372 (1713): 20150485. https://doi.org/10.1098/rstb.2015.0485.

Joron, Mathieu, and James Mallet. 1998. “Diversity in Mimicry: Paradox or Paradigm?” *Trends in Ecology and Evolution* 13 (11): 461–466. https://doi.org/10.1016/S0169-5347(98)01483-9.

Joron, Mathieu, Riccardo Papa, Margarita Beltrán, Nicola Chamberlain, Jesús Mavárez, Simon Baxter, Moisés Abanto, et al. 2006. “A Conserved Supergene Locus Controls Colour Pattern Diversity in Heliconius Butterflies.” *PLoS Biology* 4 (10): e303. https://doi.org/10.1371/journal.pbio.0040303.

Kapan, Durrell D. 2001. “Three-Butterfly System Provides a Field Test of Mullerian Mimicry.” *Nature* 409 (January): 18–20.

Kikuchi, David W., and David W. Pfennig. 2010. “Predator Cognition Permits Imperfect Coral Snake Mimicry.” *The American Naturalist* 176 (6): 830–834. https://doi.org/10.1086/657041.

Korte, Arthur, and Ashley Farlow. 2013. “The Advantages and Limitations of Trait Analysis with GWAS: A Review.” *Plant Methods* 9 (July): 29. https://doi.org/10.1186/1746-4811-9-29.

Kristiansen, E.B. Evan B., Susan D. S.D. Finkbeiner, Ryan I. R.I. Hill, Louis Prusa, and Sean P. S.P. Mullen. 2018. “Testing the Adaptive Hypothesis of Batesian Mimicry among Hybridizing North American Admiral Butterflies.” *Evolution* 72 (7). https://doi.org/10.1111/evo.13488.

Kronforst, Marcus R., Gregory S. Barsh, Artyom Kopp, James Mallet, Antónia Monteiro, Sean P. Mullen, Meredith Protas, Erica B. Rosenblum, Christopher J. Schneider, and Hopi E. Hoekstra. 2012. “Unraveling the Thread of Nature’s Tapestry: The Genetics of Diversity and Convergence in Animal Pigmentation.” *Pigment Cell & Melanoma Research* 25 (4): 411–33. https://doi.org/10.1111/j.1755-148X.2012.01014.x.

Kronforst, Marcus R., Durrell D. Kapan, and Lawrence E. Gilbert. 2006. “Parallel Genetic Architecture of Parallel Adaptive Radiations in Mimetic Heliconius Butterflies.” *Genetics* 174 (1): 535–39. https://doi.org/10.1534/genetics.106.059527.

Kronforst, Marcus R., and Riccardo Papa. 2015. “The Functional Basis of Wing Patterning in Heliconius Butterflies: The Molecules Behind Mimicry.” *Genetics* 200 (1): 1–19. https://doi.org/10.1534/genetics.114.172387.

Kunte, K, W Zhang, a Tenger-Trolander, D H Palmer, A Martin, R D Reed, S P Mullen, and M R Kronforst. 2014. “Doublesex Is a Mimicry Supergene.” *Nature* 507 (7491): 229–232. https://doi.org/10.1038/nature13112.

Lander, E. S., and D. Botstein. 1989. “Mapping Mendelian Factors Underlying Quantitative Traits Using RFLP Linkage Maps.” *Genetics* 121 (1): 185–99.

Lange, Kenneth, and Michael Boehnke. 1982. “How Many Polymorphic Marker Genes Will It Take to Span the Human Genome?” *American Journal of Human Genetics* 34 (6): 842.

Lecuit, Thomas, William J. Brook, Medard Ng, Manuel Calleja, Henry Sun, and Stephen M. Cohen. 1996. “Two Distinct Mechanisms for Long-Range Patterning by Decapentaplegic in the Drosophila Wing.” *Nature* 381 (6581): 387. https://doi.org/10.1038/381387a0.

Ledersouse, Robert C. 1993. “Territoriality along Flyways as Mate-Locating Behavior in Male Limenitis Arthemis (Nymphalidae).” *Journal of the Lepidopterists’ Society* 47 (1): 22–31.

Lepidopterist’s Society. 2016. *Lepidopterist’s Society Database*. https://www.floridamuseum.ufl.edu/lepsoc/.

Li, H., and R. Durbin. 2009. “Fast and Accurate Short Read Alignment with Burrows-Wheeler Transform.” *Bioinformatics* 25 (14): 1754–60. https://doi.org/10.1093/bioinformatics/btp324.

Li, H., B. Handsaker, A. Wysoker, T. Fennell, J. Ruan, N. Homer, G. Marth, G. Abecasis, R. Durbin, and 1000 Genome Project Data Processing Subgroup. 2009. “The Sequence Alignment/Map Format and SAMtools.” *Bioinformatics* 25 (16): 2078–79. https://doi.org/10.1093/bioinformatics/btp352.

Li, Heng. 2013. “Aligning Sequence Reads, Clone Sequences and Assembly Contigs with BWA-MEM.” *ArXiv:1303.3997 [q-Bio]*, March. http://arxiv.org/abs/1303.3997.

Lindström, L., Rauno V. Alatalo, Johanna Mappes, Marianna Riipi, and Laura Vertainen. 1999. “Can Aposematic Signals Evolve by Gradual Change?” *Nature* 397 (January): 249–251. https://doi.org/10.1038/16692.

Liu, Hai-Jun, and Jianbing Yan. 2019. “Crop Genome-Wide Association Study: A Harvest of Biological Relevance.” *The Plant Journal* 97 (1): 8–18. https://doi.org/10.1111/tpj.14139.

Lotts, Kelly, and Thomas Naberhaus. 2017. *Butterflies and Moths of North America*. https://butterfliesandmoths.org.

Loveall, Brandon J., and David L. Deitcher. 2010. “The Essential Role of Bursicon during Drosophiladevelopment.” *BMC Developmental Biology* 10 (1): 92. https://doi.org/10.1186/1471-213X-10-92.

Maia, Rafael, Chad M. Eliason, Pierre-Paul Bitton, Stéphanie M. Doucet, and Matthew D. Shawkey. 2013. “Pavo : An R Package for the Analysis, Visualization and Organization of Spectral Data.” Edited by Andrew Tatem. *Methods in Ecology and Evolution* 4 (10): 906–913. https://doi.org/10.1111/2041-210X.12069.

Malcolm, S. B. 1990. “Mimicry: Status of a Classical Evolutionary Paradigm.” *Trends in Ecology & Evolution* 5 (2): 57–62. https://doi.org/10.1016/0169-5347(90)90049-J.

Mallet, James, N. Barton, G. Lamas, J. Santisteban, M. Muedas, and H. Eeley. 1990. “Estimates of Selection and Gene Flow from Measures of Cline Width and Linkage Disequilibrium in Hybrid Zones.” *Genetics* 124 (4): 921–936.

Mallet, James, and Nicholas H Barton. 1989. “Strong Natural Selection in a Warning-Color Hybrid Zone.” *Evolution* 43 (2): 421–431.

Mallet, James, and Mathieu Joron. 1999. “Evolution of Diversity in Warning Color and Mimicry: Polymorphisms, Shifting Balance, and Speciation.” *Annual Review of Ecology and Systematics* 30 (1): 201–33. https://doi.org/10.1146/annurev.ecolsys.30.1.201.

Marples, Nicola M., Timothy J. Roper, and David G. C. Harper. 1998. “Responses of Wild Birds to Novel Prey: Evidence of Dietary Conservatism.” *Oikos* 83 (1): 161–65. https://doi.org/10.2307/3546557.

Marques, David A., Kay Lucek, Joana I. Meier, Salome Mwaiko, Catherine E. Wagner, Laurent Excoffier, and Ole Seehausen. 2016. “Genomics of Rapid Incipient Speciation in Sympatric Threespine Stickleback.” *PLoS Genetics* 12 (2): 1–34. https://doi.org/10.1371/journal.pgen.1005887.

Martin, Arnaud, Kyle J McCulloch, Nipam H Patel, Adriana D Briscoe, Lawrence E Gilbert, and Robert D Reed. 2014. “Multiple Recent Co-Options of Optix Associated with Novel Traits in Adaptive Butterfly Wing Radiations.” *EvoDevo* 5 (1): 7. https://doi.org/10.1186/2041-9139-5-7.

Martin, Arnaud, and Virginie Orgogozo. 2013. “The Loci of Repeated Evolution: A Catalog of Genetic Hotspots of Phenotypic Variation.” *Evolution* 67 (5): 1235–50. https://doi.org/10.1111/evo.12081.

Martin, Arnaud, Riccardo Papa, Nicola J Nadeau, Ryan I Hill, Brian A Counterman, and Georg Halder. 2012. “Diversification of Complex Butterfly Wing Patterns by

Repeated Regulatory Evolution of a Wnt Ligand." *Proceedings of the National Academy of Sciences of the United States of America* 109 (31). https://doi.org/10.1073/pnas.1204800109/-/DCSupplemental.www.pnas.org/cgi/doi/10.1073/pnas.1204800109.

Martin, Arnaud, and Robert D. Reed. 2014. "Wnt Signaling Underlies Evolution and Development of the Butterfly Wing Pattern Symmetry Systems." *Developmental Biology* 395 (2): 367–78. https://doi.org/10.1016/j.ydbio.2014.08.031.

Mazo-Vargas, Anyi, Carolina Concha, Luca Livraghi, Darli Massardo, Richard W. R. Wallbank, Linlin Zhang, Joseph D. Papador, et al. 2017. "Macroevolutionary Shifts of WntA Function Potentiate Butterfly Wing-Pattern Diversity." *Proceedings of the National Academy of Sciences of the United States of America* 114 (40): 10701–10706. https://doi.org/10.1073/pnas.1708149114.

McKenna, A., M. Hanna, E. Banks, A. Sivachenko, K. Cibulskis, A. Kernytsky, K. Garimella, et al. 2010. "The Genome Analysis Toolkit: A MapReduce Framework for Analyzing next-Generation DNA Sequencing Data." *Genome Research* 20 (9): 1297–1303. https://doi.org/10.1101/gr.107524.110.

McMillan, W. Owen, Antónia Monteiro, and Durrell D. Kapan. 2002. "Development and Evolution on the Wing." *Trends in Ecology & Evolution* 17 (3): 125–33. https://doi.org/10.1016/S0169-5347(01)02427-2.

Mullen, Sean P. 2006. "Wing Pattern Evolution and the Origins of Mimicry among North American Admiral Butterflies (Nymphalidae: Limenitis)." *Molecular Phylogenetics and Evolution* 39 (3): 747–758. https://doi.org/10.1016/j.ympev.2006.01.021.

Mullen, Sean P., Erik B. Dopman, and Richard G. Harrison. 2008. "Hybrid Zone Origins, Species Boundaries, and the Evolution of Wing-Pattern Diversity in a Polytypic Species Complex of North American Admiral Butterflies (Nymphalidae: Limenitis)." *Evolution* 62 (6): 1400–1417. https://doi.org/10.1111/j.1558-5646.2008.00366.x.

Mullen, Sean P., Wesley K. Savage, Niklas Wahlberg, and Keith R. Willmott. 2011. "Rapid Diversification and Not Clade Age Explains High Diversity in Neotropical Adelpha Butterflies." *Proceedings of the Royal Society B: Biological Sciences* 278 (1713): 1777–85. https://doi.org/10.1098/rspb.2010.2140.

Mullen, Sean P, and Kerry L Shaw. 2014. "Insect Speciation Rules: Unifying Concepts in Speciation Research." *Annual Review of Entomology* 59: 339–61. https://doi.org/10.1146/annurev-ento-120710-100621.

Nadeau, Nicola J., Carolina Pardo-Diaz, Annabel Whibley, Megan A. Supple, Suzanne V. Saenko, Richard W. R. Wallbank, Grace C. Wu, et al. 2016. "The Gene *Cortex* Controls Mimicry and Crypsis in Butterflies and Moths." *Nature* 534 (7605): 106–10. https://doi.org/10.1038/nature17961.

Nadeau, Nicola J., Mayté Ruiz, Patricio Salazar, Brian Counterman, Jose Alejandro Medina, Humberto Ortiz-Zuazaga, Anna Morrison, W. Owen McMillan, Chris D. Jiggins, and Riccardo Papa. 2014. "Population Genomics of Parallel Hybrid Zones in the Mimetic Butterflies, H. Melpomene and H. Erato." *Genome Research* 24 (8): 1316–1333. https://doi.org/10.1101/gr.169292.113.

Naisbit, Russell. 2001. "Ecological Divergence and Speciation in Heliconius Cydno and H. Melpomene." The University of London. https://www.ucl.ac.uk/taxome/lit/naisbitthesis02.pdf.

Naisbit, Russell, Chris D. Jiggins, and James Mallet. 2003. "Mimicry: Developmental Genes That Contribute to Speciation." *Evolution and Development* 5 (3): 269–80. https://doi.org/10.1046/j.1525-142X.2003.03034.x.

Nellen, Denise, Richard Burke, Gary Struhl, and Konrad Basler. 1996. "Direct and Long-Range Action of a DPP Morphogen Gradient." *Cell* 85 (3): 357–68. https://doi.org/10.1016/S0092-8674(00)81114-9.

Neumann, C. J., and S. M. Cohen. 1997. "Long-Range Action of Wingless Organizes the Dorsal-Ventral Axis of the Drosophila Wing." *Development* 124 (4): 871–80.

Nicholson, A J. 1927. *A New Theory of Mimicry in Insects*. Australian Zoologist. Australian Zoologist. https://books.google.com/books?id=k9jeMQAACAAJ.

Nijhout, H. F. 2001. "Elements of Butterfly Wing Patterns." *Journal of Experimental Zoology* 291 (3): 213–25. https://doi.org/10.1002/jez.1099.

Ozaki, Kouichi, Yozo Ohnishi, Aritoshi Iida, Akihiko Sekine, Ryo Yamada, Tatsuhiko Tsunoda, Hiroshi Sato, et al. 2002. "Functional SNPs in the Lymphotoxin-α Gene That Are Associated with Susceptibility to Myocardial Infarction." *Nature Genetics* 32 (4): 650–54. https://doi.org/10.1038/ng1047.

Pallares, Luisa F., Bettina Harr, Leslie M. Turner, and Diethard Tautz. 2014. "Use of a Natural Hybrid Zone for Genomewide Association Mapping of Craniofacial Traits in the House Mouse." *Molecular Ecology* 23 (23): 5756–70. https://doi.org/10.1111/mec.12968.

Palmer, Daniela H., Yue Qian Tan, Susan D. Finkbeiner, Adriana D. Briscoe, Antónia Monteiro, and Marcus R. Kronforst. 2018. "Experimental Field Tests of Batesian

Mimicry in the Swallowtail Butterfly Papilio Polytes." *Ecology and Evolution* 8 (15): 7657–66. https://doi.org/10.1002/ece3.4207.

Papa, Riccardo, Durrell D. Kapan, Brian A. Counterman, Karla Maldonado, Daniel P. Lindstrom, Robert D. Reed, H. Frederik Nijhout, Tomas Hrbek, and W. Owen McMillan. 2013. "Multi-Allelic Major Effect Genes Interact with Minor Effect QTLs to Control Adaptive Color Pattern Variation in Heliconius Erato." *PLoS ONE* 8 (3): e57033. https://doi.org/10.1371/journal.pone.0057033.

Papa, Riccardo, Arnaud Martin, and Robert D Reed. 2008. "Genomic Hotspots of Adaptation in Butterfly Wing Pattern Evolution." *Current Opinion in Genetics & Development*, Genomes and evolution, 18 (6): 559–64. https://doi.org/10.1016/j.gde.2008.11.007.

Pearson, Joseph C., Derek Lemons, and William McGinnis. 2005. "Modulating Hox Gene Functions during Animal Body Patterning." *Nature Reviews. Genetics* 6 (12): 893. https://doi.org/10.1038/nrg1726.

Pfennig, David W., Christopher K. Akcali, and David W. Kikuchi. 2015. "Batesian Mimicry Promotes Pre- and Postmating Isolation in a Snake Mimicry Complex." *Evolution* 69 (4): 1085–1090. https://doi.org/10.1111/evo.12624.

Pfennig, David W., William R. Harcombe, and Karin S. Pfennig. 2001. "Frequency-Dependent Batesian Mimicry." *Nature* 410 (6826): 323. https://doi.org/10.1038/35066628.

Pfennig, David W., George R. Harper, Abel F. Brumo, William R. Harcombe, and Karin S. Pfennig. 2007. "Population Differences in Predation on Batesian Mimics in Allopatry with Their Model: Selection against Mimics Is Strongest When They Are Common." *Behavioral Ecology and Sociobiology* 61 (4): 505–511. https://doi.org/10.1007/s00265-006-0278-x.

Pfennig, David W., and Sean P. Mullen. 2010. "Mimics without Models: Causes and Consequences of Allopatry in Batesian Mimicry Complexes." *Proceedings. Biological Sciences / The Royal Society* 277 (1694): 2577–2585. https://doi.org/10.1098/rspb.2010.0586.

Platt, Austin P., and Lincoln P. Brower. 1968. "Mimetic Versus Disruptive Coloration in Intergrading Populations of Limenitis Arthemis and Astyanax Butterflies." *Evolution* 22 (4): 699–718. https://doi.org/10.2307/2406897.

Platt, Austin P., Raymond P. Coppinger, and Lincoln P. Brower. 1971. "Demonstration of the Selective Advantage of Mimetic Limenitis Butterflies Presented to Caged Avian Predators." *Evolution* 25 (4): 692–701. https://doi.org/10.2307/2406950.

Porter, Adam H. 1989. “Genetic Evidence for Reproductive Isolation between Hybridizing Limenitis Butterflies (Lepidoptera: Nymphalidae) in Southwestern New Mexico.” *American Midland Naturalist* 122 (2): 275–280.

———. 1990. “Testing Nominal Species Boundaries Using Gene Flow Statistics: The Taxonomy of Two Hybridizing Admiral Butterflies (Limenitis: Nymphalidae).” *Systematic Zoology* 39 (2): 131. https://doi.org/10.2307/2992451.

Poulton, E.B. B. 1909. “Mimicry in the Butterflies of North America.” *Annals of the Entomological Society of America* 2 (4): 203–242.

Prudic, Kathleen L. 2007. “Warning and Deception: Chemical, Behavioral, and Phylogenetic Studies of Aposematic Coloration and Mimicry.”

Prudic, Kathleen L., Arthur M. Shapiro, and Nicola S. Clayton. 2002. “Evaluating a Putative Mimetic Relationship between Two Butterflies, Adelpha Bredowii and Limenitis Lorquini.” *Ecological Entomology* 27 (1): 68–75. https://doi.org/10.1046/j.0307-6946.2001.00384.x.

Pryszcz, Leszek P., and Toni Gabaldón. 2016. “Redundans: An Assembly Pipeline for Highly Heterozygous Genomes.” *Nucleic Acids Research* 44 (12): e113. https://doi.org/10.1093/nar/gkw294.

Purcell, Shaun, Benjamin Neale, Kathe Todd-Brown, Lori Thomas, Manuel A. R. Ferreira, David Bender, Julian Maller, et al. 2007. “PLINK: A Tool Set for Whole-Genome Association and Population-Based Linkage Analyses.” *The American Journal of Human Genetics* 81 (3): 559–75. https://doi.org/10.1086/519795.

R Core Team. 2016. *R: A Language and Environment for Statistical Computing*. Vienna, Austria: R Foundation for Statistical Computing. https://www.r-project.org/.

Rabosky, Daniel L. 2016. “Reproductive Isolation and the Causes of Speciation Rate Variation in Nature.” *Biological Journal of the Linnean Society* 118 (1): 13–25. https://doi.org/10.1111/bij.12703.

Rashed, Arash, and Thomas N. Sherratt. 2007. “Mimicry in Hoverflies (Diptera: Syrphidae): A Field Test of the Competitive Mimicry Hypothesis.” *Behavioral Ecology* 18 (2): 337–344. https://doi.org/10.1093/beheco/arl089.

Rastas, Pasi. 2017. “Lep-MAP3: Robust Linkage Mapping Even for Low-Coverage Whole Genome Sequencing Data.” Edited by Bonnie Berger. *Bioinformatics* 33 (23): 3726–32. https://doi.org/10.1093/bioinformatics/btx494.

Reed, Robert D., Riccardo Papa, Arnaud Martin, Heather M. Hines, Brian A. Counterman, Carolina Pardo-Diaz, Chris D. Jiggins, et al. 2011. "Optix Drives the Repeated Convergent Evolution of Butterfly Wing Pattern Mimicry." *Science* 333 (6046): 1137–41. https://doi.org/10.1126/science.1208227.

Reed, Robert D, and Michael S Serfas. 2004. "Butterfly Wing Pattern Evolution Is Associated with Changes in a Notch/Distal-Less Temporal Pattern Formation Process." *Current Biology* 14 (13): 1159–66. https://doi.org/10.1016/j.cub.2004.06.046.

Remington, C. L. 1968. "Suture-Zones of Hybrid Interaction between Recently Joined Biotas." In *Evolutionary Biology*, edited by Theodosius Dobzhansky, Max K Hecht, and William C Steere, 321–428. Boston, MA: Springer US. https://doi.org/10.1007/978-1-4684-8094-8_8.

Ries, Leslie, and Sean P. Mullen. 2008. "A Rare Model Limits the Distribution of Its More Common Mimic: A Twist on Frequency-Dependent Batesian Mimicry." *Evolution* 62 (7): 1798–1803. https://doi.org/10.1111/j.1558-5646.2008.00401.x.

Ritland, David B., and Lincoln P. Brower. 1991. "The Viceroy Butterfly Is Not a Batesian Mimic." *Nature* 350 (6318): 497–498. https://doi.org/10.1038/350497a0.

Ronshaugen, Matthew, Nadine McGinnis, and William McGinnis. 2002. "Hox Protein Mutation and Macroevolution of the Insect Body Plan." *Nature* 415 (6874): 914–17. https://doi.org/10.1038/nature716.

Rosenberg, Risa H., and Magnus Enquist. 1991. "Contest Behaviour in Weidemeyer's Admiral Butterfly Limenitis Weidemeyerii (Nymphalidae): The Effect of Size and Residency." *Animal Behaviour* 42 (5): 805–811. https://doi.org/10.1016/S0003-3472(05)80124-1.

Ruxton, Graeme D., Thomas N. Sherratt, and Michael P. Speed. 2004. *Avoiding Attack: The Evolutionary Ecology of Crypsis, Warning Signals and Mimicry*. Edited by Thomas N Sherratt and Michael Patrick Speed. Vol. 17. Oxford: Oxford University Press. https://doi.org/10.1093/acprof.

Sansom, Roger, and Robert Brandon. 2007. *Integrating Evolution and Development: From Theory to Practice*. MIT Press. https://mitpress.mit.edu/books/integrating-evolution-and-development.

Sassone-Corsi, Paolo, and Emiliana Borrelli. 1986. "Transcriptional Regulation by Trans-Acting Factors." *Trends in Genetics* 2 (January): 215–19. https://doi.org/10.1016/0168-9525(86)90233-7.

Savage, Wesley K, and Sean P Mullen. 2009. “A Single Origin of Batesian Mimicry among Hybridizing Populations of Admiral Butterflies (Limenitis Arthemis) Rejects an Evolutionary Reversion to the Ancestral Phenotype.” *Proceedings of the Royal Society Biological Sciences* 276 (1667): 2557–2565. https://doi.org/10.1098/rspb.2009.0256.

Scott, James A. 1992. *The Butterflies of North America: A Natural History and Field Guide*. Stanford, Calif: Stanford University Press.

Seymoure, B. M., and A. Aiello. 2015. “Keeping the Band Together: Evidence for False Boundary Disruptive Coloration in a Butterfly.” *Journal of Evolutionary Biology* 28 (9): 1618–1624. https://doi.org/10.1111/jeb.12681.

Shapiro, Arthur M. 2016. *Art Shapiro’s Butterfly Site*. http://butterfly.ucdavis.edu/.

Shaw, Kerry L., and Sean P. Mullen. 2011. “Genes versus Phenotypes in the Study of Speciation.” *Genetica* 139 (5): 649–61. https://doi.org/10.1007/s10709-011-9562-4.

———. 2014. “Speciation Continuum.” *Journal of Heredity* 105 (S1): 741–742. https://doi.org/10.1093/jhered/esu060.

Sheppard, P. M., John R. G. Turner, K. S. Brown, W. W. Benson, and M. C. Singer. 1985a. “Introduction.” In *Genetics and the Evolution of Müllerian Mimicry in Heliconius Butterflies*, 309:5 LP – 9. 1138. Philosophical Transactions of the Royal Society in London: Biology.

Sheppard, P.M., J.R.G. Turner, K.S. Brown, W.W. Benson, and M.C. Singer. 1985b. *Genetics and the Evolution of Müllerian Mimicry in Heliconius Butterflies*. Vol. 161. March. Philosophical Transactions of the Royal Society in London: Biology.

Silberglied, R E, a Aiello, and D M Windsor. 1980. “Disruptive Coloration in Butterflies: Lack of Support in Anartia Fatima.” *Science* 209 (4456): 617–619. https://doi.org/10.1126/science.209.4456.617.

Speed, Michael P. 1993. “Muellerian Mimicry and the Psychology of Predation.” *Animal Behaviour* 45 (3): 571–80. https://doi.org/10.1006/anbe.1993.1067.

Speed, Michael P., and John R. G. Turner. 1999. “Learning and Memory in Mimicry: II. Do We Understand the Mimicry Spectrum?” *Biological Journal of the Linnean Society* 67 (3): 281–312. https://doi.org/10.1111/j.1095-8312.1999.tb01935.x.

Stern, David L. 2013. “The Genetic Causes of Convergent Evolution.” *Nature Reviews. Genetics* 14 (11): 751–64. https://doi.org/10.1038/nrg3483.

Stryjewski, Katherine Faust, and Michael D. Sorenson. 2017. "Mosaic Genome Evolution in a Recent and Rapid Avian Radiation." *Nature Ecology & Evolution* 1 (12): 1912. https://doi.org/10.1038/s41559-017-0364-7.

Thayer, Rachel. 2019. "Genetic Basis and Evolutionary Context for Structural Color Shift in the Buckeye Butterfly (Junonia Coenia)." SE Hamilton Award Symposium presented at the Evolution 2019, June 22.

Toy, J., J.-M. Yang, G. S. Leppert, and O. H. Sundin. 1998. "The Optx2 Homeobox Gene Is Expressed in Early Precursors of the Eye and Activates Retina-Specific Genes." *Proceedings of the National Academy of Sciences of the United States of America* 95 (18): 10643–10648. https://doi.org/10.1073/pnas.95.18.10643.

Turner, John R. G. 1987. "The Evolutionary Dynamics of Batesian and Muellerian Mimicry: Similarities and Differences." *Ecological Entomology* 12 (1): 81–95. https://doi.org/10.1111/j.1365-2311.1987.tb00987.x.

Turner, Stephen D. 2018. "Qqman: An R Package for Visualizing GWAS Results Using Q-Q and Manhattan Plots." *Journal of Open Source Software* 3: 731. https://doi.org/10.21105/joss.00731.

Twomey, Evan, Jacob S Vestergaard, and Kyle Summers. 2014. "Reproductive Isolation Related to Mimetic Divergence in the Poison Frog Ranitomeya Imitator." *Nature Communications* 5: 4749. https://doi.org/10.1038/ncomms5749.

Vane-Wright, R. I. 1980. "On the Definition of Mimicry." *Biological Journal of the Linnean Society* 13 (1): 1–6. https://doi.org/10.1111/j.1095-8312.1980.tb00066.x.

Visscher, Peter M., Naomi R. Wray, Qian Zhang, Pamela Sklar, Mark I. McCarthy, Matthew A. Brown, and Jian Yang. 2017. "10 Years of GWAS Discovery: Biology, Function, and Translation." *The American Journal of Human Genetics* 101 (1): 5–22. https://doi.org/10.1016/j.ajhg.2017.06.005.

Vorobyev, M, and D Osorio. 1998. "Receptor Noise as a Determinant of Colour Thresholds." *Proceedings. Biological Sciences / The Royal Society* 265 (1394): 351–358. https://doi.org/10.1098/rspb.1998.0302.

Waldbauer, G P. 1988. "Aposematism and Batesian Mimicry," 227–259. https://doi.org/10.1007/978-1-4613-0931-4.

Wang, Jian, and Sanjay Shete. 2012. "Testing Departure from Hardy–Weinberg Proportions." In *Statistical Human Genetics: Methods and Protocols*, edited by Robert C. Elston, Jaya M. Satagopan, and Shuying Sun, 77–102. Methods in Molecular Biology. Totowa, NJ: Humana Press. https://doi.org/10.1007/978-1-61779-555-8_6.

Watt, WB, FS Chew, LRG Snyder, AG Watt, and DE Rothschild. 1977. "Population Structure of Pierid Butterflies." *Oecologia*, no. 27: 1–22.

Willmott, Keith R. 2003. "Cladistic Analysis of the Neotropical Butterfly Genus Adelpha (Lepidoptera: Nymphalidae), with Comments on the Subtribal Classification of Limenitidini." *Systematic Entomology* 28 (3): 279–322. https://doi.org/10.1046/j.1365-3113.2003.00209.x.

Willmott, Keith R, Julia C Robinson Willmott, Marianne Elias, and Chris D. Jiggins. 2017. "Maintaining Mimicry Diversity: Optimal Warning Colour Patterns Differ among Microhabitats in Amazonian Clearwing Butterflies." *Proceedings of the Royal Society B* 284: 20170744. https://doi.org/10.1016/j.anbehav.2014.09.005.

Winand, Dittrich, Francis Gilbert, Patrick Green, Peter McGregor, and David Grewcock. 1993. "Imperfect Mimicry: A Pigeon's Perspective." *Proceedings of the Royal Society B*, no. 251: 195–200.

Wster, Wolfgang, Christopher S. E. Allum, I. Birta Bjargardttir, Kimberley L. Bailey, Karen J. Dawson, Jamel Guenioui, John Lewis, et al. 2004. "Do Aposematism and Batesian Mimicry Require Bright Colours? A Test, Using European Viper Markings." *Proceedings of the Royal Society B: Biological Sciences* 271 (1556): 2495–2499. https://doi.org/10.1098/rspb.2004.2894.

Xu, Jianfeng, Aubrey Turner, Joy Little, Eugene R. Bleecker, and Deborah A. Meyers. 2002. "Positive Results in Association Studies Are Associated with Departure from Hardy-Weinberg Equilibrium: Hint for Genotyping Error?" *Human Genetics* 111 (6): 573–74. https://doi.org/10.1007/s00439-002-0819-y.

Yamamoto, Kimiko, Junko Nohata, Keiko Kadono-Okuda, Junko Narukawa, Motoe Sasanuma, Shun-ichi Sasanuma, Hiroshi Minami, et al. 2008. "A BAC-Based Integrated Linkage Map of the Silkworm Bombyx Mori." *Genome Biology* 9 (1): R21. https://doi.org/10.1186/gb-2008-9-1-r21.

Zecca, Myriam, Konrad Basler, and Gary Struhl. 1996. "Direct and Long-Range Action of a Wingless Morphogen Gradient." *Cell* 87 (5): 833–44. https://doi.org/10.1016/S0092-8674(00)81991-1.

Zhou, Xiang, and Matthew Stephens. 2012. "Genome-Wide Efficient Mixed Model Analysis for Association Studies." *Nature Genetics* 44 (7): 821–24. https://doi.org/10.1038/ng.2310.